SYNTHESIS & CHARACTERIZATION OF IMMOBILIZING MATERIALS FOR BIOSENSING APPLICATION

Thesis submitted to the

FACULTY OF TECHNOLOGY
UNIVERSITY OF DELHI

for the award of the degree of the

DOCTOR OF PHILOSOPHY

in

APPLIED CHEMISTRY

by

TARUSHEE AHUJA

Department of Applied Chemistry,
DELHI COLLEGE OF ENGINEERING,
BAWANA ROAD, DELHI-110042
2010

CERTIFICATE

This is to certify that the thesis titled **"SYNTHESIS & CHARACTERIZATION OF IMMOBILIZING MATERIALS FOR BIOSENSING APPLICATION"** submitted to the Faculty of Technology, University of Delhi, Delhi, in fulfilment of the requirements for the award of the degree of Doctor of Philosophy in Applied Chemistry embodies the original research work carried out by Ms.Tarushee Ahuja under our supervision. This work has not been submitted in part or full for any degree or diploma of this or any other University. It is further certified that the scholar has devoted more than two years, the minimum stipulated period, for the completion of this work.

DR. D. KUMAR,
Supervisor,
Department of Applied Chemistry,
DELHI TECHNOLOGICAL UNIVERSITY,
(formerly Delhi College of Engineering)
BAWANA ROAD,
DELHI-110042

DR. RAJESH
Co-Supervisor,
Liquid Crystal & SAM Section,
National Physical Laboratory,
(Council of Scientific & Industrial Research)
Dr. K.S.Krishnan Marg,
New Delhi-110012

PROF. A. TRIVEDI,
Dean, FOT &
Head,
Applied Sciences & Humanities Deptt.
Faculty of Technology,
University of Delhi,
Delhi

DEDICATED TO

MY FAMILY

Acknowledgments

First and foremost, a special thanks to God, for the blessings without which this endeavor was never possible.

I wish to express my deep sense of gratitude to my supervisors, Dr. D. Kumar, Associate Professor, Department of Applied Chemistry, Delhi Technological University and Dr. Rajesh, Scientist E1, National Physical Laboratory (Council Scientific of Industrial Research), for their invaluable guidance, encouragement and constructive criticism during this work. It would not have been possible for me to bring this work in the present form without their support. Working with them has been a rich experience and shall always be a pleasant memory.

I owe my most sincere gratitude to Professor P.B. Sharma, Vice Chancellor, Delhi Technological University, Professor G.L. Verma, Head, Department of Applied Chemistry, Delhi Technological University, and Dr. A.M. Biradar, Scientist G, National Physical Laboratory, for their encouragement and support throughout the work.

I am also thankful to Council of Scientific and Industrial Research and Delhi Technological University, for providing me financial aid.

It is also true that this work would be impossible without the cooperation and support of my friends, all Laboratory and Office Staff members and colleagues of DTU and NPL. In naming them, first I would like to thank Mr. Irfan Mir, Ms. Sapna Jain, Mr. Navdeep Grover, Ms. Kusum Solanki and Mr. Satya Sadhan Singh for the valuable discussions,

help and for their awesome company. My special thanks to Dr. Nahar Singh, Mr. V.K. Tanwar, Mr. Vikash Sharma, Mr. Mange Ram, Ms. Nidhi Puri, Mr. Sujeet K. Mishra, Ms. Chhavi and Ms. Namrata from NPL, and Dr. Neetika Gupta, Dr. Shalini Sharma, Ms. Sudha and Ms. Ritu from DTU for their timely help.

Many thanks are due to my pride and joy, my huge family. Starting from my grandmother (Mrs. Taravanti Ahuja), my parents (Mrs. Veena and Mr. Surinder Ahuja), my inlaws (Mrs. Saroj and Mr. Ramesh Lamba), my sisters Parul and Prachi, my Brother-in-law Mr. Kamal Gulati and my nephew Chayan for their love, support and unabated faith in me, which kept me going through this work.

This thesis would not have been possible without the support of my husband Mr. Gaurav Lamba, who has loved me unconditionally and stood by my side like a rock.

(Tarushee Ahuja)

Abstract

The development of biosensors has come from the rapid advances in health care technology as a frequent measurement of biochemical parameters such as blood cations, gases and metabolites required for effective patient care. The need for cheap and reliable sensors for monitoring such parameters has lead to exponential increase in the research and development of biosensors.

Electrochemical biosensors have emerged as the most commonly used biosensors as they have been found to overcome most of the disadvantages, which inhibit the use of other types of biosensors. They are rapid, easy to handle, simple and are of low cost. The basic fact behind this bio-interaction process is that the electrochemical species such as electrons are consumed or generated producing an electrochemical signal, which can be measured by the detector. These biosensors are usually based on potentiometry and amperometry.

Urea and uric acid are the most important end product of protein degradation and purine metabolism, thus their proper balance in blood is essential for overall well being and for renal health specifically. The optimal concentration of urea in blood is an indication of proper renal functioning, its high level in blood causes urinary tract obstruction, dehyradation, shock, burns and gastrointestinal bleeding, whereas a substantial low level of urea concentration causes hepatic failure, nephrotic syndrome, cachexia. Similarly abnormal uric acid levels lead to gout, chronic renal disease, some organic acidemias, leukemia, pneumonia and Lesch–Nyhan syndrome. Hence, the detection of these analytes in body fluids is clinically important indicator. Although direct spectroscopic methods can be used for their determination, but these methods are dependent on the pre-treatment of sample and cannot be used for onsite monitoring. The primary focus of this work

is to develop urea and uric acid biosensors with improved properties such as sensitivity and response time by using different substrates on indium tin-oxide (ITO) glass plates and different methods of immobilization.

This study identifies the already established materials for developing different biosensor which may be used for the detection of urea and uric acid in aqueous solution. The main objective of this dissertation is to use modified electrode such as BSA/PPy, MWCNT/SiO_2, APTES/BS^3 and GNPs/APTES as matrix for the development of urea and uric acid biosensors.

Organization of the thesis

This thesis is organized into 5 chapters,

Chapter 1 gives introduction to several topics that are related to this research. These include fundamentals of biosensors, immobilization techniques, materials for immobilization.

Chapter 2 investigates the use of bovine serum albumin during electropolymerization of pyrrole which improves the enzyme loading.

Chapter 3 shows the impact of using carbon nanotubes in a sol matrix and its use in developing urea biosensor.

Chapter 4 discusses the use of another matrix based on self assembled monolayer and its modification to develop uric acid biosensor.

Chapter 5 signifies the use of Au nanoparticles in self assembled monolayer. Response characteristics were studied as a function of uric acid concentration.

CONTENTS

List of Tables

List of Figures

KCl solution containing 2 mM $[Fe(CN)_6]^{3-}$; scan rate 25 mV/s; 3rd cycle voltammogram is shown

Fig.4.7: Nyquist plots obtained for bare ITO glass, APTES/ITO glass, BS^3/APTES/ITO glass and Uricase/BS^3/APTES/ITO glass electrodes in 0.1 M KCl solution containing 2 mM $[Fe(CN)_6]^{3-}$. Inset shows a schematic diagram of equivalent circuit for impedance spectroscopy in the presence of redox couple: R_s, resistance of the electrolyte solution; Ret, electron-transfer resistance; Z_w, Warburg impedance; C_{dl}, double-layer capacitance

Fig.4.8: Enzymatic reaction mechanism of working of Uricase/BS^3/APTES/ITO electrode

Fig.4.9: (a) Chronoamperometric response curve of Uricase/BS^3/APTES/ITO with addition of different concentration of uric acid; repeatability performance of the same electrode from n = 2-6 time (b-f)

Fig.4.10: Steady state current dependence calibration curve of Uricase/BS^3/ APTES/ITO biosensor to uric acid

Fig.4.11: Reusability performance (n = 3-5) of the Uricase/BS^3/APTES/ITO electrode in terms of relative standard deviation at different concentrations of uric acid in PBS

Fig.4.12: Effect of storage time on the amperometric response of Uricase/BS^3/APTES/ITO electrode

Fig.5.1: (A) Self-assembled monolayer formation of Au nanoparticles on solid surfaces enhances the redox process that provides the electrochemical detection of the enzymatic product (P) from the substrate (S); (B) Metal nanoparticles embedded inside the matrices

Chapter I

(Part A)

Introduction

Improvement of “life quality” is one of the most important objectives of global research efforts, and is closely linked to the control of diseases, food quality and safety, and the quality of our environment. There is a lot of global emphasis these days towards environment consciousness and health monitoring. This has led to the development of accurate, fast, sensitive and low cost miniaturized monitoring devices generally called as Biosensors. Biosensors combine the high specificity of biological catalysts such as enzymes with the sensitivity and accuracy of electrochemical indicator reactions. They have not only become an impeccable part of the fields of biomedicine and environmental science but also received as a lot of attention of researchers across the globe. The rapid advancements in this field have created a niche for the research and development in areas specific or related to biosensors. Our attempt too is a step forward in this direction and thus forms the crust of the research work presented in this dissertation. A brief overview related to biosensors is discussed in the following sections.

1.1 A BRIEF HISTORY

In 1956, Clark published his definitive research paper on the oxygen electrode [1]. Based on this experience and addressing his desire to expand the range of analytes that could be measured in the body, he made a landmark address in 1962 at a New York Academy of Sciences symposium in which he described how "to make electrochemical sensors (pH, polarographic, potentiometric or conductometric) more intelligent by adding

"enzyme transducers as membrane enclosed sandwiches". The concept was illustrated by an experiment in which glucose oxidase was entrapped at a Clark oxygen electrode using dialysis membrane. The decrease in measured oxygen concentration was proportional to glucose concentration. Guilbault and Montalvo [2] were the first to detail a potentiometric enzyme electrode. They described a urea sensor based on urease immobilized at an ammonium-selective liquid membrane electrode. Clark's ideas became commercial reality in 1975 with the successful re-launch (first launch 1973) of the Yellow Springs Instrument Company (Ohio) glucose analyser based on the amperometric detection of hydrogen peroxide. This was the first of many biosensor-based laboratory analyzers to be built by companies around the world.

Since then, research communities from various fields such as Physics, Chemistry, and Material Science have come together to develop more sophisticated, reliable and mature biosensing devices for applications in the fields of medicine, agriculture, biotechnology, as well as the military and bioterrorism detection and prevention. Selective determination of various blood analytes, viz., glucose, urea, lactate, uric acid, cholesterol etc. is of utmost importance for the screening and treatment of a number of diseases. The developments of such detection tools and similar techniques have made considerable progress since then. Early techniques of biosensor in the analysis of chemical and biological species involved reactions that took place in a solution, in addition to catalysts and samples. In recent years, however, the biosensor techniques have provided alternative systems that allowed the reactions, without adding reagents, to take place at a surface of an electrode.

Since the reagents have been already immobilized in the systems, the biological and chemical sensors have performed the task of identifying composition of species with minimum human interventions.

The use of thermal transducers for biosensors was proposed in 1974 and the new devices were christened *thermal enzyme probes* [3] and *enzyme thermistors* (Mosbach) [4], respectively. The biosensor took a further fresh evolutionary route in 1975, when Divis [5] suggested that bacteria could be harnessed as the biological element in *microbial electrodes* for the measurement of alcohol. This paper marked the beginning of a major research effort in Japan and elsewhere into biotechnological and environmental applications of biosensors. Lubbers and Opitz [6] coined the term *optode* in 1975 to describe a fibre-optic sensor with immobilized indicator to measure carbon dioxide or oxygen. They extended the concept to make an optical biosensor for alcohol by immobilizing alcohol oxidase on the end of a fibre-optic oxygen sensor [7]. Commercial optodes are now showing excellent performance for *in vivo* measurement of pH, pCO_2 and pO_2, but enzyme optodes are not yet widely available. In 1976, Clemens *et al.* [8] incorporated an electrochemical glucose biosensor in a bedside artificial pancreas and this was later marketed by Miles (Elkhart) as the Biostator. Although, the Biostator is no longer commercially available, a new semi-continuous catheter-based blood glucose analyser has recently been introduced by VIA Medical (San Diego, USA). In the same year, La Roche (Switzerland) introduced the Lactate Analyser LA 640 in which the soluble mediator, hexacyanoferrate, was used to shuttle electrons from lactate dehydrogenase to an electrode.

Although this was not a commercial success at the time, it turned out in retrospect to be an important forerunner of a new generation of mediated-biosensors and of lactate analyzers for sports and clinical applications. A major advance in the *in vivo* application of glucose biosensors was reported by Shichiri *et al.* [9] who described the first needle-type enzyme electrode for subcutaneous implantation in 1982. Companies are still pursuing this possibility, but no device for general use is available yet. The idea of building direct *immunosensors* by fixing antibodies to a piezoelectric or potentiometric transducer had been explored since the early 70's, but it was a paper by Liedberg *et al.* [10] that was to pave the way for commercial success. They described the use of surface plasmon resonance to monitor affinity reactions in real time. The BIAcore (Pharmacia, Sweden) launched in 1990 is based on this technology. A screen-printed enzyme electrode was launched by MediSense (Cambridge, USA) in 1987 with a pen-sized meter for home blood-glucose monitoring. The electronics were redesigned into popular credit-card and computer-mouse style formats, and MediSense's sales showed exponential growth reaching US$175 million by 1996 when they were purchased by Abbott Boehringer Mannheim and Bayer now have competing mediated biosensors and the combined sales of the three companies dominate 85% of the world market for biosensors and are rapidly displacing conventional reflectance photometry technology for home diagnostics. Academic journals now contain descriptions of a wide variety of devices exploiting enzymes, nucleic acids, cell receptors, antibodies and intact cells, in combination with electrochemical, optical, piezoelectric and thermometric

transducers, [11]. Within each permutation lies a myriad of alternative transduction strategies and each approach can be applied to numerous analytical problems in health care [12], food and drink [13], the process industries [14], environmental monitoring [15], defense and security. Generic goals may be identified which underpin more applied biosensor programmes and tackle some of the principal hurdles to the more widespread adoption of biosensor technology for analysis. The design of integrated systems approaches to patterning sensitive elements and methods to improve the sensitivity, stability and selectivity of biosensors are key areas.

1.2 FUNDAMENTALS OF BIOSENSORS

The name biosensor has been variously applied to a number of devices either used to monitor living systems or incorporating biotic elements. A biosensor is a chemical sensing device in which a biologically derived recognition entity is coupled to a transducer, to allow the quantitative development of some complex biochemical parameter [16]. The term 'biosensor' is often used to cover sensor devices used in order to determine the concentration of substances and other parameters of biological interest even where they do not utilise a biological system directly. The name “biosensor” signifies that the device is a combination of two parts: (i) a bio-element (bioreceptor), and (ii) a sensor-element (transducer). A specific “bio” element (say, enzyme) recognizes a specific analyte and the “sensor” element transduces the change in the biomolecule into an electrical signal. The

bioelement is very specific to the analyte to which it is sensitive. It does not recognize other analytes. The usual aim of a biosensor is to produce either discrete or continuous digital electronic signals, which are proportional to a single analyte or related group of analytes. Different components of biosensors are shown in figure 1.1.

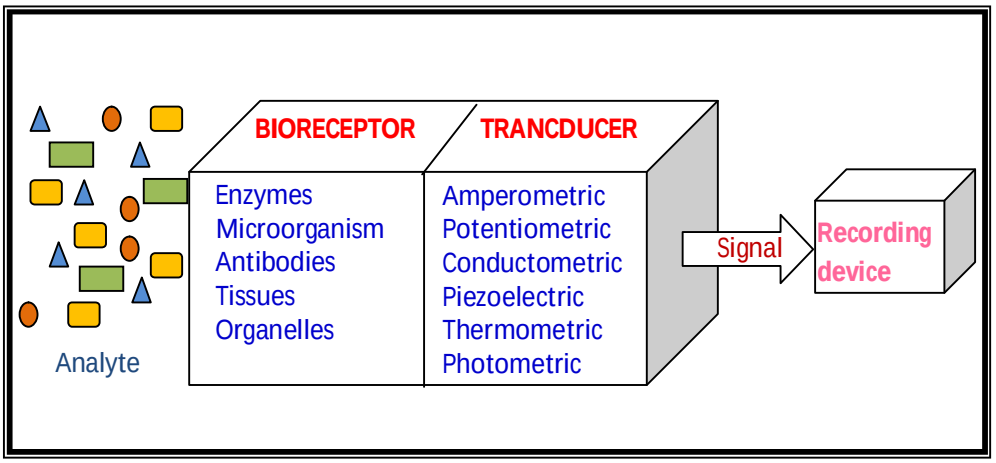

Fig. 1.1: Schematic representation of a biosensor

In biosensors the following sequence of processes takes place:

- specific recognition of the analyte;
- transduction of the physiochemical effect caused by the interaction with the receptor into an electrical signal;
- signal processing and amplification

A successful biosensor must possess at least some of the following beneficial features:

- The biocatalyst must be highly specific for the purpose of the analysis, be stable under normal storage conditions and, show good stability over a large number of assays.

- The reaction should be as independent of such physical parameters as stirring, pH and temperature as is manageable. This would allow the analysis of samples with minimal pre-treatment. If the reaction involves cofactors or coenzymes these should, preferably, also be co-immobilized with the enzyme.

- The response should be fast, accurate, precise, reproducible and linear over the useful analytical range and also should be free from electrical noise.

- If the biosensor is to be used for invasive monitoring in clinical situations, the probe must be tiny and biocompatible, having no toxic or antigenic effects.

- The complete biosensor should be cheap, small, portable and capable of being used by semi-skilled operators.

1.2.1 Bioreceptors

Bioreceptors are biomolecules such as enzymes, tissues, bacteria, yeast, antibodies/ antigens, liposomes, organelles which work as biochemical transducers and are capable of recognizing the specific analytes, and also

regulate the specificity and sensitivity of the device. Due to the high substrate specificity of enzymes and the interference free indication of the reaction product, biosensors based on enzymes are commonly developed and are highly selective. Most of these biological molecules have very short lifetime in solution phase, thus they have to be fixed in a suitable matrix. Since, enzymes form the core bioreceptors in this study a detailed purview of their use is given below.

Enzymes are proteins that catalyse biochemical reactions. These biomaterials include amide linked amino acids and typically have molecular weights of 5,000 or greater. Enzymes have a number of distinct advantages over conventional chemical catalyst like their specificity and selectivity not only for particular reactions but also in their discrimination between similar parts of molecules or optical isomers. All enzymes have active site. In metallo-enzymes there are co-factors in the active sites which contain metal ions. These metal ions present in the active site of the enzymes play an active role in oxido-reductive reaction and are responsible for the redox reaction when they come in contact with a substrate. These enzymes work on the principle of key-lock system. When the active site of the enzyme comes in contact with the substrate only then redox reaction starts proceeding and continues till whole of the substrate is converted into product. Figure 1.2 shows a schematic representation of the specificity of enzymes.

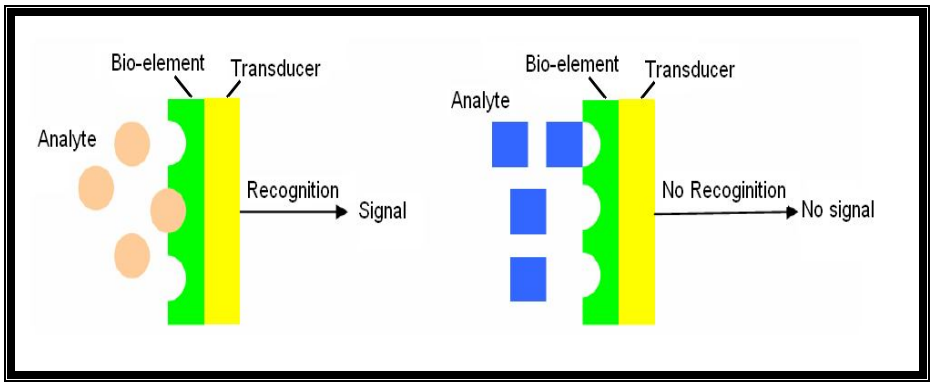

Fig. 1.2: Specificity of the enzyme in biosensor

Redox enzymes (also known as oxidoreductases) are extensively used to construct enzyme electrodes. In addition to these, hydrolytic enzymes like lipases [17, 18] and esterase [19, 20] are also used along with the redox enzymes for added specificity to sense a substrate where no oxidoreductase is known to work. A promising example is the composite enzyme electrode that consists of cholesterol oxidase and esterase used to detect blood cholesterol [21]. A wide range of redox enzymes have been used for the construction of enzyme electrodes. They include: alcohol dehydrogenase, aldehyde dehydrogenase, glucose oxidase (GOx), glutaminase, horse radish peroxidase (HRP), catalase, xanthine oxidase, choline oxidase, urease, billirubin oxidase, uricase and lactate oxidase. The major problem of enzyme electrodes for biosensor applications are their dependence on co-substrates like oxygen and hydrogen peroxide. A need of high over potential for these co-substrates impair the usefulness of these enzymes based biosensors. This problem may be substantially overcome by the use of ‘mediators’ which transfer the electrons directly to the electrode by passing the reduction of the

co-substrate [22]. Thus, in addition to the enzyme and electrode material, the mediators have also been considered a vital component of enzyme electrodes for many applications. These mediators, which are basically synthetic or biologically active charged carriers, act as intermediates between the redox center of the enzyme and the electrode. These mediators must possess a number of useful properties for such applications: (a) they must react rapidly with the reduced form of the enzyme and (b) they should be adequately soluble in both the oxidised and reduced forms for rapid diffusion between the redox center of the enzyme and the electrode surface. The over potential for the regeneration of the oxidised mediator at the electrode surface should be low and independent of pH and the reduced form of the mediator should not readily react with oxygen. Historically, ferrocene and quinine derivatives are the widely used mediators as evident from the open literature [23, 24].

1.2.2 Transducer

The main function of a transducer is to convert the physico-chemical change in the biologically active material resulting from the interaction with the analyte into an output signal. The transducer of an electrical device responds in a way that a signal can be electronically amplified, stored and displayed. Suitable transducing system can be adapted in a sensor assembly depending on the nature of the biochemical interaction with the species of interest. The physical transducers vary from electrochemical, spectroscopic, thermal, piezoelectric and surface acoustic wave technology.

1.3 CHARACTERISTICS OF BIOSENSOR

1.3.1 Sensitivity

Clinicians, food technologists and environmentalists all have an interest in generally increased sensitivity and limits of detection for a range of analytes. While the precise demands to meet today's requirements may be modest in these respects, few would contest the longer-term benefits of reliable detection of trace amounts of various indicators, additives or contaminants. Enzyme electrodes have been designed which preconcentrate the analyte of interest [25]. A gas-phase microbiosensor for phenol has been reported in which polyphenol oxidase was immobilized in a glycerol gel on an interdigitated microelectrode array [26]. Phenol vapour partitioned directly into the gel where it was oxidized to quinone. Signal amplification was enhanced by redox recycling of the quinone/catechol couple resulting in a sensor able to measure 30 parts per billion (ppb) phenol. Detection limits of parts per trillion volatile organic carbons are feasible with this approach. Ultra-low detection limits are achievable with affinity sensors and electrochemical detection may be readily integrated with chromatographic techniques to yield user-friendly devices [27].

1.3.2 Stability

Arguably the most obvious disadvantage in exploiting the exquisite specificity and sensitivity of complex biological molecules is their inherent instability. Many strategies may be employed to restrain or modify the structure of biological receptors to enhance their longevity. Some reports have confirmed the effectiveness of sol gels as an immobilization matrix for glucose using simultaneous fluorescence quenching of two indicators, (2,2'-bipyridyl)ruthenium(II) chloride hexahydrate and 1-hydroxypyrene-3,6,8-trisulphonic acid. In addition to the excellent optical properties of the gel, enhanced stability of the glucose oxidase catalyst was clearly evident [28].

1.3.3 Selectivity

Improvement in the selectivity of biosensors may be sought at two levels; the interface between the transducer and the biological receptor may be made more exclusive thus reducing interference, and new receptors can be developed with improved or new affinities. The use of mediators as a strategy to improve performance in amperometric biosensors has proved extremely popular. A recent publication [29] describes the use of pyrroloquinoline quinone as a "natural" mediator, but used with glucose oxidase in an enzyme electrode for the measurement of sugar in drinks. Alternatively, electrocatalytic detection of the products of enzymatic reactions may be enhanced by the use of chemically modified electrodes such as

rhodinised [30] or hexacyanoferrate-modified [31] carbon. The latter method results in a Prussian Blue coating on the electrode which may then be used for amperometric detection of hydrogen peroxide at both oxidative and reductive potentials in enzyme electrodes for lactate [32] and glucose [30]. Arguably a more elegant solution is to seek connection of the redox centre of an enzyme to an electrode via a molecular wire. Much has been published about so called "wired" enzymes, but these papers have generally been concerned with immobilized mediators on various polymer backbones.

1.4 GENERATIONS OF BIOSENSORS

Biosensors have been divided into three generations. In the first generation biosensor, the normal product of the reaction diffuses to the transducer and causes the electrical response, as shown in figure 1.3.

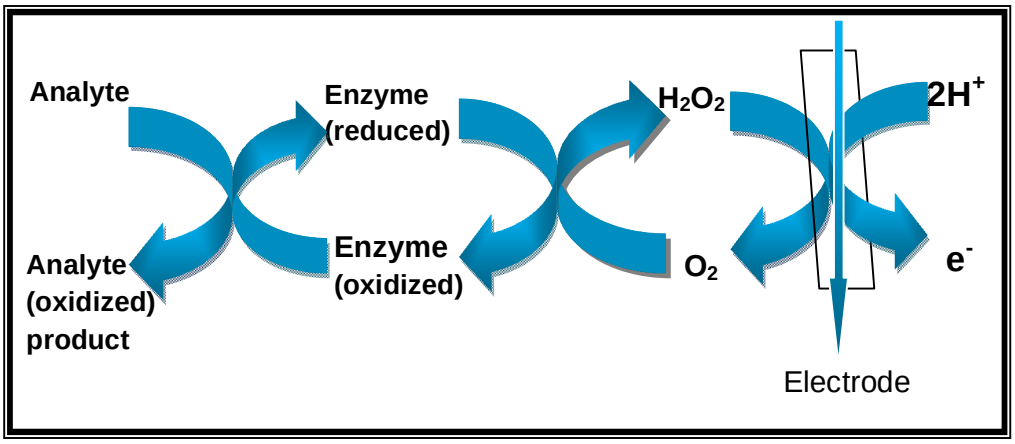

Fig.1.3: Schematic representation of first generation biosensor

The first-generation biosensors were proposed by Clark and Lyons and implemented by Updike and Hicks, who coined the term enzyme electrode [33, 34]. Typically, an oxidase enzyme, i.e., glucose oxidase (GOx), is immobilized behind a dialysis membrane at the surface of a platinum electrode. The enzyme's function is to selectively oxidize analyte by the reduction of O_2 to H_2O_2; i.e., GOx selectively catalyzes the following two reactions:

Glucose + GOx-FAD $\longleftrightarrow$ Gluconolactone + GOx-$FADH_2$

GOx-$FADH_2$ $\longleftrightarrow$ GOx-FAD + H_2O_2

GOx-FAD and GOx-$FADH_2$ represent the oxidized and reduced states of the glucose oxidase enzyme's flavin active site. The consumption of O_2, or, as first described by Guilbault and Lubrano, the formation of H_2O_2, is subsequently measured at a platinum electrode [35]. In the 1970s, Yellow Springs Instruments (Yellow Springs, OH) was the first company to successfully market an amperometric biosensor, a benchtop glucose analyzer. Most commercial benchtop amperometric biosensors rely on reactions catalyzed by oxidase enzyme and subsequent detection of H_2O_2 on platinum electrodes. A universal problem with this sensor arrangement is the loss in selectivity between the biorecognition event and the amperometric H_2O_2 detection. The highly oxidizing potential (700 mV vs Ag/AgCl) necessary for H_2O_2 oxidation results in substantial interference from the oxidation of other compounds in complex matrices.

Second generation biosensors involve specific 'mediators' between the reaction and the transducer in order to generate improved response. The second generation biosensors involve two steps: first, there is a redox reaction between enzyme and substrate that is reoxidized by the mediator, and in second step eventually the mediator is oxidized by the electrode, as shown in figure 1.4.

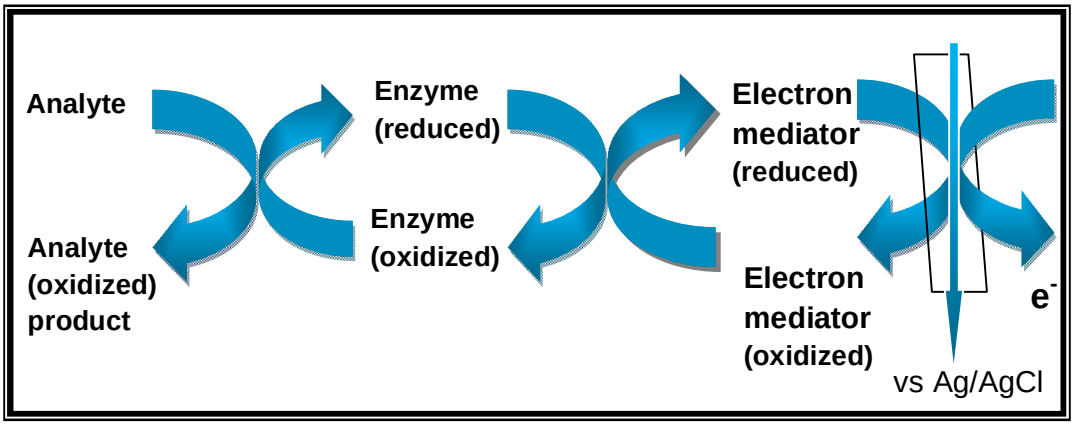

Fig.1.4: Schematic representation of second generation biosensor

Second-generation biosensors use an artificial electron mediator, which replaces O_2 as the electron shuttle. Ferrocene, quinones, quinoid like dyes, organic conducting salts, and viologens have been used as mediators. Most oxidase enzymes are not selective with respect to oxidizing agent, allowing substitution of a variety of artificial oxidizing agents, as in the following reaction.

$$GOx\text{-}FADH_2 + Mediator_{ox} \longleftrightarrow GOx\text{-}FAD + Mediator_{red}$$

Eliminating the O_2 dependence of the first-generation method facilitated control of the enzymatic reaction and sensor performance. Specifically, the selection of mediators with appropriate redox potentials allows poising of the working electrode in a potential range where other components in the sample matrix are not oxidized or reduced. Low O_2 solubility in aqueous solutions and the difficulty associated with controlling the O_2 partial pressure were disadvantages of biosensors based on the O_2/H_2O_2 reaction. When a highly soluble artificial mediator is used, the enzyme turnover rate is not limited by the co substrate (O_2) concentration. Use of mediators other than O_2 allows exploitation of other oxidoreductase enzymes, including peroxidases and dehydrogenases. Unlike oxidases, these enzymes cannot use O_2 as an electron-accepting cosubstrate. Second-generation biosensors have been commercialized, mostly in single-use testing format. MediSense (Waltham, MA, USA) was the first company to launch a second-generation product. Again, the application was blood glucose monitoring, but this device was for home use. The mediation was provided by a ferrocene species. Other second-generation amperometric biosensors have subsequently come onto the market.

Third-generation sensors are marked by the progression from use of a freely diffusing mediator (O_2 or artificial) to a system where enzyme and mediator are co-immobilized at an electrode surface, making the biorecognition component an integral part of the electrode transducer. Co-immobilization of enzyme and mediator can be accomplished by redox mediator labeling of the enzyme followed by enzyme immobilization, enzyme

immobilization in a redox polymer, or enzyme and mediator immobilization in a conducting polymer. There are even reported cases of direct electrical contact of enzyme to electrode. Whether this is direct electrical connection or mediation by surface functionalities is a matter of debate.

Third-generation biosensors offer all the benefits of second-generation biosensors and some new ones as well. The latter arise from the self-contained nature of the sensor. Since neither mediator nor enzyme must be added, this design facilitates repeated measurements. Sensor use for multiple analyses minimizes cost pressures on sensor design. It also follows that such a sensor could allow for continuous analyte monitoring.

1.5 TYPES OF BIOSENSORS

Based on the type of recognition element (by analyte), the biosensors are divided into the following four categories

- Enzyme electrode (enzymes)
- Immunosensor (proteins, antibodies)
- DNA sensor (DNA)
- Microbial sensor (organelles, microbial cells, plant and animal tissue)

Based on the detection method, the biosensors are divided into the following:

1.5.1 Electrochemical Biosensors

Electrochemical biosensors have emerged as the most commonly used biosensors as they have been found to overcome most of the disadvantages, which inhibit the use of other types of biosensors. They are rapid, easy to handle, simple and are of low cost. The basic fact behind this bio-interaction process is that the electrochemical species such as electrons are consumed or generated producing an electrochemical signal, which can be measured by the detector. These biosensors are usually based on potentiometry and amperometry.

1.5.1.1 Potentiometric Biosensors

Potentiometric biosensors are the most important subgroup of electrochemical biosensors. They measure the voltage produced during the oxidation or reduction of a product or reactant, usually at a constant current. These transducers measure potentials under zero-current conditions according to the Nernst equation [36].

$$E = E^{0} + nFRT\ln a_i \qquad \text{(i)}$$

Reactions involving the release or absorption of ions that may be utilized by potentiometric biosensors are,

(a) H^+ cation,

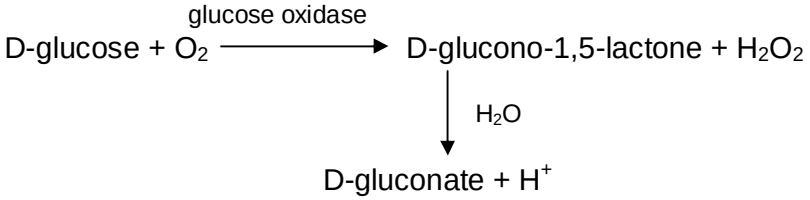

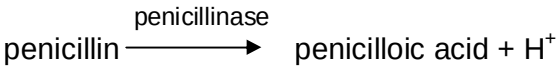

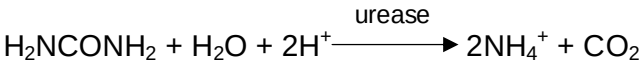

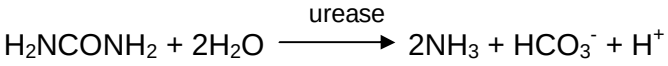

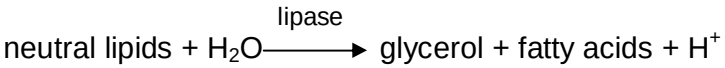

(b) NH_4^+ cation,

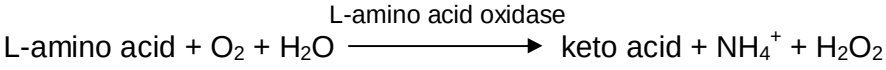

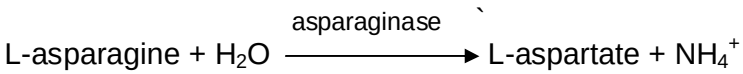

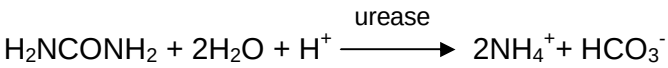

(c) I^- anion,

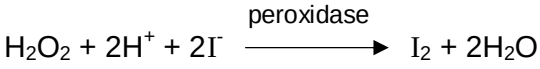

(d) CN^-anion,

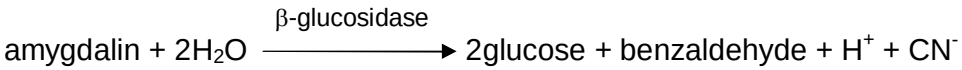

This type of measurement technique is very attractive for practical applications as it allows the use of small size, portable and low cost

instruments. These devices operate under equilibrium conditions and measure the accumulation of charge density at the electrode surface brought about by some selective process. It addresses to the need for application of potentiometry for the determination of simple ions especially for pH and physiological electrolytes. Also, it focuses on emerging trends in the development of integrated multi-sensor and biosensor arrays.

A potentiometric biosensor can be made of enzyme electrode in which an immobilized enzyme is coated over a conventional ion-sensitive electrode (ISE). In ISE, a potentiometric device, the ions in solution are quantified by observing changes in electrode potential. These devices, i.e., ISEs have been successfully developed for monitoring Na^{+}, K^{+}, Ca^{2+}, Li^{+}, NH^{4+}, also a variety of anions, drugs and other materials. These are able to measure the specific substrate or product produced or consumed at the electrode surface. Enzymes in conjunction with potentiometric biosensors offer advantages in terms of cost, speed, accuracy, convenience and non-dependence on sample turbidity or optical properties if compared to other methods.

Various biosensors based on potentiometric analysis using different matrices have been developed for the detection of glucose [37, 38], urea [39, 40], lactate [41] etc. A composite film consisting of electro polymerized electro inactive PPy with the polyion complex containing urease was used to fabricate a high-sensitivity urea sensor. This sensor showed potential response to urea within 20 sec by detecting pH change during enzymatic reaction with a pH-sensitive electro-inactive PPy [42]. Similarly, a potentiometric urea biosensor containing urease was fabricated by combining the pH response of the electro

inactive PPy with the pH changes associated with the enzymatic reaction of urease. Urease was immobilized in an inactive PPy by electro-polymerization from aqueous solution of pyrrole, $NaHCO_3$ and urease [43]. A cholinesterase potentiometric biosensor based on a glassy electrode modified with processible polyaniline (PANI) has been developed and explored for the detection of organophosphorous and carbamic pesticides by Ivanov et al [44]. Acetyl and butyryl-cholinesterase from various sources were immobilized on the surface of PANI modified electrode by cross linking with gluteraldehyde. The detection limits of the pesticides investigated were found lower than those obtained with other similar cholinesterase.

1.5.1.2 Amperometric biosensors

Amperometric biosensor measures the current produced during the oxidation or reduction of a product or reactant, usually at a constant applied potential. These types of biosensors are considered promising for various analyte determinations because of their effectiveness and simplicity. The application of pH-sensitive amperometric biosensors is widespread now days because of their utilization in turbid media, instrumental sensitivity and amenability to miniaturization. The amperometric biosensors are known to be reliable, cheaper and highly sensitive for the clinical, environmental and industrial purposes.

The simplest amperometric biosensors are based on the Clark oxygen electrode. This consists of a platinum cathode (where oxygen is reduced) and

an Ag/AgCl reference electrode when a potential of −0.6 V vs Ag/AgCl electrode is applied to the Pt electrode, a current proportional to the oxygen concentration is produced.

Ag anode: $4Ag+4Cl^- \longrightarrow 4AgCl+4e^-$

Pt cathode: $O_2+4H^++4e^- \longrightarrow 2H_2O$

In this case the rate of electrochemical reduction of O_2 depends on the rate of diffusion of the oxygen from the bulk solution, which in turn is dependent on the concentration gradient and hence the bulk oxygen concentration. Alternatively, the rate of production of H_2O_2 directly, by applying a potential of 0.68 V versus Ag/AgCl to the Pt electrode.

Pt anode: $H_2O_2 \longrightarrow O_2+2H^++2e^-$

Ag cathode: $2AgCl+2e^- \longrightarrow 2Ag+2Cl^-$

An amperometric biosensor has been developed for the estimation of galactose, lactose and glucose by immobilizing galactose oxidase, β-galactoside and glucose with poly (3-hexyl thiphene)/stearic acid on indium tin-oxide (ITO) glass plate by using Langmuir-blodgett technique [45]. An amperometric biosensor for the quantitative determination of urea in aqueous solution based on the use of pH-sensitive redox active dissolved hematein molecule is described [46]. Urease was immobilized, covalently; over a conducting copolymer poly (*N*-3-aminopropylpyrrole-co-pyrrole) film which was electrochemically prepared onto an ITO-coated glass plate. An anodically polarized platinum electrode modified with PPy as the working electrode for the amperometric detection of ammonia was employed as the internal detector in amperometric biosensor for urea and creatinine by immobilization

in a different way at the PPy surface of urease and creatinine iminohydrolase respectively [47].

An amperometric glucose biosensor based on immobilization of glucose oxidase in a composite film of poly (o-aminophenol) and carbon nanotube (CNT), which are electrochemically copolymerized at a gold electrode, was also developed. The biosensor has a detection limit of 0.01–10mM with a good stability and reproducibility [48]. Metheby et al. developed an amperometric biosensor by *in situ* deposition of horseradish peroxide (HRP) enzyme on PANI doped Pt disk electrode. HRP was electrostatically immobilized onto the surface of the PANI film and voltammetry was used to monitor the electro catalytic reduction of H_2O_2 under diffusion controlled conditions. The linear range of this biosensor was from 2.5×10^{-4} to 5×10^{-3} M [49]. Earlier, Nakabayashi et al. had reported an amperometric biosensor for sensing H_2O_2 based on electron transfer between HRP and ferrocene as a mediator [50]. Similarly, a novel H_2O_2 sensor based on peroxide carrying poly {pyrrole-co-[4-(3-pyrrolyl) butanesulfonate]} copolymer was developed by Thanachasai et al. [51].

1.5.1.3 Conductometric biosensor

Conductometric biosensor measures the changes in the conductance of the biological component arising between a pair of metal electrodes. These types of biosensors do not require any reference electrode and exhibit no light sensitivity. Their driving voltage can be sufficiently small to minimize

substantially the sensor's power consumption and to reduce safety problems when they are used *in vivo*. As bioreactions involve charge production or consumption, which leads to an ionic composition modification of the bio-membranes, conductometric electrodes were used to realize enzymatic sensors sensitive to urea, glucose, amino acids, pesticides etc. These types of biosensors are however not efficient when used for measuring samples having high ionic strength. Also, the response is highly dependent on buffer capacity of sample and exhibit narrow dynamic ranges and low sensitivity. The use of additional perm selective membranes on top of enzymatic membrane could substantially reduce the dependence of sensor response on buffer concentration and significantly extends its dynamic range. Many biosensors have been prepared for the estimation of glucose, urea, lipase, hemoglobin etc by monitoring the change in the electronic conductivity arising as a change in redox potential and/or pH of the microenvironment in the polymer matrix. A conductometric biosensor was prepared from electroconductive polyaniline-poly(*n*-butyl methacrylate) (PANI-PBMA) homogeneous composite films by casting [52]. The sensor offered precision, however the detection limits had a small range 3–20 mM. Homogeneous films of PANI-PBMA composite having poly(vinylmethyl ether) as dispersant was used to detect H_2O_2, NH_3 , urea and uric acid.

1.5.2 Optical biosensors

Optical biosensors are based on the measurement of light absorbed or emitted as consequence of a biochemical reaction. In such type of biosensors, light waves are guided by means of optical fibers to suitable detectors. The added advantage that optical transducers have over other methods is the use of visible radiation allowing versatile detection in many different areas. In particular, the development of fibre optic sensing has significantly enhanced optical sensing and increased the diversity of optical analytical devices, due to adaptation of such systems to miniaturisation. Optical sensing usually takes the form of total internal reflection, so that light propagates through the fibre. Fibre optical waveguides have typically been used in biosensors to carry light between the optical instrument and the biological element, which can often be immobilised on the distal end of the fibre. This improves the sensitivity and speed of immunoassays. These types of biosensors have been used for the detection of pH, O_2 and CO_2 etc.

Enzymatic hydrolysis of urea results in an increase in the pH of the medium, thus causing the colour change of the pH probe. Most of the urea optical biosensors developed use a pH/NH_3 optical transducer for determination of urea. The use of simple fibre optic technology to device reflective, transmission or fluorescence-based biosensors by immobilization of reactive chemicals at the termination of small fibre optic probes has been described. pH sensitive polymer PPy/prussian blue transparent film can be used for spectrophotometric measurement of urea [53, 54].

1.5.3 Thermal & Piezoelectric biosensors

The basic concept of heat change, through absorption, which occurs during reactions, is exploited in thermal transducers. The total heat produced or consumed in a reaction is proportional to the molar enthalpy and the number of moles produced; these temperature changes are reflected in the reaction medium. Temperature changes are recorded sensitively using thermistors.

Piezoelectric biosensors operate on the principle of generation of electric dipoles on subjecting an anisotropic natural crystal to mechanical stress. Due to the adsorption of an analyte, the mass of the crystal is increased resulting in altered frequency of oscillation. Such type of biosensors has been utilized for the measurement of ammonia, hydrogen, methane, carbon monoxide, nitrous oxide and other organophosphorous compounds.

1.6 BIOCOMPATIBLE MATERIALS FOR ENZYME IMMOBILIZATION

The immobilization of the enzymes on the electrode surface is considered as one of the critical steps that dictates the effectiveness of the enzyme electrode. For construction of these enzyme electrodes, polymeric materials (like nafion, chitosan, polypyrrole, polyaniline, polythiophene, polyvinyl alcohol, polycarbonate etc.) nanomaterials (metal nanoparticles, carbon nanotubes, nanowires etc.), sol-gel materials and composites have been widely used for the construction of enzyme electrodes for biosensing

applications. In order to prevent enzyme leaching and thus loss of activity, enzyme must be immobilized in a suitable matrix. Hence, the role of matrix is supreme for the overall functioning of biosensors. Much like the diversity of biosensors, the matrices used for immobilization too show a lot of variety.

1.6.1 Conducting Polymers

Since the chemical and physical properties of polymers may be tailored by the chemist for particular needs, they gained importance in the construction of sensor devices. A new class of polymers known as intrinsically conducting polymer or electro active conjugated polymers has recently emerged. Conducting polymers (CPs) show unusual electrochemical properties like high electrical conductivity, low ionization potential, high electronic affinities, and optical properties. These properties are only because of conjugated π-electron backbones in CPs. There must be high degree of overlapping of the polymer molecular orbital, which permits the formation of a delocalized molecular wave function and partial occupation of the molecular orbital if there is to be free movement of electrons through out the lattice [55]. CPs exhibit intrinsic electronic conductivity ranging from about 10^{-14} to 10^{2} S cm^{-1} due to extension of the doped state [56]. In the neutral (undoped) state these materials are only semi-conducting and electronic conductivity only appears when the material is doped with small sized ions (when electrons or holes are injected into the super orbital). This kind of doping is normally produced by chemical or electrochemical oxidation of the monomer, in which the polymer

chains acquire positive charges and the electro neutrality of the resulting material is preserved by the incorporation of small counter ions from the electrolyte solution. Some of the conducting polymers that have been used for fabrication of biosensors are given in figure 1.5.

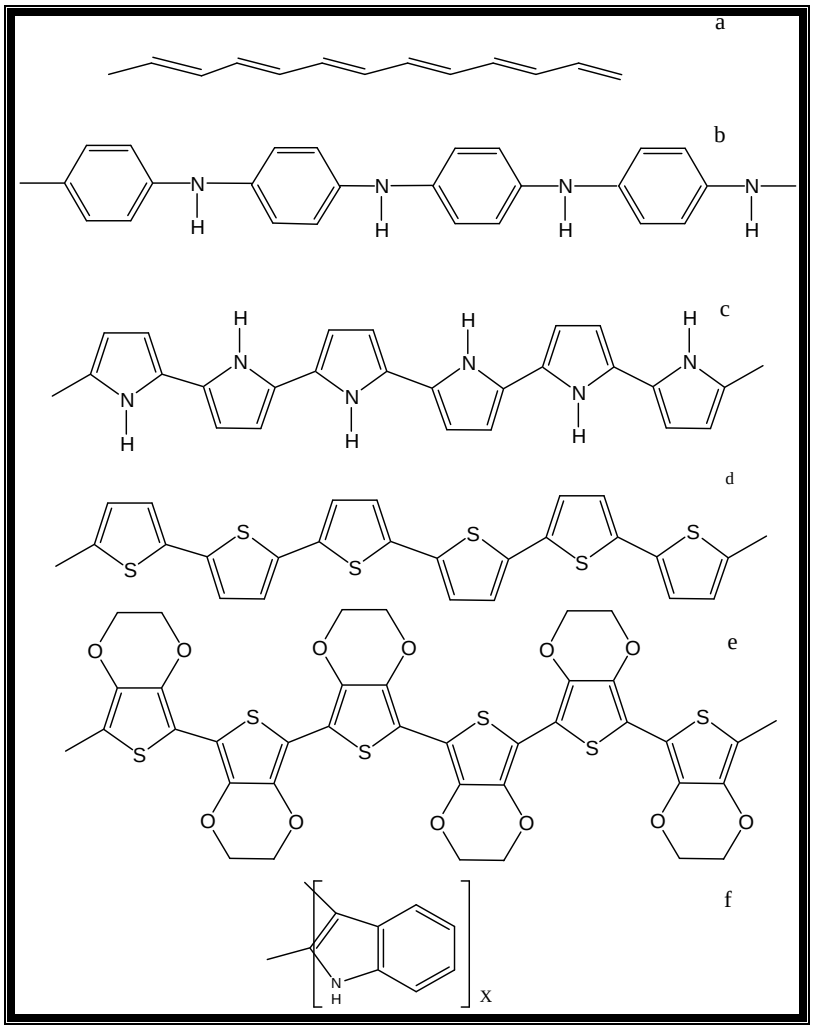

Fig. 1.5: Commonly used conducting polymers in the fabrication of biosensors: (a) polyacetylene, (b) polyaniline, (c) polypyrrole, (d) polythiophene, (e) poly(3,4-ethylenedioxythiophene) and (f) poly(indole).

The major challenge when using CPs in the design of biosensor with electrochemical transducer is to understand the mechanism of the electron transfer in configuration that usually runs parallel to the charging of a double layer at the electrode surface and the mass transport processes at the polymer interface [57]. CPs have an organized molecular structure on metal substrates, which permit them to function as a three dimensional matrix for the immobilization of active catalyst and preserve the activity for long duration. This property of CPs together with their functionality as a membrane has provided opportunities to investigate the development of sensors [58, 59]. CPs serve as the immobilizing matrices for biomolecules and provides a suitable environment for their immobilization. The redox properties of these materials especially PPy, have been intensively studied in recent years, with much emphasis on their synthesis and characterization. PPy is presently considered as the most promising among CPs for the development of advanced sensor devices due to its relative stability, ease of preparation, and good conductivity [60, 61].

These types of polymers are usually prepared by electrochemical polymerization which is normally carried out in a single or dual compartment cell by adopting a standard three-electrode configuration in a typical electrochemical bath consisting of a monomer and a supporting electrolyte both dissolved in an appropriate solvent. Generally, electrochemical polymerization can be carried out either potentiostatically (to obtain thin films) or galvanostatically (to obtain thick films) [62]. A standard three-electrode system used comprises of a working electrode, a counter electrode and a

reference electrode. The function of working electrode is to support the polymer film. Metals like gold, platinum, titanium, nickel, palladium, and carbon are used. Glass coated with tin oxide or indium tin oxide can also be employed. Counter electrode supplies current required by the working electrode. Metallic foil of platinum, gold, nickel is generally used as counter electrode. Common reference electrodes for aqueous system are saturated calomel electrode (SCE), normal calomel electrode (NCE), silver electrode and mercurous sulfate. Those compounds, which possess relatively low anodic oxidation potential and are susceptible to electrophilic substitution reaction, can give CPs by electrochemical techniques. Mechanism of electro polymerization of CP can be best explained by using PPy as an example [63, 64]. The electrochemical polymerization of PPy is illustrated in figure 1.6.

The first step involves the formation of pyrrole radical cation by electrode surface. It is followed by dimerization by deprotonation. The dimer oxidizes slightly more easily than the monomer and thus gets reoxidized to allow further coupling reaction to proceed. The oxidation potential of the polymer is always lower than that of monomer. The polymer is electrochemically ionized to a conducting state and the overall electrical neutrality is maintained by incorporation of the counter ion from the supporting electrolyte. This is essential because precipitation of the unoxidized, insulating polymer would stop the reaction. During the process of electrochemical polymerization negatively charged molecules are present in the electrolytic solution such as anions. Polymers and enzymes can be embedded into the positively charged backbone as dopants [65, 66]. This promotes an attractive

route to trap functional molecules within organic polymers during their electro generation of electrode, and offers a new means to fabricate a range of novel composite material with novel properties.

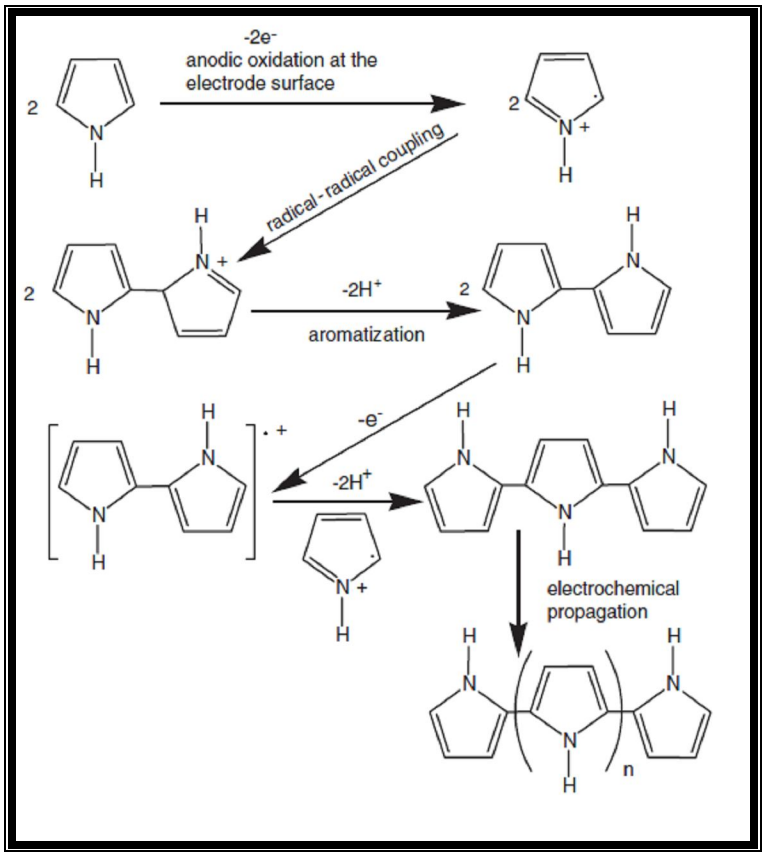

Fig.1.6: Mechanism of electrochemical polymerization of PPy

In electrochemical polymerization, doping and processing takes place simultaneously. Also uniform doping is accomplished. It is also possible to produce freestanding films, homogenous and coherent films even at room temperature. Yasuzawa et al. discussed the properties of glucose sensors

based on the immobilization of GOx in *N*-substituted PPy film [67]. Sensors were prepared by electro polymerization of 3-(1-pyrrolyl) propionic acid in the presence of the enzyme following the treatment with water soluble carbodiimide to provide covalent bonding between GOx and PPy derivatives. The treatment with water-soluble carbodiimide improves the response stability of the enzyme immobilized electrodes.

1.6.2 Sol-gel materials

Sol–gel materials provide a versatile way for bio-immobilization due to the presence of inorganic M–O–M or M–OH–M bridges forming a continuous network containing a liquid phase which can then be dried out to form a solid, porous polymeric matrix. In biosensors, this technique could result in the development of novel strategies to generate advanced materials for the immobilization of biological receptors within silica, metal oxide, organosiloxane, and hybrid sol–gel polymers [68, 69]. An extensive review of sol-gel materials and their uses for construction of enzyme electrodes was reported by Wang [70]. This class of sol–gel matrices possesses chemical inertness, physical rigidity, negligible swelling in aqueous solution, tunable porosity, high photochemical and thermal stability and are thus suitable for the construction of biosensor. Although, the problems of diffusional limitations through the porous network, poor reproducibility, and control of pore size require further optimization for biosensor purposes [71].

Sol–gel technology provides unique means to prepare three-dimensional networks suited for the encapsulation of biomolecules. Sol–gel hybrid materials prepared by physically encapsulating gold nanoparticles into porous sol–gel networks have been used for the fabrication of biosensors. An example is the construction of an acetylcholinesterase biosensor in which the sol–gel-derived silicate network assembling gold nanoparticles provided a biocompatible microenvironment that stabilized the enzyme bioactivity and prevented its leaking out from the interface. Typical pesticides such as monocrotophos, methyl parathion and carbaryl were determined with high sensitivity, accuracy, low cost and simplified procedures [72].

Braun et al. reported the first attempt to encapsulate proteins inside SiO_2 glasses in 1990 [73]. Since then, these new kinds of inorganic materials are particularly attractive to the development of electrochemical biosensor. The enzymes and proteins can be immobilized within sol–gel matrices whilst maintaining their native properties, which make a potential tool for the development of biosensors. The pore size in sol–gel can be controlled into an appropriate size for the diffusion of the analyte to the redox active sites, at the same time preventing enzyme leakage. This property is suitable for the development of new biosensors. Unfortunately, it has also been observed that some gels lose their activities after the first few cycles, primarily ascribed to leaching of enzymes from the sol–gel matrix [74].

1.6.3 Composites

Mixtures of materials can be homogenous or heterogeneous. In the case of polymers, the homogenous mixtures are classified by plastic technologists as blends and heterogeneous mixtures as composites. The basic principle underlying the development of the technology of composites is that the combination of two dissimilar materials results in a product with properties different from those of the starting materials. For example, combination of an organic polymer with an inorganic material, the property of polymer, i.e., flexibility, toughness, and processibility with the property of inorganic material like hardness, good chemical stability, better barrier properties and also brittleness results in a composite having both these properties. Depending on the type of filler for sensing applications they are divided as (i) metal oxide-metal oxide based composites, (ii) polymer based composites, (iii) carbon based composites, and (iv) noble-metal based composites.

Metal oxide-metal oxide composites are based on metal oxide matrix in which the filler is also metal oxide particles or wires etc. Metal oxides are important semiconductors which can be used as sensing material in sensors because of the advantages offered by wide band gap semiconductor oxides which include their stability in air, relative inexpensiveness, and easy preparation in the ultra dispersed state. Since porous metal oxides have attractive properties like simplicity of preparation, tunable porosity, good chemical stability, low temperature encapsulation, negligible swelling, mechanical and biodegradable stability, high sensitivity at lower operating

temperature for detection of reducing and oxidizing gases, they have been used for the fabrication of biosensors. It was found that sensors designed on the basis of metal oxide nanocomposites have good chemical stability and high selectivity to specific target gases.

Polymer based composite materials have also attracted the interest of a number of researchers, due to their synergistic and hybrid properties derived from several components. A simple representation for the formation of composites is given in figure 1.7. Ease of processability of an organic polymer combined with the improved mechanical and optical properties of some other particles has led to the fabrication of many devices.

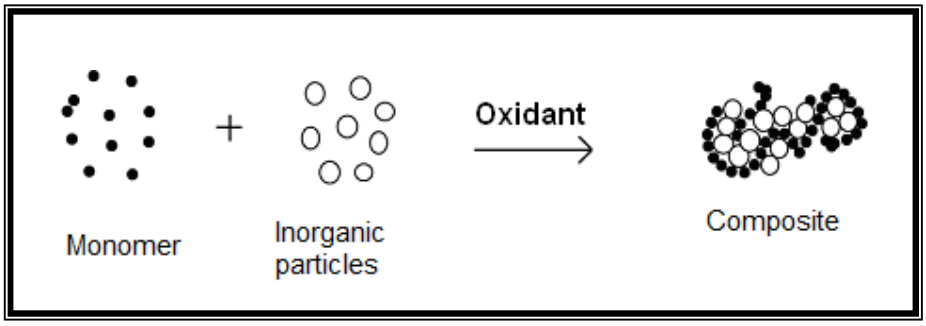

Fig. 1.7: Formation of composites

A large number of methods for synthesis and fabrication of polymer based composites have been demonstrated, of which a simple and effective approach is to introduce nanoparticles/nanotubes or biomolecules into polymer matrices, or simply to mix them with the polymer matrices [75]. Polymers with nanostructures can also be prepared by template method and non-template approach. Inorganic aluminum oxide, zeolite with channels and

polymer membranes with porosity have been commonly used as templates where as in non template approach, either the polymerization takes place at interface or surfactant, and polyelectrolytes are added for structural direction. Nanocomposites of poly(o-anisidine) containing TiO_2 nanoparticles, carbon black and multiwalled carbon nanotubes (MWCNT) were prepared by Carrora et al [76]. The synthesized materials were deposited in thin films and analysis of such films demonstrated that materials based on polymeric nanocomposites are best suited for biosensor applications because they provide the best electron transfer and assure the faster ion mass transfer.

CNTs based composites have attracted a lot of attention of researchers for their applications in sensors. The extended surface area provides greater substrate binding sites for sensing molecule attachment. Moreover, they are hollow tubes with high aspect ratio and propagate a signal fast. They serve as ideal substrates after being functionalized to form bonds with sensing molecules. Since their composition is uniform, they tend to give specificity to the overall sensing property.

Due to the large aspect ratio, i.e., size to volume ratio and submicron size, and unique properties, nanosensors, nanoprobes and other nanosystems designed on the base of such nanomaterials are revolutionizing the fields of chemical and biological analysis. Despite the variety of approaches to synthesize different nanostructures, the need for a method capable of making pure, uniform, template free nanostructures arises. This is a fabrication strategy, which requires only the mixing of components to achieve an ordered structure and is appealing both for its simplicity and its

potential efficiency. Template free method of synthesizing nanostructures has several advantages like simple synthesis, purification with no template removing steps needed. Also, uniform nanofibres are formed, which are easily scalable and reproducible. They show superior performance as sensors because the diameter of nanomaterials is at nanoscale and are water dispersible which facilitates environmental friendly processing and biological application.

A wide range of nanostructured materials have been reported for efficient immobilization of enzymes for application in biosensors. A novel sensitive electrochemical biosensor based on magnetite nanoparticles for monitoring DNA hybridization was prepared by using MWNT-COOH/PPy-modified glassy carbon electrode. The range of the biosensor was found to be $6.9 \cdot 10^{-14}$ to $8.6 \cdot 10^{-13}$ mol/L and the detection limit is 2.3×10^{-14} mol/L [77].The 3-D structure of CNTs provides a good template for a large enzyme loading in an ultra thin polymer layer, leading to a glucose response of 10-20 times higher than that from a corresponding flat electrode. Kong et al. developed a hydroquinone sensor based on the synergistic effect of MWCNT and conducting poly (N-acetylaniline) polymer and the accumulation effect of β-cyclodextrin, with a sensitive detection, stability and reproducibility of the electrode [78]. Tu et al. studied the over oxidation of PPy-MWCNT composite film in neutral and alkaline solutions by electrochemical quartz crystal impedance and used this PPy/CNT/NaOH/Au electrode for sensing dopamine with a limit of detection down to 1.7 nmol L^{-1} [79].

The use of nanomaterials for the construction of biosensing devices constitutes one of the most exciting approaches. The extremely promising prospects of these devices accrue from the unique properties of nanomaterials [80]. The ability of noble metals especially gold nanoparticles provides a stable immobilization of biomolecules. Retaining their bioactivity is a major advantage for the preparation of biosensors. Furthermore, gold nanoparticles permit direct electron transfer between redox proteins and bulk electrode materials, thus allowing electrochemical sensing to be performed with no need for electron transfer mediators. Characteristics of gold nanoparticles such as high surface-to-volume ratio, high surface energy, ability to decrease proteins–metal particles distance, and the functioning as electron-conducting pathways between prosthetic groups and the electrode surface, have been claimed as reasons to facilitate electron transfer between redox proteins and electrode surfaces [81, 82]. Gold nanoparticles also constitute useful interfaces for the electrocatalysis of redox processes of molecules such as H_2O_2, O_2 or NADH involved in many significant biochemical reactions [83]. Modification of electrode surfaces with self-assembled monolayers (SAMs) of thiols provides a simple way to design tailored materials that can be further used as functionalized sites to immobilize gold nanoparticles and enzymes [84].

1.6.4 Self assembled biocompatible materials

Self-assembled monolayer (SAM) is a layer of molecular thickness formed by self-organization of molecules in an ordered manner by chemisorption on a solid surface. SAM is the most elementary form of nanometer-scale organic thin-film material. SAM comprises of three significant parts: a surface-active head group that binds strongly to a substrate, an alkyl chain giving stability to the assembly by Van der Waals interactions and functionality that plays an important role in terms of coupling of a biomolecule to a monolayer. Through proper selection of terminal functional group, specific surface/solution interactions (covalent, electrostatic or hydrophobic) can be exploited to immobilize molecules at an interface. The use of SAMs in various fields of research is rapidly growing. In particular, biosensors apply SAMs as an interface-layer between a metal surface and a solution or vapor. The most common compounds that are able to undergo the process of SAMs are alkanothiols, dialkyl disulfides or dialkyl sulfides on gold. The use of SAMs in the construction of enzyme electrodes is not widespread to a large variety of enzymes, however, a growing trend is observed. A comprehensive review dealing with the application of alkanethiol self assembled monolayers to enzyme electrodes has been published by Gooding and Hibbert [84].

The advantages of SAMs lie in their integration with a biological recognition element for development of biosensors. For fabrication of a biosensor, immobilization of a biomolecule on a SAM surface is an important concern. SAMs for biosensing applications can be modified by adopting many

strategies like modification via physical adsorption [85], using chemical activators [86], using chemical crosslinkers [87], and using exchange process [88].

SAM can be utilized for efficient self-assembling of gold nanoparticles and biomolecules for fabrication of a biosensor. Such assembling of gold nanoparticles onto SAM increases surface area and hence enzyme loading in near vicinity of a surface resulting in higher sensitivity of the fabricated biosensor. A glucose biosensor has been developed by immobilizing glucose oxidase (GOx) onto preformed SAM on nanoscopic gold tubes [89]. The results indicate that in SAM-modified gold nanotubes based system; sensitivity to glucose can be achieved up to 400 $nAmM^{-1}cm^{-2}$. GOx has been covalently attached with SAM of *N*-hydroxysuccinimide esters of 16-mercaptohexandecanoic acids for (NHS-MHDA) obtaining improved sensitivity, stability, and reproducibility of enzyme-based amperometric microbiosensors [90]. These results have been attributed to the NHS-MHDA layer (enzymatic recognition interface) spacing resulting in minimized quenching of the enzyme activity.

1.7 METHODS OF IMMOBILIZATION

With the advance in the development of biosensors, several problems surfaced relating to functioning of enzyme system like loss of enzyme (especially expensive enzymes), maintenance of enzyme stability and shelf life of the biosensors. In addition to this, there grew a need to reduce the time

of enzymatic response and offer disposable devices, which can easily be used in stationary or in, flow systems [91]. In order to overcome these problems, several immobilization procedures have been developed. The procedure of biomolecule immobilization on conductive surfaces remains a key step for the performance of the resulting electrochemical devices. For efficient deposition of a biomolecule, it must satisfy a few pre-requisites, that;

- There must be an efficient and stable immobilization of the biological macromolecules on transducer surfaces
- It must retain its biological properties completely
- It should be compatible & chemically inert towards host structure
- It should be accessible when immobilized [92]

Immobilized enzyme has many operational advantages over free enzyme such as reusability, enhanced stability, continuous operational mode, rapid termination of reaction, easy separation of biocatalyst from product, and reduced cost of operation [93].

Immobilization of biomolecules can be carried out using many different procedures, like physical adsorption, covalent linking and electro immobilization, while retaining the biological recognition properties of the biomolecules as shown in figure 1.8.

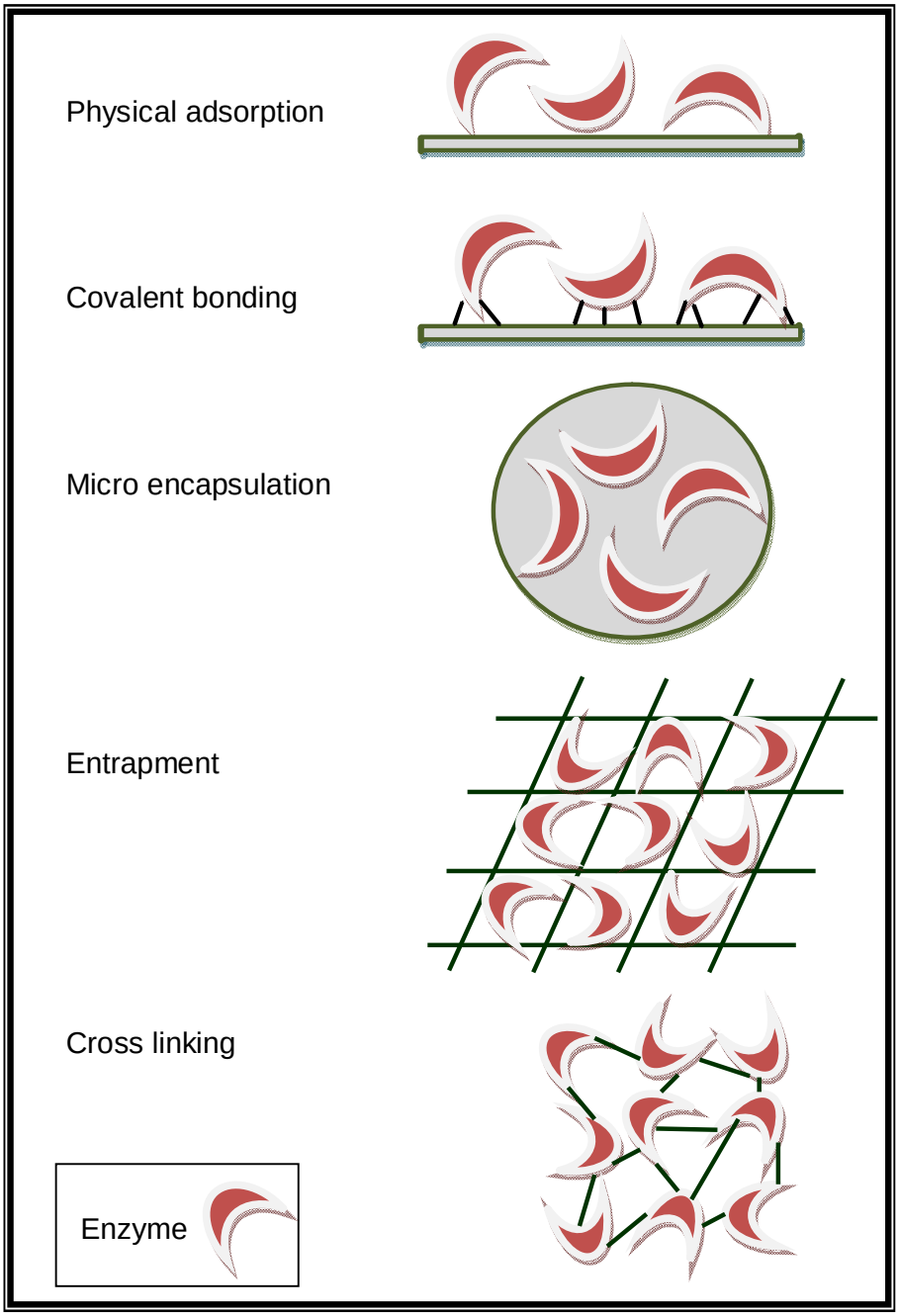

Fig 1.8: Presentation of various methods of enzyme immobilization

1.7.1 Physical Adsorption

In physical adsorption process, the biomolecule gets adsorbed in the polymer/solution interface due to static interactions between the polycationic matrix of the oxidated polymer and the total negative enzyme charge, provided pH is higher than the isoelectric point of the enzyme [95]. But this process has some known disadvantages like binding forces can change with pH, adsorption is limited to one monolayer on the polymer surface hence amount of enzyme incorporated is very small [96]. Also, since biomaterial is immobilized on the outer layer of conducting polymer, it gets leached out into sample solution during measurements. This decreases the lifetime stability of enzyme electrode [97-103].

Immobilization by physical adsorption also involves cross-linking. Cross-linking gives sensors with short response times but poor stability because enzyme is directly exposed to the bulk solution and partly denatured by the cross-linking. Immobilization of acetylcholine esterase (AChE) by cross-linking involving glutaraldehyde significantly increased the attachment of enzyme to the transducer and hence led to a more direct electron exchange. Here AChE was co immobilized with choline oxidase (ChOx) on to a Pt surface using a solution of gluteraldehyde [91]. Immobilization of AChE in nylon net using gluteraldehyde has been reported by Gulla et al. [104]. The method involves immobilization by sandwiching the enzyme layer between two cellophane membranes kept in close contact with a gold electrode. Milagres et al. [105] immobilized salicylate hydroxylase by cross-linking.

Similarly, immobilization of tyrosinase [106] and lactate dehydroganase [107] has also been reported in literature.

1.7.2 Covalent Immobilization

In order to achieve an increased lifetime stability of enzyme electrode, it is necessary that there should be a strong and an efficient bonding between the enzyme and the immobilizing material. Hence, covalent linking of biomolecules on transducer is an efficient method of immobilization. It comes with an advantage of low diffusional resistance and such a sensor shows good stability under adverse conditions.

As depicted in figure 1.9, the carbodiimide-mediated coupling of a carboxylic acid (**I**) with a primary amine first progresses through an unstable intermediate, an O-acylisourea ester (**III**) compound formed by the reaction of the carbodiimide (**II**) with the carboxylic acid (**I**). Because this intermediate is unstable, it is often the case that either NHS (N-hydroxysuccinimide) (**IV**) or sulfo-NHS is added to the carboxylic acid together with the carbodiimide, in order to form an NHS-ester (**V**), which is a much more stable compound that remains reactive with amines. Upon the final addition of an amine (**VI**), the final desired coupling product, an amide (**VII**), is formed by displacement of the NHS.

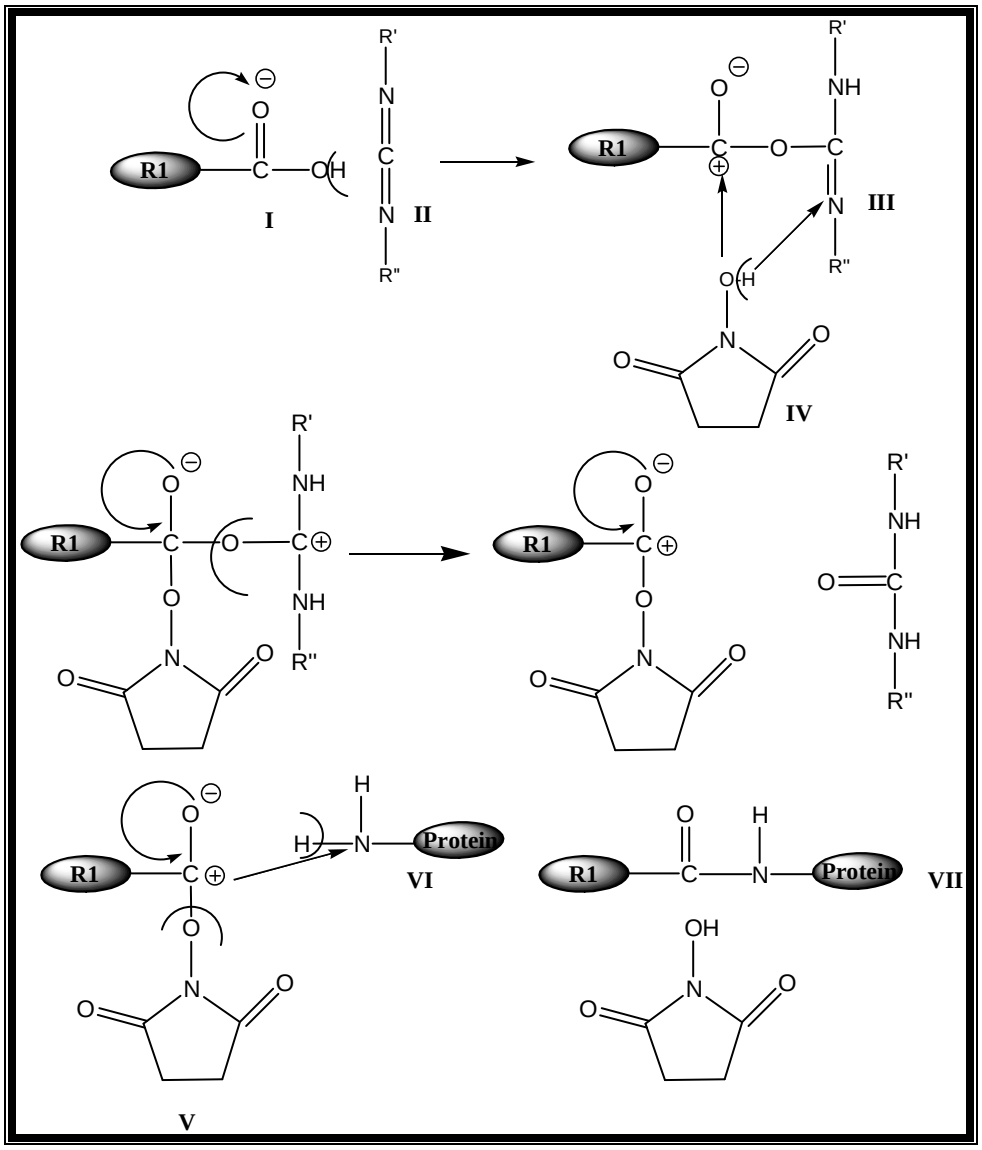

Fig. 1.9: Coupling of a carboxylic acid and a primary amine via O-acylisourea ester and NHS ester intermediates

1.7.3 Electrochemical immobilization

Although, the conventional procedures for deposition of biomolecules on to the transducers like, physical adsorption, covalent linkage, entrapment and cross-linking have been used extensively, they suffer from a low reproducibility and have a poor spatially controlled deposition. In recent years, the focus of immobilization has been shifted towards the entrapment of biomolecules in the layers of electrochemically synthesized polymers. Aizawa and Yabuki had pioneered the application of PPy and PANI to the immobilization of enzymes [108]. Since, then hundreds of papers have been published and patents have been granted on this subject. Serge Cosnier reviewed different electrochemical procedures for biomolecule immobilization based on electro polymerized films and describes the adsorption of amphiphilic monomers and biomolecule before the polymerization step. Examples of organic phase enzyme electrode and electrical wiring of immobilized enzymes are presented. Furthermore, the construction of controlled architectures based on spatially segregated multilayers, exhibiting complimentary biological activities is described [109]. The electrochemical formation of polymer layers of controlled thickness and enzyme activity in galvanostatic or potentiostatic conditions offers numerous advantages over conventional procedures for the design of biosensors, such as complete coverage of the active surface, greater control over film thickness and greater reproducibility. The major advantages of the electrochemical immobilization techniques are: it is a one step, fast than in all immobilization procedures; the

distribution of the immobilized enzyme is spatially controlled irrespective of geometry, shape and dimension of the electrode; the film thickness can be precisely controlled through, e.g. the charge involved in the deposition step and it can be used to build up multiplayer/multienzyme structures; it allows the reproducible and precise formation of a polymer coating over surfaces whatever their size and geometry may be. The fabrication of biosensor by entrapment of biomolecules in electro-polymerized films is the most popular approach. Since, the pioneering work by Umana and Waller [110] and Bartlett et al. [111] numerous papers have been published on this approach [112-114].

Immobilization by enzyme entrapment involves electrochemical oxidation of the monomer in the presence of the enzyme to form a polymer, which incorporates the homogenously distributed enzyme molecules during its growth process. This method is the most straightforward method of immobilization with some inherent advantages like simplicity and reproducibility of the one step preparation procedure and the possibility of immobilizing of mediators, co-enzymes or the other enzymes simultaneously simply by adding them to the polymerization solution as shown in figure 1.10.

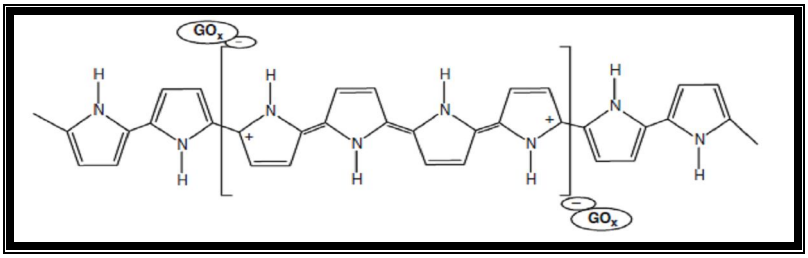

Fig. 1.10: Schematic representation of electrochemical immobilization of enzyme in polypyrrole

The mechanism of incorporation of the enzyme into electro synthesized polymer films has been an object of various speculations. It has been suggested that electrostatic interaction plays the major role in enzyme incorporation and this assumption has been adequately supported by indirect experimental evidence. This is not the case for non-ionic polymer films where pre-adsorption of enzyme onto the electrode surface seems to be the important step in determining the enzyme loading. In this respect, enzyme/polymer interaction is of paramount importance to improve the fundamental knowledge about the biological interface of the biosensor. Incorporation of the enzyme results in changes in the apparent optical properties and density of the polymeric films, suggesting a mutual stabilization of polymer and the enzyme. Griffith et al. have reported the amount of GOx entrapped in conducting and non-conducting electro polymerized film (on gold surface) at different adsorption time and enzyme concentrations in the growing solution [115]. Although, biomolecules are only physically confined near transducer, it has a high diffusion barrier. Entrapment of GOx during the growth of PANI films at low pH due to its high tolerance has been extensively reported [116-123]. Compagnone et al. used thiophene derivative polymers synthesized in organic solvents for entrapment [124], while Gambhir et al. entrapped urease and glutamate dehydrogenase in PPy/polyvinyl sulfonate films for urea detection [102]. This process involves application of an appropriate potential to the working electrode soaked in aqueous solution containing both biomolecule and electro polymerizable monomer. Biomolecules present in the immediate vicinity of the electrode surface are

thus physically incorporated into the growing polymer. This, reagentless electrochemical approach is easily applicable to a wide variety of biological macromolecules. Ramanathan [125] has immobilized GOx on different conducting matrices such as PPy, PANI, polyammino benzoic acid (PAB) and studied the response characteristics, lifetime detail, etc.

Chapter I

(Part B)

Characterization Techniques

1.8 FOURIER TRANSFORM INFRARED (FTIR) SPECTROSCOPY

Infrared spectroscopy (IR) exploits the fact that molecules absorb specific frequencies that are characteristic of their structure. These absorptions are resonant frequencies i.e. the frequency of the absorbed radiation matches the frequency of the bond or group that vibrates. The energies are determined by the shape of the molecular potential energy surfaces, the masses of the atoms, and the associated vibronic coupling.

In particular, in the Born–Oppenheimer and harmonic approximations, i.e. when the molecular Hamiltonian corresponding to the electronic ground state is approximated by a harmonic oscillator in the neighborhood of the equilibrium molecular geometry, the resonant frequencies are determined by the normal modes corresponding to the molecular electronic ground state potential energy surface. The resonant frequencies relates to the strength of the bond, and the mass of the atoms at either end of it and thus are associated with a particular bond type.

Fourier Transform Infrared (FTIR) spectroscopy is a technique used to determine qualitative and quantitative features of IR-active molecules in organic or inorganic solid, liquid or gas samples. Infrared light is guided through an interferometer and then through the sample (or vice versa). A moving mirror inside the apparatus alters the distribution of infrared light that passes through the interferometer. The signal directly recorded, called an "interferogram", represents light output as a function of mirror position. A data-processing technique called fourier transform turns this raw data into the

desired result (the sample's spectrum): Light output as a function of infrared wavelength (or equivalently, wavenumber).

In order for a vibrational mode in a molecule to be "IR active," it must be associated with changes in the permanent dipole. A molecule can vibrate in many ways, and each way is called a *vibrational mode.* Linear molecules have 3N–5 degrees of vibrational modes whereas nonlinear molecules have 3N–6 degrees of vibrational modes (also called vibrational degrees of freedom). For example, H_2O is a non-linear molecule and will have 3×3–6 = 3 degrees of vibrational freedom, or modes. Simple diatomic molecules have only one bond and only one vibrational band. If the molecule is symmetrical, e.g. N_2, the band is not observed in the IR spectrum, but only in the Raman spectrum. Unsymmetrical diatomic molecules, e.g. CO, absorb in the IR spectrum. The exact frequency at which a given vibration occurs is determined by the strengths of the bonds involved and the mass of the component atoms. In practice, infrared spectra do not normally display separate absorption signals for each of the 3n-6 fundamental vibrational modes of a molecule. The number of observed absorptions may be increased by additive and subtractive interactions leading to combination tones and overtones of the fundamental vibrations. Furthermore, the number of observed absorptions may be decreased by molecular symmetry, spectrometer limitations, and spectroscopic selection rules. One selection rule that influences the intensity of infrared absorptions is that a change in dipole moment should occur for a vibration to absorb infrared energy. Absorption

bands associated with C=O bond stretching are usually very strong because a large change in the dipole takes place in that mode, as shown in figure 1.11.

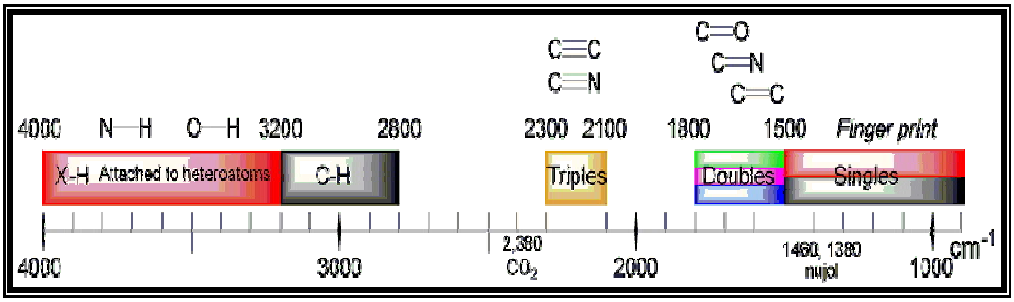

Fig.1.11: Absorption bands corresponding to single, double and triple bond stretchings

The basic components of an FTIR are shown schematically in figure 1.12. Most interferometers employ a beam splitter which takes the incoming infrared beam and divides it into two optical beams. One beam reflects off of a flat mirror which is fixed in place. The other beam reflects off of a flat mirror which is on a mechanism which allows this mirror to move a very short distance (typically a few millimeters) away from the beamsplitter. The two beams reflect off of their respective mirrors and are recombined when they meet back at the beamsplitter. Because the path that one beam travels is a fixed length and the other is constantly changing as its mirror moves, the signal which exits the interferometer is the result of these two beams "interfering" with each other. The resulting signal is called an interferogram which has the unique property that every data point which makes up the signal has information about every infrared frequency which comes from the source. Because there needs to be a relative scale for the absorption intensity, a background spectrum must also be measured. This is normally a

measurement with no sample in the beam. This can be compared to the measurement with the sample in the beam to determine the "percent transmittance." This technique results in a spectrum which has all of the instrumental characteristics removed. Thus, all spectral features which are present are strictly due to the sample. A single background measurement can be used for many sample measurements because this spectrum is characteristic of the instrument itself.

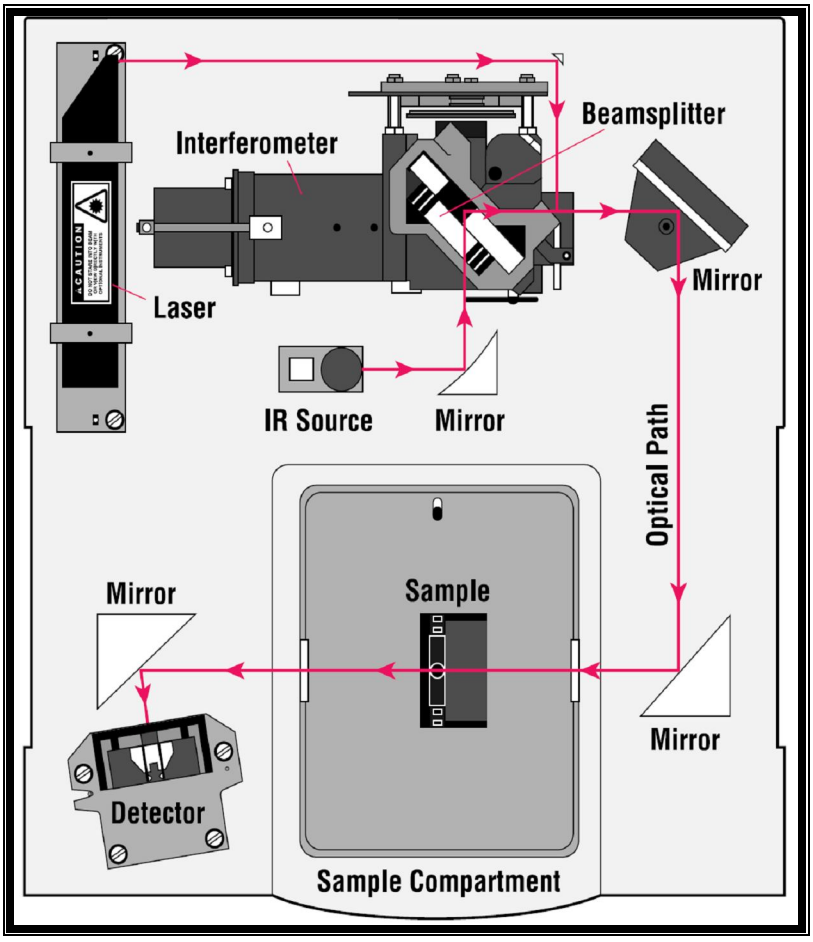

Fig.1.12: A simple layout of an FTIR instrument

1.9 UV VISIBLE SPECTROSCOPY

Ultraviolet/visible spectroscopy is useful as an analytical technique for two reasons. First it can be used to identify some functional groups in molecules and secondly, it can be used for assaying. This second role determining the content and strength of a substance is extremely useful. When light either visible or ultraviolet is absorbed by valence (outer) electrons these electrons are promoted from their normal (ground) states to higher energy (excited) states.

Samples are used in solution and are placed in a small transparent cell known as cuvette. Two lamps are used; a hydrogen or deuterium lamp for the ultraviolet region and a tungsten/halogen lamp for the visible region. In this way radiation across the whole range is scanned by the spectrometer. A reference cell containing only solvent is used. When light is passed simultaneously through the sample cell and reference cell, the spectrometer compares the light and the transmitted radiation is detected and the spectrometer records the absorption spectrum by scanning the wavelength of the light passing through the cells.

For most spectra the solution obeys Beer's Law. This states that the light absorbed is proportional to the number of absorbing molecules, i.e., to the concentration of absorbing molecules. A second law; Lambert's law tells us that the fraction of radiation absorbed is independent of the intensity of the radiation. Combining these two laws gives the Beer–Lambert law:

$A = -log_{10} (I/I_0) = \varepsilon . l . c$ (ii)

I_O = the intensity of the incident light at a given wavelength

I = the intensity of the transmitted light

ε = the molar absorption coefficient

l = the path length of the absorbing solution (cm)

c = the concentration of the absorbing species in mol dm^{-3}

Two useful pieces of information are the molar absorption coefficient, ε and λ_{max} which is the wavelength at which maximum absorption occurs. However, if ε and λ_{max} are known for a compound the concentration of the solution can be calculated.

The energy associated with electromagnetic radiation is defined by the following equation:

$E = h \upsilon$ (iii)

Where E is energy (in joules), h is Planck's constant (6.62×10^{-34} Js), and υ is frequency expressed in sec. Electromagnetic radiation can be considered a combination of alternating electric and magnetic fields that travel through space with a wave motion. Because radiation acts as a wave, it can be classified in terms of either wavelength or frequencies, which are related by the following equation:

$\upsilon = c \ / \ \lambda$ (iv)

where υ is frequency (in seconds), *c* is the speed of light ($3x10^8$ ms^{-1}), and λ is wavelength (in meters). In UV-visible spectroscopy, wavelength usually is expressed in nanometers (1 nm = 10^{-9} m). It follows from the above equations that radiation with shorter wavelength has higher energy. In UV-visible spectroscopy, the low-wavelength UV light has the highest energy. In some cases, this energy is sufficient to cause unwanted photochemical reactions when measuring sample spectra (remember, it is the UV component of light that causes sunburn).

1.10 SCANNING ELECTRON MICROSCOPY (SEM)

SEM is an instrument that produces a largely magnified image by using electrons instead of light to form an image. It utilizes an electron beam that interacts with the surface of the sample and supplies information on the surface morphology of a sample. A beam of electrons is produced at the top of the microscope by an electron gun. The electron beam follows a vertical path through the microscope, which is held within a vacuum. The beam travels through electromagnetic fields and lenses, which focus the beam down toward the sample. Once the beam hits the sample, electrons and X-rays are ejected from the sample. Detectors collect these X-rays, backscattered electrons, and secondary electrons and convert them into a signal to produce the final image.

The secondary electron detectors are common in all SEMs, but it is rare that a single machine would have detectors for all possible signals. The

signals result from interactions of the electron beam with atoms at or near the surface of the sample. Due to the very narrow electron beam, SEM micrographs have a large depth of field yielding a characteristic three-dimensional appearance useful for understanding the surface structure of a sample. A wide range of magnifications is possible, from about 10 times (about equivalent to that of a powerful hand-lens) to more than 500,000 times, about 250 times the magnification limit of the best light microscopes. Back-scattered electrons (BSE) are beam electrons that are reflected from the sample by elastic scattering. BSE are often used in analytical SEM along with the spectra made from the characteristic X-rays. Characteristic X-rays are emitted when the electron beam removes an inner shell electron from the sample, causing a higher energy electron to fill the shell and release energy. These characteristic X-rays are used to identify the composition and measure the abundance of elements in the sample.

In a typical SEM, as shown in figure 1.13, an electron beam is thermionically emitted from an electron gun fitted with a tungsten filament cathode. Tungsten is normally used in thermionic electron guns because it has the highest melting point and lowest vapour pressure of all metals, thereby allowing it to be heated for electron emission, and because of its low cost. The electron beam, which typically has an energy ranging from a few hundred eV to 40 k eV, is focused by one or two condenser lenses to a spot about 0.4 to 5 nm in diameter. The beam passes through pairs of scanning coils or pairs of deflector plates in the electron column, typically in the final lens, which deflect the beam in the *x* and *y* axes so that it scans in a raster

fashion over a rectangular area of the sample surface. When the primary electron beam interacts with the sample, the electrons lose energy by repeated random scattering and absorption within a teardrop-shaped volume of the specimen known as the interaction volume, which extends from less than 100 nm to around 5 µm into the surface. The size of the interaction volume depends on the electron's landing energy, the atomic number of the specimen and the specimen's density. The energy exchange between the electron beam and the sample results in the reflection of high-energy electrons by elastic scattering, emission of secondary electrons by inelastic scattering and the emission of electromagnetic radiation, each of which can be detected by specialized detectors. The beam current absorbed by the specimen is used to create images of the distribution of specimen current. Electronic amplifiers of various types are used to amplify the signals which are displayed as variations in brightness on a cathode ray tube.

For conventional imaging in the SEM, specimens must be electrically conductive, at least at the surface, and electrically grounded to prevent the accumulation of electrostatic charge at the surface. Metal objects require little special preparation for SEM except for cleaning and mounting on a specimen stub. Nonconductive specimens tend to charge when scanned by the electron beam, and especially in secondary electron imaging mode, this causes scanning faults and other image artifacts. They are therefore usually coated with an ultrathin coating of electrically-conducting material, commonly gold, deposited on the sample either by low vacuum sputter coating or by high vacuum evaporation. Conductive materials in current use for specimen

coating include gold, gold/palladium alloy, platinum, osmium, iridium, tungsten, chromium and graphite. Coating prevents the accumulation of static charge on the specimen during electron irradiation. Two reasons for coating, even when there is enough specimen conductivity to prevent charging, are to increase signal and surface resolution, especially with samples of low atomic number (Z). The improvement in resolution arises because backscattering and secondary electron emission near the surface are enhanced and thus an image of the surface is formed.

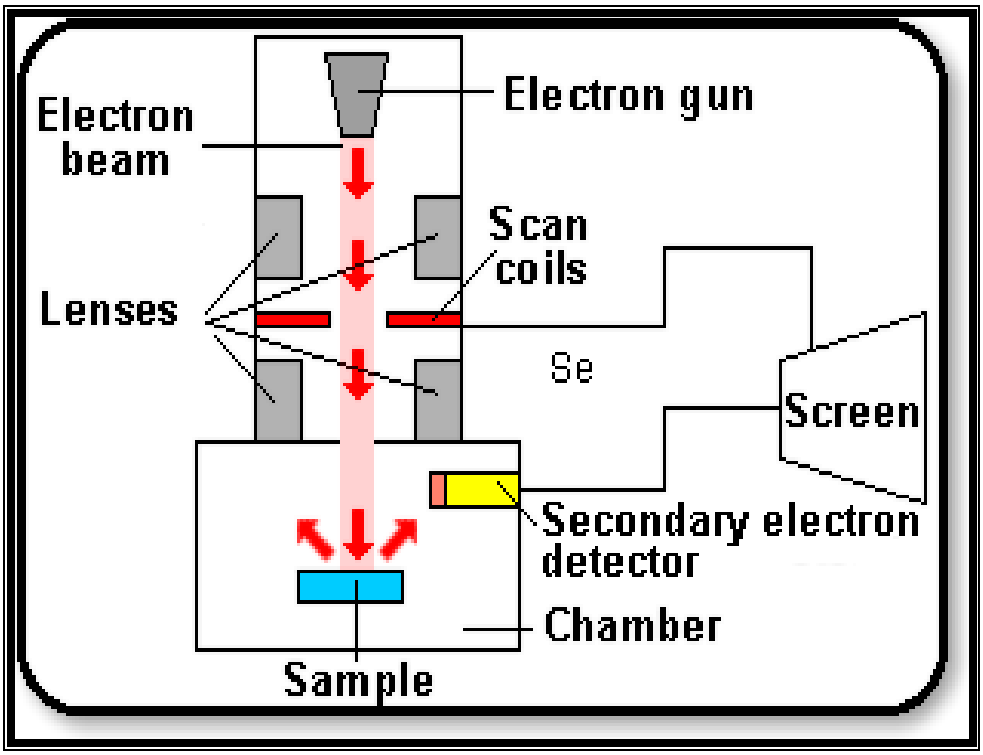

Fig. 1.13: A schematic layout of SEM

1.11 ATOMIC FORCE MICROSCOPY

The atomic force microscope (AFM) relies on the forces between the tip and sample as shown in the figure 1.14. Depending on the situation, forces that are measured in AFM include mechanical contact force, Van der Waals forces, capillary forces, chemical bonding, electrostatic forces, magnetic forces (see magnetic force microscope, MFM), casimir forces, solvation forces, etc. The force is not measured directly, but calculated by measuring the deflection of the lever, and knowing the stiffness of the cantilever. Hook's law gives F = -kz, where F is the force, k is the stiffness of the lever, and z is the distance the lever is bent.

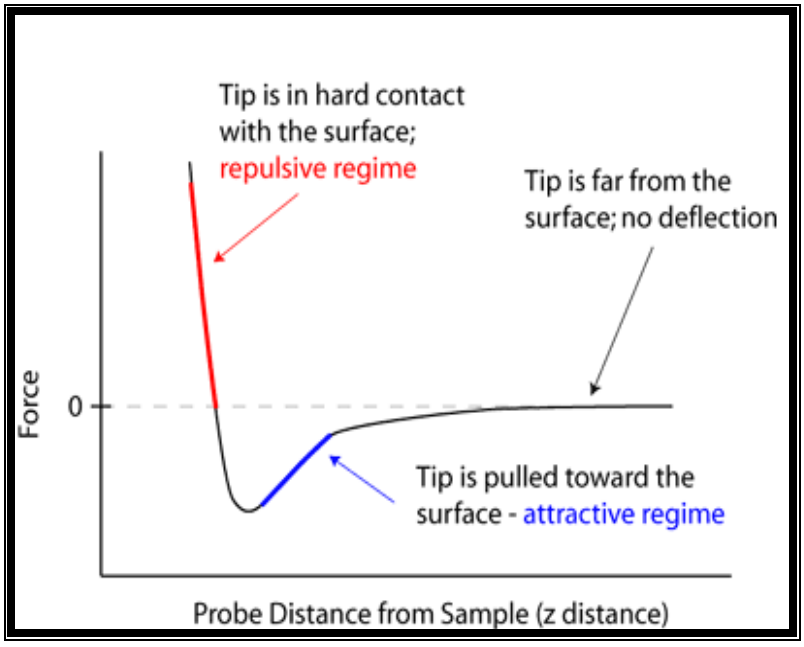

Fig. 1.14: Forces generated between the tip and sample surface

The AFM consists of a cantilever with a sharp tip (probe) at its end that is used to scan the specimen surface. The cantilever is typically silicon or silicon nitride with a tip radius of curvature on the order of nanometers. Typically, the deflection is measured using a laser spot reflected from the top surface of the cantilever into an array of photodiodes, as shown in figure 1.15. If the tip was scanned at a constant height, a risk would exist that the tip collides with the surface, causing damage. Hence, in most cases a feedback mechanism is employed to adjust the tip-to-sample distance to maintain a constant force between the tip and the sample. Traditionally, the sample is mounted on a piezoelectric tube that can move the sample in the *z* direction for maintaining a constant force, and the *x* and *y* directions for scanning the sample.

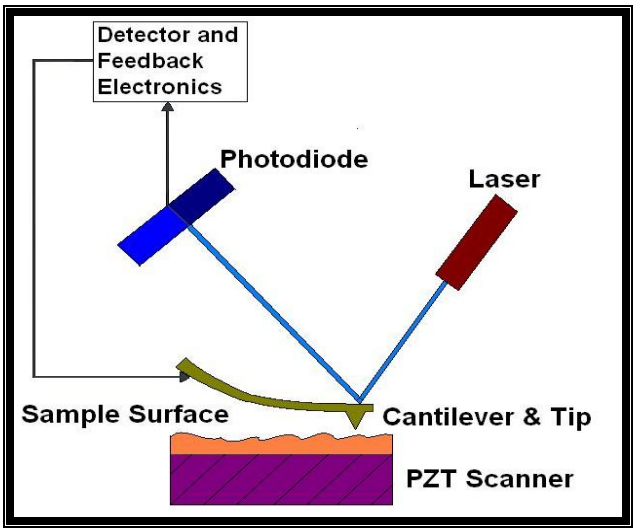

Fig. 1.15: Block diagram of atomic force microscope

1.11.1 Mode of operation

The most commonly used modes of operation of an AFM are:

- Contact mode AFM
- Tapping mode AFM
- Noncontact mode

Contact is often called a static mode. As the tip is raster-scanned across the surface, it is deflected as it moves over the surface corrugation. In constant force mode, the tip is constantly adjusted to maintain a constant deflection, and therefore constant height above the surface. It is this adjustment that is displayed as data. However, the ability to track the surface in this manner is limited by the feedback circuit. Sometimes the tip is allowed to scan without this adjustment, and one measures only the deflection. This is useful for small, high-speed atomic resolution scans, and is known as variable-deflection mode. Because the tip is in hard contact with the surface, the stiffness of the lever needs to be less that the effective spring constant holding atoms together, which is on the order of 1 - 10 nN nm^{-1}. Most contact mode levers have a spring constant of < 1N m^{-1}.

Tapping (TM-AFM) and noncontact (NC-AFM) called dynamic modes, as the cantilever is oscillated in tapping and noncontact modes. AFM works by vibrating a tip which is at the end of a cantilever and bringing the tip into intermittent contact with a sample surface, as shown in figure 1.16. The distance from the cantilever equilibrium position and the surface is defined as z_e, while the displacement from equilibrium is defined as z. thus, as the tip

moves towards the surface, z<0. When the tip interacts with a surface feature, its amplitude is decreased from its previous amplitude of oscillation. The AFM senses this decrease, and the tip is raised away from the sample in order to re-attain the previous amplitude of oscillation. In this way, the tip can be rastered across the sample to generate topographical images. Because the reaction of the tip is sensitive to sample mechanical properties, such as visco-elasticity, we can also gain an understanding of these quantities through TM-AFM.

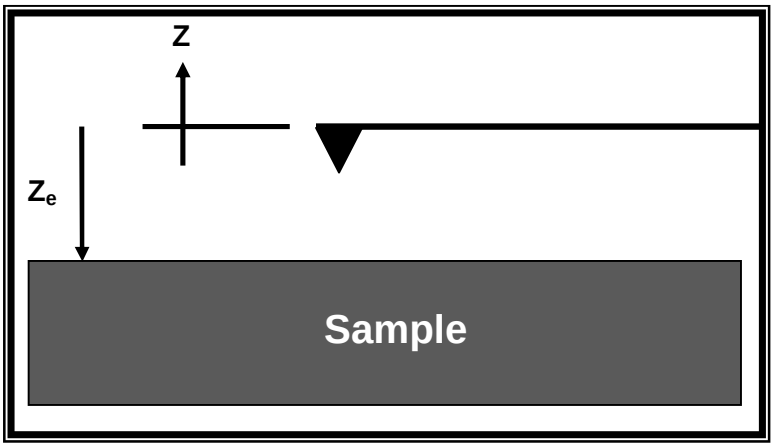

Fig. 1.16: The equilibrium position of the cantilever in AFM

Typically this is done by adding an extra piezoelectric element that oscillates up and down to the cantilever holder. Tapping mode is also known by many other names, e.g., intermittent contact (IC-AFM), AC mode and vibrating mode. Some authors prefer to refer to the modes by their detection mechanisms, Tapping mode would then be called Amplitude Modulation AFM (AM-AFM), and noncontact mode would be Frequency Modulation AFM (FM-

AFM). The main difference between tapping mode and noncontact mode is that in tapping mode, the tip of the probe actually touches the sample, and moves completely away from the sample in each oscillation cycle. When the tip is not in contact, the only force it feels from the sample is Van der Waals, which is attractive. When in contact, there is the attractive Van der Waals force over the interatomic distances, and the repulsive force due to sample hardness (the Young's modulus term). The third term is due to viscosity and acts like a friction force, opposing the motion of the tip. While the terms involving Young's modulus and viscosity make the model more difficult, if we model the system correctly, we can obtain these two sample parameters that cannot be obtained by other microscopic techniques.

In NC-AFM, the cantilever stays close to the sample all the times, and has much smaller oscilaltion amplitude. The forces between the tip and sample are quite low, on the order of 10^{-12} N. NC-AFM is more sensitive to small oscillations of the cantilever, so may be operated in close contact (almost touching). AM-AFM is typically used for tapping mode, where the tip actually taps the sample during each oscillation. This is often the most stable mode to use in air, and so is currently more commonly used than either noncontact or contact modes for most applications.

The AFM has several advantages over the SEM. Unlike the electron microscope which provides a two-dimensional projection or a two-dimensional image of a sample, the AFM provides a true three-dimensional surface profile. Additionally, samples viewed by AFM do not require any special treatments (such as metal/carbon coatings) that would irreversibly change or damage the

sample. While an electron microscope needs an expensive vacuum environment for proper operation, most AFM modes can work perfectly well in ambient air or even a liquid environment. This makes it possible to study biological macromolecules and even living organisms. In principle, AFM can provide higher resolution than SEM. It has been shown to give true atomic resolution in ultra-high vacuum (UHV) and, more recently, in liquid environments. High resolution AFM is comparable in resolution to scanning tunneling microscopy and transmission electron microscopy.

1.12 CYCLIC VOLTAMMETRY

Cyclic voltammetry (CV) is the most widely used technique for acquiring qualitative information about electrochemical reactions. The cyclic voltammetry provides considerable information on the thermodynamics results of redox processes and the kinetics of heterogeneous electron-transfer reactions, and on coupled chemical reactions (figure 1.17) or adsorption processes.

An extension of voltage-sweep voltammetry is called cyclic voltammetry and involves reversing the triangular scan after the peak of the reduction process has been passed. Thus the voltage is scanned negatively beyond the peak and then reversed in a linear positive sweep.

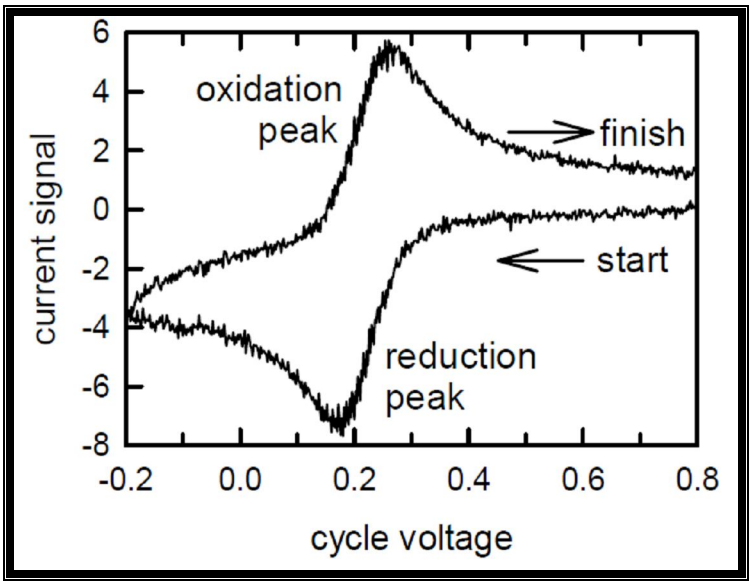

Fig. 1.17: A typical cyclic voltammogram showing reduction and oxidation peak

Such a technique provides even more information concerning the properties and characteristics of the electrochemical process and also given insight into any complicating side processes such a pre and post chemical reactions as well as kinetic considerations [126].

For a reversible process the ratio of the peak current for the cathodic process relative to the peak current for the anodic process is equal to unity. To measure the peak current for the anodic process the extrapolated baseline going from the foot of the cathodic wave to the extension of this cathodic current beyond the peak must be used as a resonance. If a post chemical process destroys the product before the reverse scan occurs then the ratio of the cathodic peak current to the anodic peak current will be grater than unity.

$$|E_{\lambda} - E_{p/2}| \geq 0.141 / n \qquad \text{(v)}$$

where E_λ is the extent of the voltage sweep. The difference in the peak potentials between the anodic and the cathodic processes of a reversible reaction at 25°C is given by the relationship.

$$(E_p)_a - (E_p)_c = 0.0595 / n \quad \text{(vi)}$$

Again, this provides a very rapid and convenient means for establishing the number of electrons involved in the electro-chemical reaction. Cyclic voltammetry is of particular value for the study of electrochemical processes that are limited by finite rates of electron transfer.

1.13 ELECTROCHEMICAL IMPEDANCE SPECTROSCOPY

Electrochemical impedance spectroscopy (EIS) involves applying an AC probe voltage to an electrochemical system and measuring the current response. By fitting an equivalent circuit to the electrochemical reaction, the components of the circuit can be determined using EIS [127]. One such circuit is known as Randles circuit [128] as shown below in figure 1.18, where in R_Ω is uncompensated resistance, R_P is polarization resistance and C_{DL} is double layer capacitance. In a Randles circuit a resistor is in series with a parallel combination of a capacitor and another resistor, as seen below:

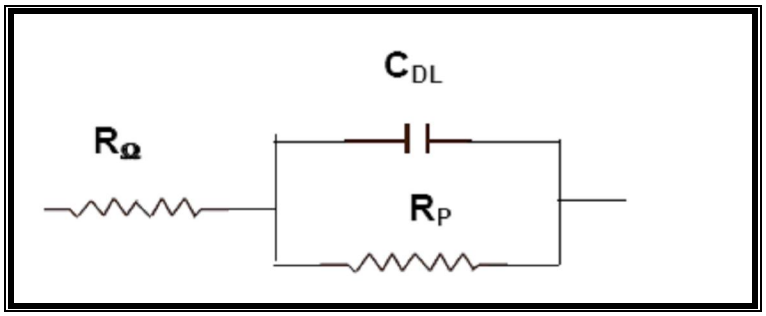

Fig. 1.18: A Randles circuit

Impedance data can be analyzed to determine the components of the Randles circuit. By graphing the imaginary (out of phase) vs the real (in phase) impedance values, a Nyquist plot can be generated. Through understanding of the Nyquist plot, information can be learned about the electrochemical system. For the Randles circuit, the following Nyquist plot is formed as shown in figure 1.19.

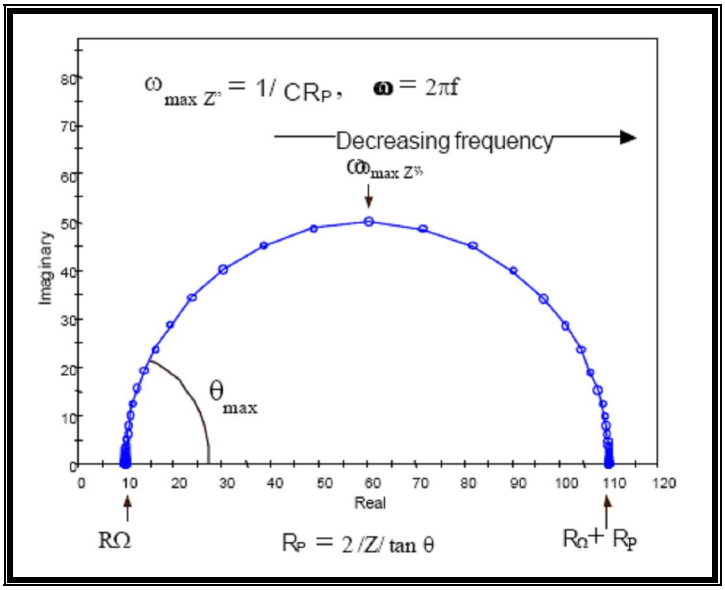

Fig. 1.19: A Nyquist plot

The semicircular shape is formed under ideal conditions for the Randles circuit. The diameter of the circle, which corresponds to the charge transfer resistance (R_{ct}), is most useful for biosensing.

Impedance measurements are performed with a three-electrode system, including a working electrode, a counter electrode, and a reference electrode. All three electrodes are connected to a common potentiostat that controls the impedance measurements and immersed into a electrolyte solution containing $K_3Fe(CN)_6$ / $K_4Fe(CN)_6$. The working electrode is the active element of the biosensor and is modified to detect the species of interest.

In order to observe changes in the biosensor due to protein, the charge-transfer resistance is monitored. At each stage of modification of the working electrode, an AC sweep can be performed and the impedance monitored. By analyzing the impedance after each step of surface modification of working electrode including the enzyme immobilization cause changes in charge-transfer resistance, which will determine the usefulness of this method in a biosensor application.

1.14 REFERENCES

1. Clark LC. *Trans. Am. Soc. Artif. Intern. Organs* 2 (1956) 41.
2. Guilbault GG, Montalvo J. *J Amer. Chem. Soc.* (1969) 91, 2164.
3. Cooney CL, Weaver JC, Tannebaum SR, Faller SR, Shields DV, Jahnke M. *In: "Enzyme Engineering"* (Eds. E.K. Pye and L.B. Wingard Jnr.) (1974) Plenum, New York.
4. Mosbach K, Danielsson B. *Biochim. Biophys. Acta*. 364 (1974) 140.
5. Divis C. *Annals of Microbiology* 126A (1975) 175.
6. Lubbers DW, Opitz N*Z. Naturforsch. C: Biosci*. 30c (1975) 532.
7. Voelkl KP, Opitz N, Lubbers DW. *Fres. Z. Anal. Chem*. 301 (1980) 162.
8. Clemens AH, Chang PH, Myers RW. *Proc. Journes Ann. de Diabtologie de l'Htel-Dieu*, Paris (1976).
9. Shichiri M, Kawamori R, Yamaski R, Hakai Y, Abe H. *Lancet* 2 (1982) 1129.
10. Liedberg B, Nylander C, Lundstrm I. *Sens.& Actuators* B 4 (1983) 299.
11. Turner APF. "Advances in Biosensors"*,* Suppl. I; III. JAI Press, London, UK, 1991; 1992; 1993; 1995.
12. Alcock SJ, Turner APF. *IEEE Engineering in Medicine and Biology* (1994) 319.
13. Kress-Rogers E. "Handbook of Biosensors and Electronic Noses: Medicine, Food and the Environment", CRC Press, Boca Raton, USA, 1996.

14. White SF, Turner APF. In: "Encyclopedia of Bioprocess Technology: Fermentation, Biocatalysis and Bioseparation"(Eds. M C Flickinger and S W Drew). Wiley, New York, USA, 1997.
15. Dennison MJ, Turner APF. *Biotechnol. Adv.* 13 (1995) 1.
16. Deshpande MV, Amalnerkar DP. *Prog. Polym. Sci.* 18 (1993) 623.
17. Kartal F, Kilin CA, Timur S. *Int. J. Environ. Anal. Chem.* 87 (2007) 715.
18. Huang XR, Li YZ, Yang GL, Liu LL, Qu YB, Zhang WJ. *Chin. Chem. Lett.* 12 (2001) 453.
19. Aravamudhan S, Ramgir NS, Bhansali S. *Sens. & Actuators B* 127 (2007) 29.
20. Arya SK, Datta M, Singh SP, Malhotra BD. *Anal. Bioanal. Chem.* 389 (2007) 2235.
21. Arya SK, Datta M, Malhotra BD. *Biosens. Bioelectron.* 23 (2008) 1083.
22. Reshetilov AN, Alferov SV, Tomashevskaya LG, Ponamoreva ON. Reprints of Symposia—American Chemical Society, Division of Fuel Chemistry 50 (2005) 719.
23. Harper JC, Polsky R, Wheeler DR, Brozik SM. *Langmuir* 24 (2008) 2206.
24. Yu EH, Sundmacher K. *Process Saf. Environ.* 85 (2007) 489.
25. Saini S,Turner APF. *Trends Anal. Chem.* 14 (1995) 304.
26. Dennison MJ, Hall JM, Turner APF. *Anal. Chem.* 67 (1995) 3922.
27. Alcock SJ, White SF, Turner APF, Setford S, Tothill IE, Dicks JM, Stephens S, Hall JM, Warner PJ. British Patent Application 9416002.5, 1994.

28. Psoma S, Turner APF. "3rd World Congress on Biosensors", New Orleans, USA, 1994.
29. Loughran MG, Hall JM, Turner APF. *Electroanal.* 7 (1996) 1.
30. Newman JD, White SF, Tothill IE, Turner APF. *Anal. Chem.* 67 (1995) 4594.
31. Jaffari SA, Turner APF. UK Patent Application GB9402591.3 (1994).
32. Selkirk JY, Turner APF, Saini S. "4th World Congress on Biosensors", Bangkok, Thailand, 1996.
33. Clark LC, Lyons C. *Ann. NY Acad. Sci.* 102 (1962) 29.
34. Updike SJ, Hicks GP, *Nature* 214 (1967) 986.
35. Guilbault GG, Lubrano GJ. *Anal Chim. Acta* 64 (1972) 439.
36. Wang J. Analytical Electrochemistry, VCH Publishers, New York 1994.
37. Ngeontae W, Janrungroatsakul W, Maneewattanapinyo P, Ekgasit S, Aeungmaitrepirom, W. Tuntulani T. *Sens.& Actuators B* 137 (2009) 320.
38. Usman Ali SM, Nur O, Willander M, Danielsson B. *Sens. & Actuators B* Article in Press (2010).
39. Chen X, Yang Z, Si S. *J. Electroanal. Chem.* 635 (2009) 1.
40. Ansari SG, Wahab R, Kim Y-S, Ansari ZA, Yang O-B, Shin H-S, Khang G. *Int. J. Nanomanucfacturing* 4 (2009) 290.
41. Lin Z-C, Chou J-C, Sun T-P, Hsiung S-K. *Sens. Lett.* 6 (2008) 855.
42. Osaka T, Komaba S, Seyama M, Tanabe K, *Sens. Actuators B* 35–36, 463 (1996).

43. Komaba S, Seyama M, Momma T, Osaka T. *Electrochim. Acta* 42 (1997) 383.

44. Ivanov AN, Evtugyn GA, Lukachova LV, Karyakina EE, Budnikov HC, Kiseleva SG, Orlov AV, Karpacheva GP, Karyakin AA. *IEEE Sensors J* 3 (2003) 333.

45. Malhotra BD, Singhal R, Chaubey A, Sharma SK, Kumar A. *Curr. Appl. Phys.* 5 (2005) 92.

46. Rajesh, Bisht V, Takashima W, Kaneto K. *Biomaterials* 26 (2005) 3683.

47. Trojanowicz M, Lewenstam A, Krawczyk TK Vel, Lahdesmaki I, Szczepek W. *Electroanalysis* 8 (1996) 233.

48. Pan D, Chen J, Yao S, Tao W, Nie L. *Anal. Sci.* 21 (2005) 367.

49. Mathebe NGR, Morrin A, Iwuoha EI. *Talanta* 64 (2004) 115.

50. Nakabayashi Y, Yoshikawa H. *Anal. Sci.* 16: (2000) 609.

51. Thanachasai S, Rokutanzono S, Yoshida S, Watanabe T. *Anal. Sci.* 18 (2002) 773.

52. Castillo-Ortega MM, Rodriguez DE, Encinas JC, Plascencia M, Méndez-V elarde FA, Olayo R. *Sens. Actuators B* 85 (2002) 19.

53. Koncki R, Lenarczuk T, Radomska A, Glab S. *Analyst* 126 (2001) 1080.

54. Radomska A, Glab S, Koncki R. *Analyst* 126, (2001) 1564.

55. Gerard M, Chaubey A, Malhotra BD. *Biosens. Bioelectron.* 17 (2002) 345.

56. Bidan G. *Sens Actuators B* 6 (1992) 45.

57. Trojanowicz M. *Microchim Acta* 43 (2003) 75.

58. Santhanam KV. *Pure Appl. Chem.* 70 (1998) 1259.

59. Skotheim TA, (1997). Handbook of conducting polymer. Basel: Marcel Dekker; New York.

60. Baeriswyl D, Cambell DK, Mazumdar S, (1992). Conjugated conducting polymers. In: Kiess HG, editor. Berlin, Heidelberg, New York.: Springer;

61. Ahuja T, Mir IA, Kumar D, Rajesh. *Sens. Actuators B* 134 (2008) 140.

62. Ahuja T, Mir IA, Kumar D, Rajesh. *Biomaterials* 28 (2007) 791.

63. Malhotra BD, Kumar N, Chandra S. *Prog. Polym. Sci.* 12 (1986) 179.

64. Cosnier S, Gondran C. Analysis 27 (1999) 558.

65. Wang P, Li Y. *J. Electroanal. Chem.* 408 (1996) 77.

66. Cassagneau T, Caruso F. *Adv. Mater.* 14 (2002) 1837.

67. Yasuzava M, Nieda T, Hirano T, Kunugi A. *Sens. Actuators B* 66 (2000) 77.

68. Gorton L. Comprehensive analytical chemistry volume XLIV: Biosensors and modern bio specific analytical techniques. Elsevier science 2005.

69. Pauliukaite R, Schoenleber M, Vadgama P, Brett CMA. *Anal. Bioanal. Chem.* 390 (2008) 1121.

70. Wang J. *Anal. Chim. Acta* 399 (1999) 21.

71. Zou Y, Xiang C, Sun L-X, Xu F. *Biosens. & Bioelectron.* 23 (2008) 1010.

72. Du D, Chen S, Cai J, Zhang A. *Talanta* 74 (2008) 766.

73. Braun S, Rappoport S, Zusman R, Avnir D, Ottolenghi M. *Mater. Lett.* 10 (1990) 1.

74. Shi G, Sun Z, Liu M, Zhang L, Liu Y, Qu Y, Jin L. *Anal. Chem.* 79 (2007) 3581.

75. Xiao Y, Li CM. *Electroanalysis* 20 (2008) 648.

76. Carrara S, Bavastrello V, Ricci D, Stura E, Nicolini C. *Sens. Actuators B* 104 (2005) 221.

77. Chang Z, Fan H, Zhao K, Chen M, He P, Fang Y. *Electroanalysis* 20 (2008) 131.

78. Kong B, Yin T, Liu X, Wei W. *Anal. Lett.* 40 (2007) 2141.

79. Tu X, Xie Q, Jiang S, Yao S. *Biosens. & Bioelectron.* 22 (2007) 2819.

80. Katz E, Willner I, Wang J. *Electroanalysis* 16 (2004) 19.

81. Yanez-Sedeno P, Pingarron JM. *Anal. Bioanal. Chem.* 382 (2005) 884.

82. Liu S, Leech D, Ju H. *Anal. Lett.* 36 (2003) 1.

83. Rashid MH, Bhattacharjee RR, Kota A, Mandal TK. *Langmuir* 22 (2006) 7141.

84. Gooding JJ, Hibbert DB. *Trac-Trend Anal. Chem.* 18 (1999) 525.

85. Groot MT, Evers TH, Merkx M, Koper MTM. *Langmuir* 23 (2007) 729.

86. Dannenberger O, Weiss K, Wo C, Buck M. *Phys. Chem. Chem. Phys.* 2 (2000) 1509.

87. Mendes RK, Carvalhal RF, Kubota LT. *J. Electroanal. Chem.* 612 (2008) 164.

88. Satjapipat M, Sanedrin R, Zhou F. Langmuir 17 (2001) 7637–7644.

89. Delvaux M, Champagne SD. *Biosens. Bioelectron.* 18 (2003) 943.

90. Masson JF, Kranz C, Booksh KS, Mizaikoff B. *Biosens. Bioelectron.* 23 (2007) 355.

91. Amine A, Mohammadi H, Bourais I, Palleschi G. *Biosens. Bioelectron.* 21 (2006) 1405.

92. Cosnier S. *Anal. Bioanal. Chem.* 377 (2003) 507.

93. Elif Boyukbayram A, Kiralp S, Toppare L, Yagci Y. *Bioelectrochemistry* 69 (2006) 164.

94. Vidal JC, Ruiz EG, Castillo JR. *Microchim. Acta* 143 (2003) 93.

95. Dicks JM, Cardosi MF, Turner APF, Karube I. *Electroanalysis* 5 (1993) 1.

96. Mu S, Xue H. *Sens. Actuators B* 31 (1996) 155.

97. Kumar A, Rajesh, Chaubey A, Grover SK, Malhotra BD. *J. Appl. Polym. Sci.* 82 (2001) 3486.

98. Gajovic N, Habermuller K, Warsinke A, Schuhmann W, Scheller FW. *Electroanalysis* 11 (1999) 1377.

99. Ramanathan K, Ram MK, Malhotra BD, Murthy ASN. *Mater. Sci. Eng. C* 3 (1995) 159.

100. Ramanathan K, Mehrotra R, Jayaram B, Murthy ASN, Malhotra BD. *Anal. Lett.* 29 (1996) 1477.

101. Ramanathan K, Ram MK, Verghese MM, Malhotra BD. *J. Appl. Polym. Sci.* 60 (1996) 2309.

102. Gambhir A, Gerard M, Mulchandani A, Malhotra BD. *Appl. Biochem. Biotechnol.* 96 (2001) 249.

103. Romette JL, Yang JS, Kusakabe H, Thomas D. *Biotechnol. Bioeng.* 25 (1983) 2557.

104. Gulla KC, Gouda MD, Thakur MS, Karanth NG. *Biochem. Biophys. Acta* 1597 (2002) 133.

105. Milagres BG, Neto GD, Kubota LT, Yamanka H. *Anal. Chim. Acta* 347 (1997) 35.

106. Chaubey A, Gerard M, Singhal R, Singh VS, Malhotra BD. *Electrochim. Acta* 46 (2000) 723.
107. Mc Ardle FA, Persaud KC. *Analyst* 4 (1993) 419.
108. Aizawa M, Yabuki S. In: Proceedings of the 51st annual meeting Japan chemical society, 1985.
109. Cosnier S. *Biosens. Bioelectron.* 14 (1999) 443.
110. Umana M, Waller J. *Anal. Chem.* 58 (1986) 2979.
111. Bartlett PN, Whitaker RG, Green MJ, Frew J. *J. Chem. Soc. Chem. Commun.* (1987) 1603.
112. Palmisano F, Zamborin PG, Contonzo D. Fresenius *J. Anal. Chem.* 366 (2000) 586.
113. Bakker E, Telting-Diaz M. *Anal. Chem.* 74 (2002) 2781.
114. Schuhmann W. *Rev. Mol. Biotechnol.* 82 (2002) 425.
115. Griffith A, Glidle A, Cooper JM. *Biosens. Bioelectron.* 11 (1996) 625.
116. Vidal JC, Garcia E, Castillo JR. *Biosens. Bioelectron.* 13 (1998) 371.
117. Sung WJ, Bae YH. Anal. Chem. 72 (2000) 2177.
118. Habermuller K, Schuhmann W. *Electroanalysis* 10 (1998) 1281.
119. Reiter S, Habermuller K, Schuhmann W. *Sens. Actuators B* 79 (2001) 150.
120. Tian F, Zhu G. *Anal. Chim. Acta* 451 (2000) 251.
121. Arjsiriwat S, Tanticharoen M, Kirtikara K, Aoki K, Somasundrum M. *Electrochem. Commun.* 2 (2000) 441.
122. Garjonyte R, Malianauskas A. *Sens. Actuators B* 63 (2000) 122.
123. Xue H, Shen Z, Li Y. *Synth. Met.* 124 (2001) 345.

124. Compagnone D, Federici G, Bannister JV. *Electroanalysis* 7 (1995) 1151.

125. Ramanathan K. Application of some conducting polymers to biosensors. PhD thesis, IIT Delhi, India, 1995.

126. Sawyer DN, Roberts Jr JL. Experimental electrochemistry for chemists. John Wiley & Sons, New York, 1974.

127. Princeton Applied Research. Basics of Electrochemical Impedance Spectroscopy. http://new.ametek.com/content-manager/files/PAR/078.

128. Randles, J.B.B. *Disc Faraday Soc. 1* (1947) 11.

Chapter II

Potentiometric Urea Biosensor based on Conducting Polymer Matrix

2.1 INTRODUCTION

Urea has received a considerable attention from researchers throughout world and many techniques for detection of urea in environment and humans have been developed. The well-known role of urea is as a fertilizer, which satisfies the nitrogen requirement of the plant. However, in humans, it is the most important end product of protein degradation and its proper balance in blood is essential for overall well being and for renal health specifically. The optimal concentration of urea in blood is an indication of proper renal functioning and thus the estimation of blood urea is frequently advised in clinical diagnostics. The normal level of urea in serum is 8 to 20 mg dL^{-1}. High level of urea in blood causes chronic or acute renal failure, urinary tract obstruction, dehyradation, shock, burns and gastrointestinal bleeding, whereas a substantial low level of urea concentration causes hepatic failure, nephrotic syndrome, cachexia [1].

The need for a fast sensing urea probe is an absolute requirement of the present-day society with the increasing problem of diabetes and malfunctioning of kidney and liver due to air pollution and in take of toxic compounds. The sensor will also serve as a bedside tool for rapid monitoring of urea in suspected patients and will help medical practitioners for providing preventive medicine.

Although direct spectroscopic methods can be used for determination of urea, but these methods are dependent on the pretreatment of sample and cannot be used for onsite monitoring.

The process of hydrolysis of urea is catalyzed by an enzyme, urease, accompanied by the production of ammonia and carbon dioxide.

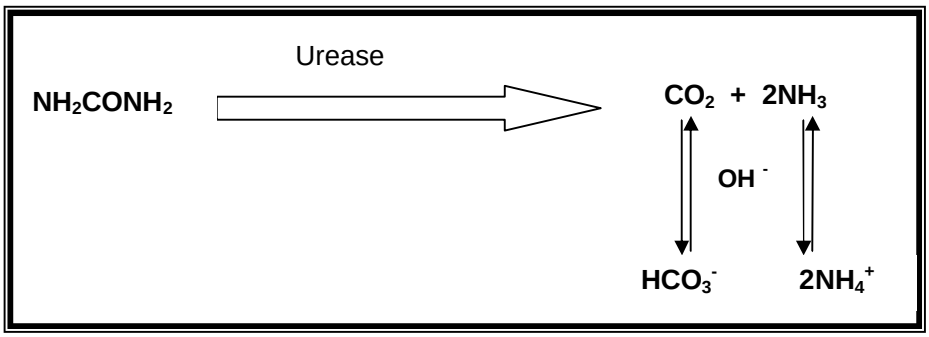

The Jack Bean urease used (E C 3.5.1.5) has an activity of 54.3 units mg^{-1} (1 unit catalyzes the formation of 1 mmol ammonia per minute at 25°C from urea) at the optimal pH of 7.4. One monomer of Jack Bean urease has a molecular weight of 82914 Da, with a 5.4 x 9.6 nm^2 average size. The molecular weight for the native urease seems to range from 480,000 to 590,000. The protein contains 840 amino acid residues in a single polypeptide chain and the subunit molecular weight calculated from the sequence is 90,790. The value of 544,740 for the hexamer, consistent with the value of 580,000 determined for intact urease by centrifugal analyses, indicated that urease consists of six subunits [2, 3].

The mechanism by which urea is hydrolyzed follows the scheme first described by Zerner's group for the jack bean urease [4]. Urea binds in *O*-coordination to one nickel ion aided by His-221. As an active base, His-322 activates a water molecule bound to the other nickel ion. Attack by the metal-coordinated hydroxide on the substrate carbon atom results in a tetrahedral intermediate that bridges the two nickel sites, a proton is transferred to the intermediate with accompanying ammonia release, and water displaces the

carbamate to complete the cycle. The detail mechanism of the enzyme, urease, catalytical reaction is shown below in figure 2.1.

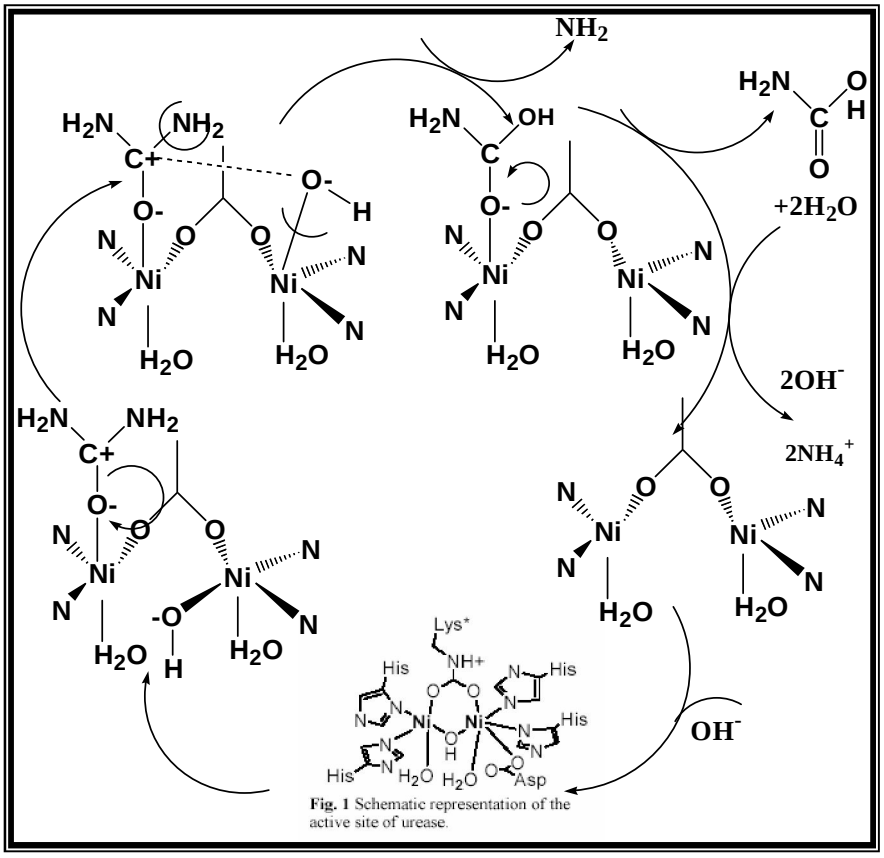

Fig. 2.1: Mechanism of the reaction enzyme, urease, with urea

This enzyme, urease, has been utilized as the biological sensing material for the fabrication of many types of urea sensors, like thermal [5-7], amperometric [1, 8-10], potentiometric [11-14], conductometric [15-17], and optical [18, 19].

Since potentiometric urea biosensors have a simple mode of construction and general availability of the instrumentation required for their

utilization, they have found a universal acceptance [20]. Several potentiometric urea biosensors based on detecting ammonia gas [21], pH change [22, 23] or ammonium ions [24, 25] generated by enzymatic reactions have been studied.

Most of the approaches utilized for fabrication of a urea biosensor involve the incorporation of an enzyme urease into a polymer film. Conducting polymers are attractive as possible materials for biosensing applications as they are used to enhance speed, sensitivity and versatility of biosensors in diagnostics to measure vital analytes [26]. Conducting polymers have attracted much interest as a suitable matrix for the entrapment of enzymes. The technique of incorporating enzymes into electro-depositable conducting polymeric films permit the localization of biologically active molecules on electrodes of any size or geometry and is particularly appropriate for the fabrication of multi-analyte micro-amperometric biosensors. These conjugated polymers are very promising supports for immobilization of enzymes due to a direct electron transfer between an enzyme and a polymer and thus potential usability as sensing materials [27].

The enzyme can be immobilized by various techniques like physical immobilization, electrochemical immobilization, entrapment or covalent binding etc. [28]. Adsorption techniques [29, 30] were used to immobilize the biological component to the outer layer of the conducting polymer to overcome the problem of burial. However, this technique suffers from the desorption (leaching out) of enzyme from the immobilizing material into the sample solution during measurement. Therefore, studies are required to stop

the desorption of enzyme to a maximum extent from immobilization materials to obtain an increased lifetime stability of the enzyme electrode. The electrochemical entrapments of enzyme induced by polymerization of the monomer in the presence of the bioactive moiety are simple and can be used to localize the bioactive component [31]. However, as the biological component is randomly oriented within the polymer matrix it is often inaccessible to the target analyte [32, 33].

Among the numerous conducting polymers prepared to date, polypyrrole is by far the most extensively studied. The reasons for this intense focus on polypyrrole lies in the fact that the monomer (pyrrole) is easily oxidized, water soluble and commercially available. Hence, polypyrrole presents several advantages including environmental stability, good redox properties and the ability to give high electrical conductivities [34, 35]. As a result of its good intrinsic properties, polypyrrole has proven promising for several applications including batteries, supercapacitors, electrochemical biosensors, conductive textiles and fabrics, mechanical actuators, electromagnetic interference (EMI) shielding, anti-static coatings and drug delivery systems [36]. The properties of conjugated polymer like polypyrrole are strongly affected by acidic solution. In an alkaline media deprotonation of oxidized polypyrrole readily occurs, resulting in significant decease in conductivity [37]. The incorporation of OH^- ions in the polymer film in the alkaline solution is also a possibility as shown in figure 2.2.

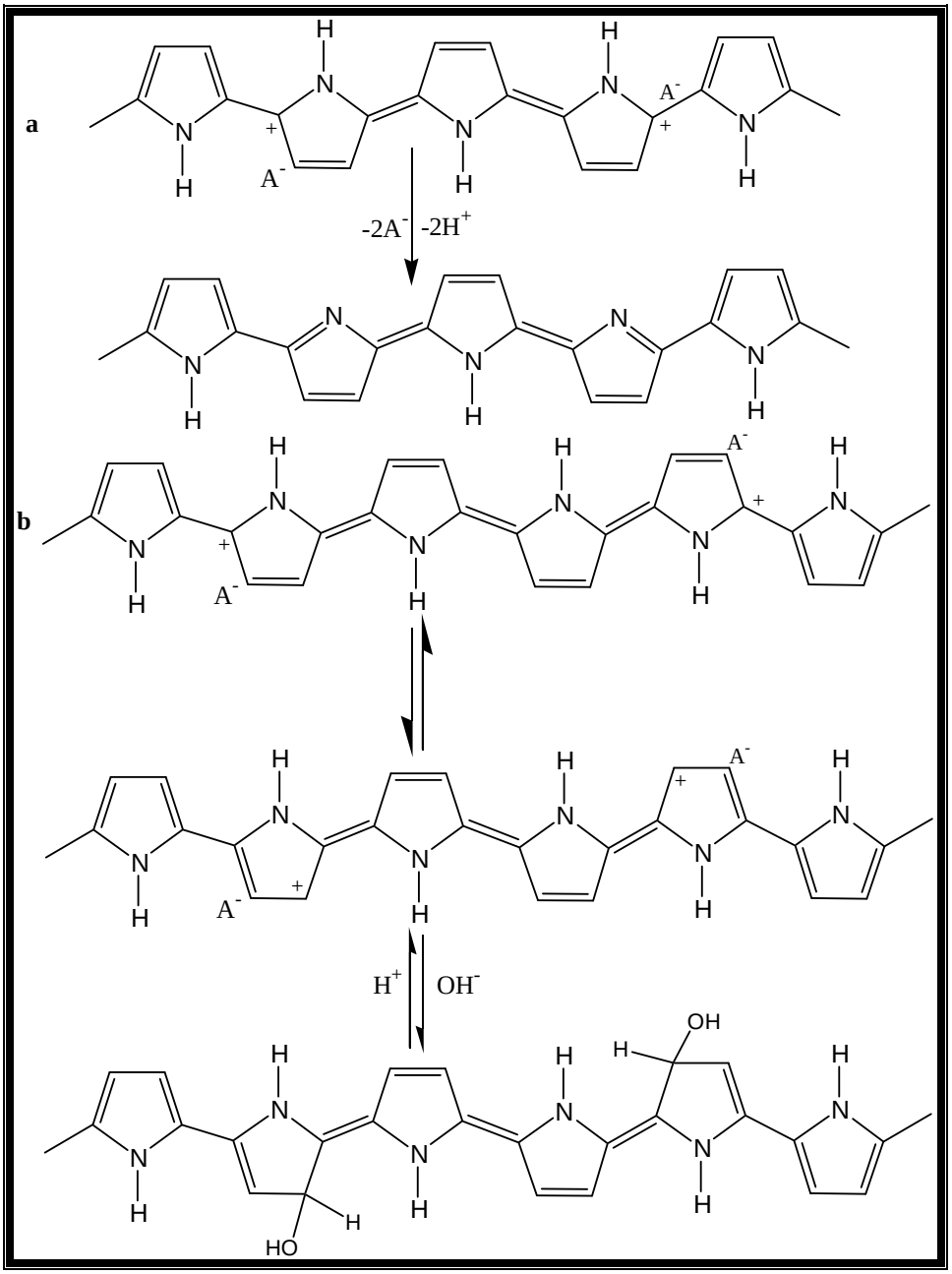

Fig. 2.2: (a) Deprotonation of polymer in alkaline solution, (b) transformation of polypyrrole in the presence of OH^- and H^+ ions

Electro-active PPy films can be doped with various anions in an electrolytic solution with the great advantage of stability. However, the

absence of active binding sites in polypyrrole, which can bind the urease, limits its application to some extent. A urea biosensor developed by Wallace et al., by simultaneous electrochemical deposition of enzyme, urease, during polymerization of pyrrole over a platinum electrode showed decrease in background current once used for individual measurement of urea solution [31]. This degradation of the polymer was attributed to the denaturing of the enzyme. This problem can be overcome by incorporating an actively binding group containing substances into the polymer film that provides free NH_2 group to enhance the immobilization as well as electrochemical properties [38]. As compared to the other immobilization methods, carbodiimide-coupling reaction has a feature of strong covalent bonding of enzyme with the matrix, which in turn is responsible for the high enzyme loading at the surface of the electrode [39].

In this investigation, the preparation and characterization of potentiometric urea biosensor has been reported by embedding Bovine serum albumin (BSA) in polypyrrole during electrochemical synthesis on an ITO glass electrode. The free NH_2 groups of embedded BSA at the surface of the polypyrrole film were exploited for the covalent binding of enzyme via carbodiimide coupling reaction. The advantage of using BSA embedded surface modified PPy films for efficient enzyme loading is described.

2.2 EXPERIMENTAL

2.2.1 Materials

Urease (EC 3.5.1.5, 104 Units/mg from jack beans) and *N*-(3-dimethylaminopropyl)-*N*'-ethyl carbodiimide hydrochloride (EDC) were obtained from Sigma Aldrich Corp. Bovine serum albumin (BSA) was purchased from Merck chemicals (Germany). *N*-Hydroxy succinimide and Pyrrole monomer were obtained from Spectrochem. p-Toluene sulphonic acid was procured from Titan biotech limited, India. Urea was procured from CDH, India. Pyrrole monomer was distilled thrice and other chemicals were of analytical grade and used without further purification. Water used in all reactions was double de-ionized (DDI) water obtained from a Millipore purification system.

2.2.2 Equipments

Fourier transform infrared (FTIR) spectra of the films were recorded on Perkin-Elmer spectrum BX. Scanning electron micrographs (SEM) were obtained with a ZEISS EVO series scanning electron micrograph model EVO50 at an acceleration voltage of 10.0 kV. UV-Vis measurements were carried out on a double beam UV-Vis spectrophotometer UV5704SS from Electronics Corporation India Ltd. Electrochemical polymerization and potentiometric measurements were done on a PGSTAT302, AUTOLAB

instrument from Eco Chemie, Netherlands. All measurements were performed at about 25°C in Tris-HCl buffer solution (pH 7.4).

2.2.3 Preparation of BSA embedded surface modified conducting polypyrrole (PPy) films

The BSA embedded surface modified conducting polypyrrole (PPy) films (0.5 x 0.5 cm^2) were electrochemically prepared on ITO glass plates from an aqueous solution containing pyrrole (0.1 M), p-toluene sulphonic acid (0.1 M) and BSA (10^{-5} M), at a fixed voltage of 0.8 V vs Ag/AgCl. The polymer films were prepared at injecting a charge density of 50-150 mC cm^{-2}. The thickness of the films obtained was about 1 to 2 µm as calculated from the injected charge.

2.2.4 Fabrication of enzyme electrode (Urs/BSA-PPy/ITO)

The enzyme, urease, was covalently attached to the exposed free amine groups (from BSA) at the surface of the polypyrrole film through carbodiimide coupling reaction. The electrode BSA/PPy/ITO was immersed in a phosphate buffer solution (0.1 M, pH 7.4) containing 0.015 M EDC, 0.03 M *N*-hydroxy succinimide and 10 mg/mL Urs for 1.5 h. The enzyme electrode was rinsed with buffer solution (pH 7.4) to remove excess unbound enzyme. All experiments were carried out at about 25°C. The enzyme electrode was stored under dry conditions at 4°C in a refrigerator when not in use.

2.3 RESULTS & DISCUSSION

2.3.1 Characterization of enzyme electrode (Urs/BSA-PPy/ITO)

The scheme given in figure 2.3 shows the fabrication of enzyme electrode (Urs/BSA-PPy/ITO), wherein the free amine groups present at the surface of the BSA modified polypyrrole film have been utilized for the covalent attachment of enzyme, Urease, through peptide linkage with a carboxylic acid group, using the linkage reagents EDC and NHS [40, 41].

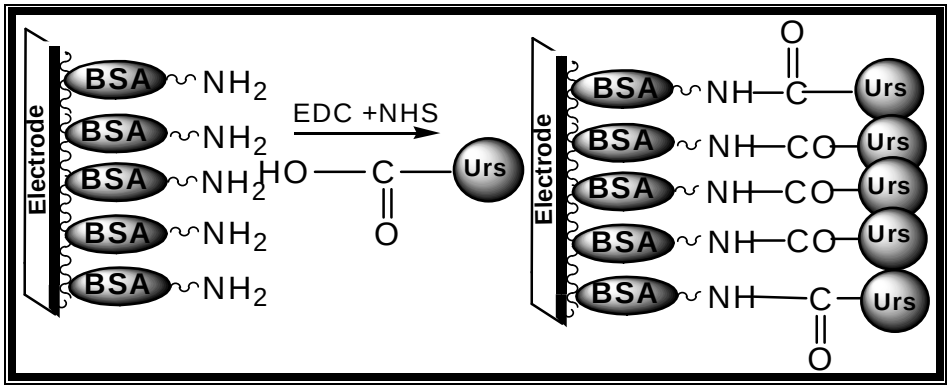

Fig. 2.3: Schematic representation of BSA modified enzyme electrode (Urs/BSA-PPy/ITO)

The enzyme electrode (Urs/BSA-PPy/ITO) was characterized by FTIR spectroscopy. Figure 2.4 shows FT-IR spectra of PPy (a), BSA-PPy (b), Urs/BSA-PPy (c) films and BSA (d). Sharp peaks were seen at 1560 cm^{-1} and 1000-1170 cm^{-1} in native PPy (a), BSA-PPy (b) and Urs/BSA-PPy (c) films, these have been assigned to C=C stretching mode and C-C stretching respectively. Prominent peaks were seen in the region 3500-3900 cm^{-1} in the

spectra of BSA embedded surface modified PPy (BSA-PPy) and enzyme immobilized polymer (Urs/BSA-PPy) films. A NH stretching region 3200-3700 cm^{-1} in the infrared spectrum of BSA film is usually strongly overlapped with the OH stretching band of hydrating H_2O molecules. Separation of these two bands with different origin is rather difficult and partially possible only when all bands of NH (Amide I, Amide II and Amide III) and H_2O (HOH deformation) are taken into account [42]. However, these peaks in the region of 3500-3900 cm^{-1} are absent in the spectra of native unmodified polymer PPy film, which is an indicative of the presence of BSA over the surface of the PPy film wherein the basic backbone structure of the PPy film is not altered by BSA.

The physical morphology of the native PPy and BSA embedded surface modified BSA-PPY/ITO film with and without enzyme (Urs) immobilization were characterized by scanning electron microscopy (SEM). A typical SEM picture of PPY/ITO (figure 2.5a) at 20,000 magnifications displays a three- dimensional porous open structure with uniform pyrrole monomers granules. However, the SEM picture of BSA embedded PPy film exhibits a large numbers of aggregated globular particles along with the pyrrole monomers granules (figure 2.5b), which indicates the presence of globular protein (BSA) over the surface of the PPy film. When the enzyme was covalently immobilized over the surface of the BSA-PPY/ITO matrix, the porous structure was disappeared and instead bright rectangular shape particles have been seen on the surface of the polymer matrix (figure 2.5c) at the magnification of 20,000, which may be assigned to enzyme (Urs) molecules.

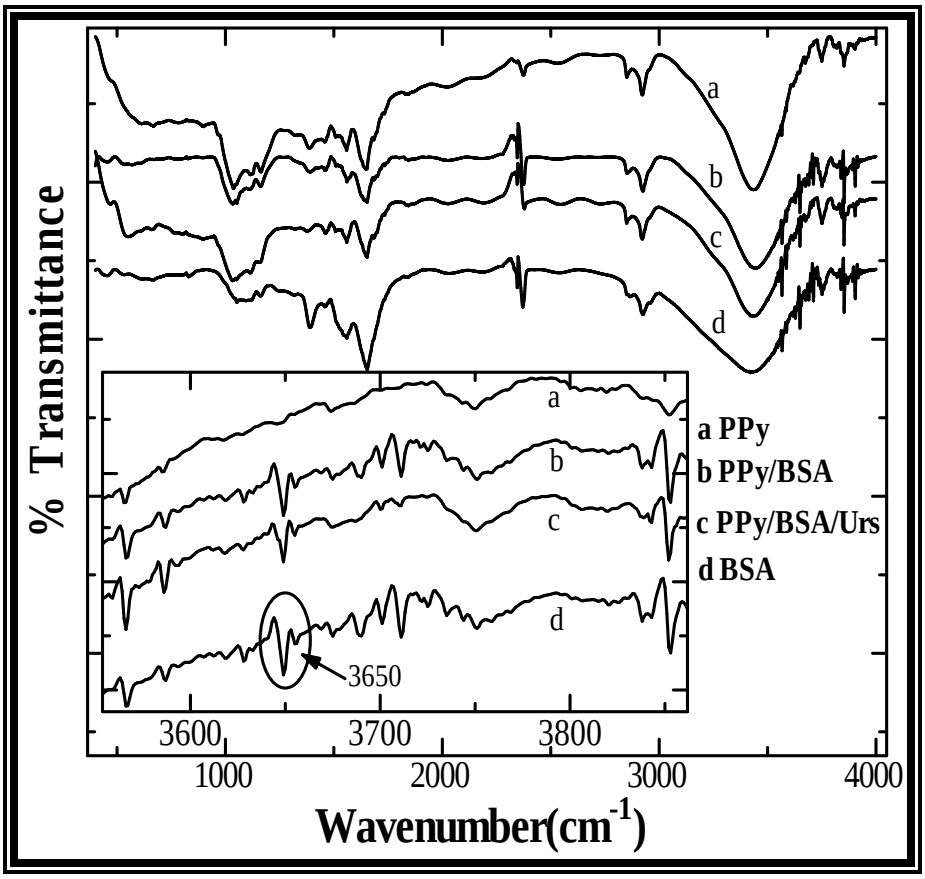

Fig. 2.4: FTIR spectra of (a) PPy; (b) BSA-PPy; (c) Urs/BSA-PPy; (d) BSA at 25°C.

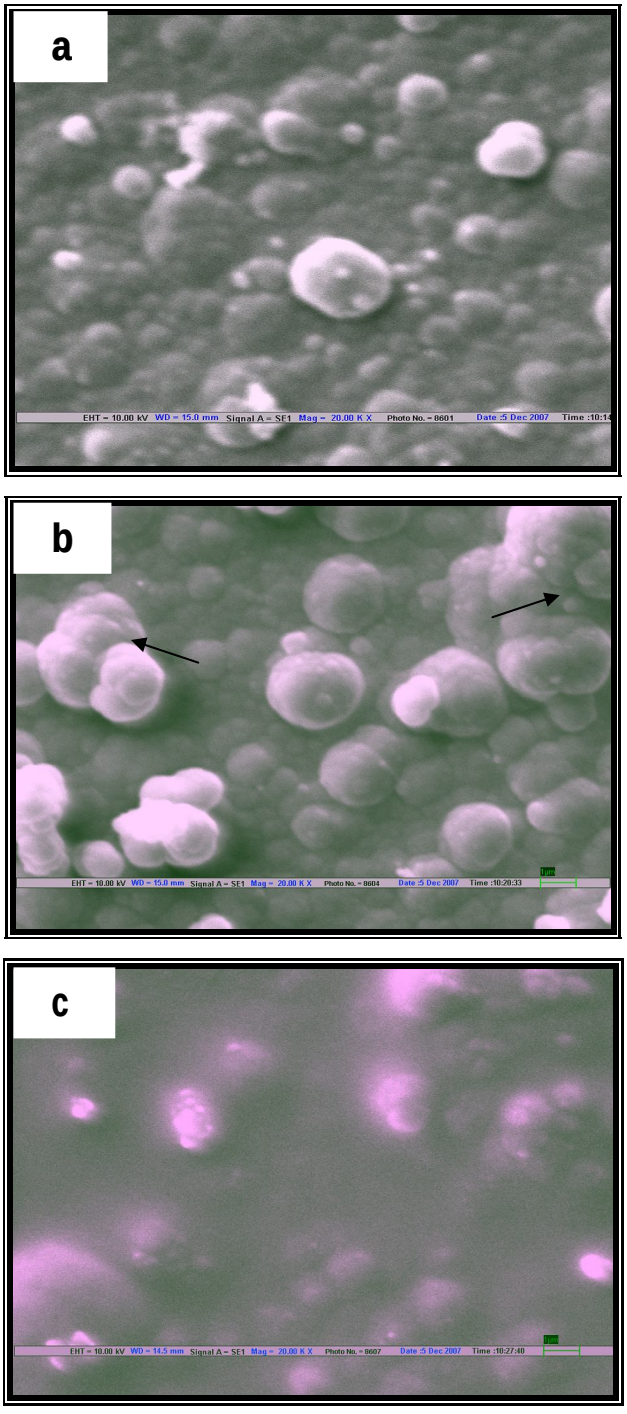

Fig. 2.5: SEM micrographs of (a) PPy/ITO; (b) BSA-PPy/ITO; (c) Urs/BSA-PPy/ITO at 20,000 magnification

2.3.2 Spectrophotometric response studies

Urease catalyzes the hydrolysis of urea to produce ammonia, which in turn reacts with Nessler's reagent ($K_2Hg^{II}I_4$) to form a colored product $NH_2Hg_2I_3$ as shown in the reaction given below:

$$NH_2CONH_2 \text{ (urea)} + H_2O \xrightarrow{\text{urease}} 2NH_3 + CO_2$$

$$2NH_3 + 2Hg^{II}I_4^{2-} \longrightarrow NH_2Hg_2I_3\ (\lambda_{max} = 380) + NH_4^+ + 5I^-$$

The electrode (Urs/BSA-PPy/ITO) was tested for the leaching of the enzyme, urease, from the surface of the polymer film by placing it in 2 mL Tris-HCl buffer (pH 7.4) solution, for 20 min and assays the solution for urease. The film was taken out after 20 min from the buffer solution and 1 mL of 10 mM urea solution containing 200 µL Nessler's solution was added to check for any possible complex formation of Nessler's reagent with enzymatically produced ammonia in solution. However, no significant absorbance for urease was found in the solution, indicating an efficient covalent entrapment of enzyme, urease, through peptide linkage to the exposed amino functional group at the surface of the polymer film. By continuously monitoring the absorbance at 380 nm for the product $NH_2Hg_2I_3$, urea can be quantified and the analytical performance of the sensor was determined. The response time of the sensor (Urs/BSA-PPy/ITO) to urea was tested by continuously monitoring the increasing absorbance at 380 nm with time period for 10 mM urea solution. The analytical response vs. time profile of Urs/BSA-PPy/ITO is shown in figure 2.6. The 95% response of the Urs/BSA-PPy/ITO film to urea is achieved in approximately 15 min and there after the absorbance at 380 nm gets almost saturated.

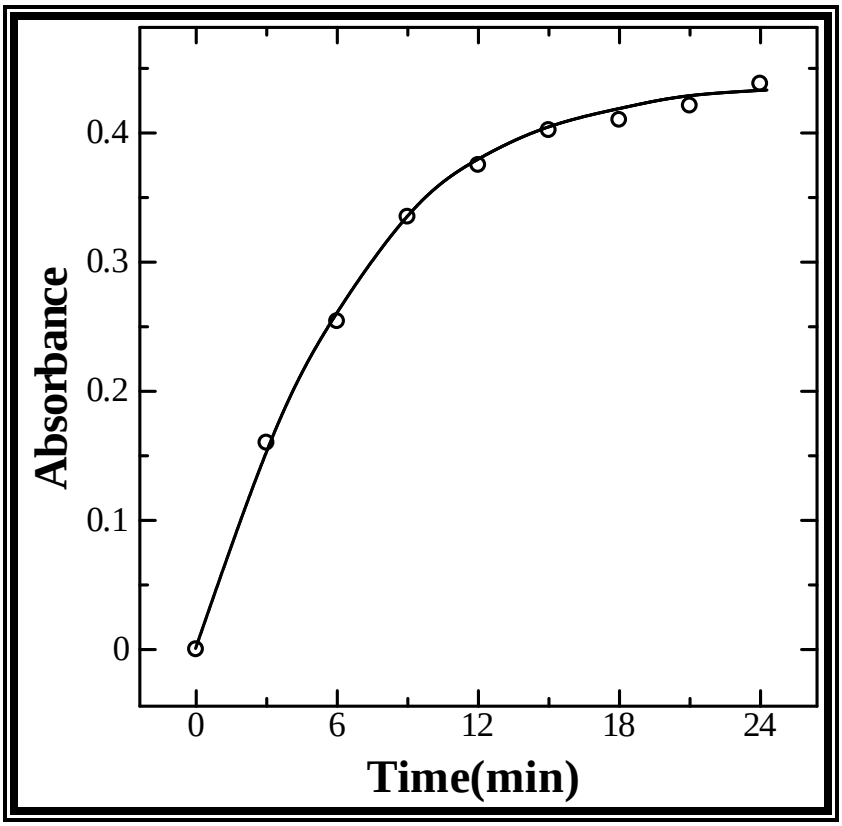

Fig. 2.6: Absorbance (380 nm) vs time profile for an Urs/BSA-PPy/ITO film on exposure to Nessler's reagent and 10 mM urea.

Figure 2.7 depicts the response of Urs/BSA-PPy/ITO film to varying concentrations of urea. The Urs/BSA-PPy/ITO films were placed in different urea concentrations in Tris-HCl buffer (pH 7.4) solution (2 mL) containing identical amount of Nessler's reagent (200 µL) for 15 minutes before taking the absorbance at 380 nm for individual urea concentration. Figure 2.7 (inset) presents a typical calibration curve for urea. The linearity response for the determination of the urea concentration was obtained in the range of 8.9×10^{-6} to 7.1×10^{-4} M.

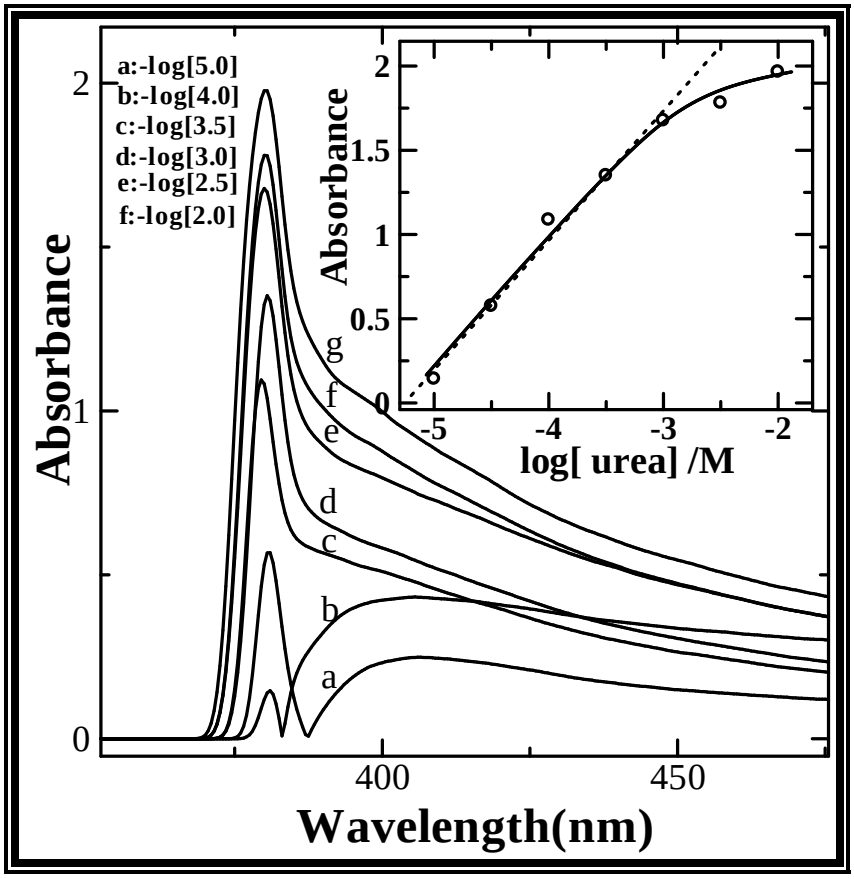

Fig. 2.7: Specrophotometric response and calibration (λ_{380}) curve (inset) using an Urs/BSA-PPy/ITO film on exposure to varying concentrations of urea and identical amounts of Nessler's reagent

2.3.3 Potentiometric response characteristics

The potentiometric biosensor is based on the enzymatic reaction of urea hydrolysis catalyzed by urease (Urs) and is represented by the reaction as given below:

$$NH_2CONH_2 \text{ (urea)} + H^+ + 2H_2O \xrightarrow{\text{Urease}} 2NH_4^+ + HCO_3^-$$

By detecting ions consumed or produced in the above enzymatic reaction, urea concentrations are determined. The Urs/BSA-PPy/ITO electrodes with varying film thickness prepared electrochemically at injecting charge density of 50-150 mC/cm^2 were tested for the potentiometric response measurements of urea concentration in working solution (10 mM Tris-HCl buffer, pH 7.4). It has been found that the thickness of the film has considerable affect on the sensitivity of the biosensor to urea. Figure 2.8 shows that the sensitivity of the enzyme electrode to urea decreases with increasing thickness of the polymer film. The polymer film prepared at injected charge density of 150 mC cm^{-2} provides a very slow response and sensitivity to urea solutions as compared to the results obtained with the polymer film prepared at low injected charge density of 100 m cm^{-2}. This slow response and sensitivity of the biosensor film prepared with higher charge density may be due to increasing diffusion barrier with increased film thickness, which tends to reduce the amount of analyte reacting at the electrode surface [8]. However, a film prepared with an injected charge density of 50 mC cm^{-2} was too thin to handle and was not found to be stable for a longer time in a working solution, therefore a thin film enzyme electrode prepared at injected charge density of 100mC cm^{-2} was selected for potentiometric detection of

urea in aqueous solution. Potentiometric response were measured after the addition of successive aliquots of urea in Tris-HCl buffer solution (10 mM, pH 7.4, 10 mL) under a slow constant stirring of 100 rpm, in accordance to the chronopotentiometric protocol. The enzyme electrode responded rapidly to the urea substrate and a 95% steady state baseline was reached within 70-90 sec. This response time of the electrode is much shorter than those of recently reported biosensors (>2 min) [43-45].

Figure 2.9 shows the steady state potential dependence calibration curve for the each individual urea concentration. The response of enzyme electrode (Urs/BSA-PPy /ITO) to urea was found to be linear in the range of 6.6×10^{-6} to 7.5×10^{-4} M ($r = 0.999$). This linearity range is in well conformity with that obtained in the spectrophotometric response studies. The slope of the linearity, i.e., the sensitivity of the enzyme electrode towards urea concentrations was 17.3 mV per decade.

The reported sensitivity of the PPy-enzyme electrode without any surface modification with BSA (Urs/PPy) is 17.5 mV per decade and it provides a linear response to urea concentration in the range of 0.5×10^{-3} to 100×10^{-3} M [12]. Though no much improvement in sensitivity was observed with BSA modified PPy enzyme electrode (Urs/BSA-PPy/ITO), but it exhibits a wide range of urea detection in low urea concentration in comparison to unmodified PPy-enzyme electrode (Urs/PPy). This shows that surface modification over the polymer film lead to better enzyme loading that makes the electrode more responsive and susceptible to the determination of urea at much lower concentration. The reproducibility of the response of the enzyme

electrode was investigated at a 1mM urea concentration. In a series of 10 Urs/BSA-PPy/ITO electrodes, a relative standard deviation of about 10% was obtained for the individual potential response for the same sample (1 mM urea). A slow and steady decrease in potential response was observed up to 3 uses of an electrode in testing but after successive uses of the same electrode a rapid reduction in potential response was observed. This reduction in potential response of the enzyme electrode may be attributed to the possible poisoning of the polymer film by urea, which binds strongly with the polymer and hence decreases the number of free active sites [12].

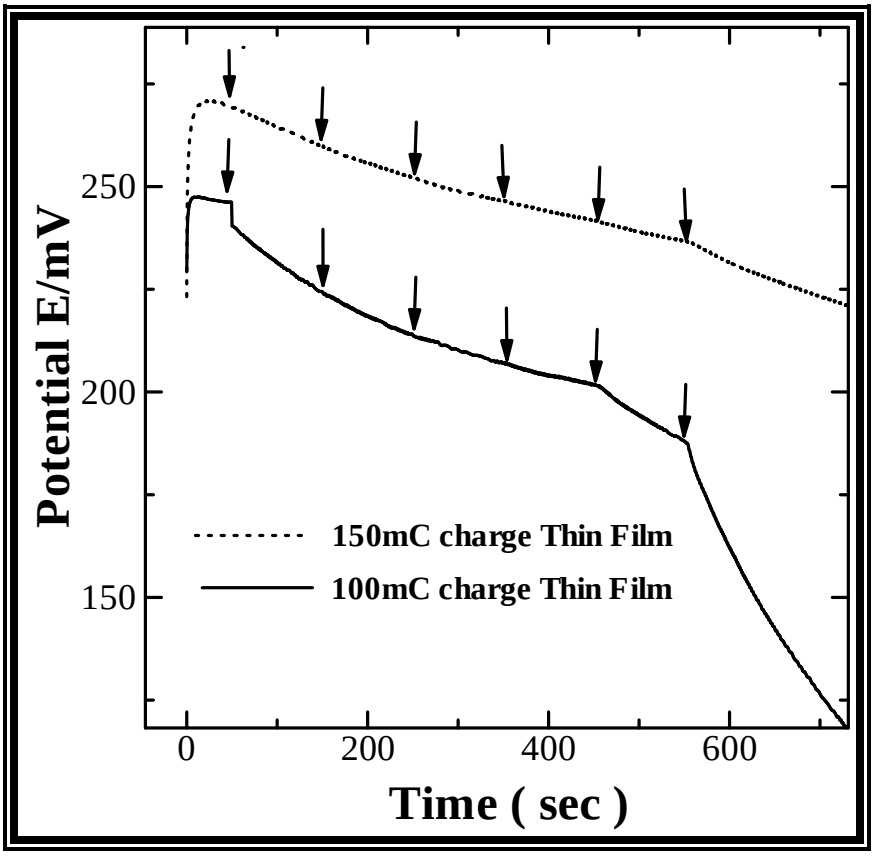

Fig. 2.8: Chronopotentiometric response of biosensor Urs/BSA-PPy/ITO to increasing urea concentration

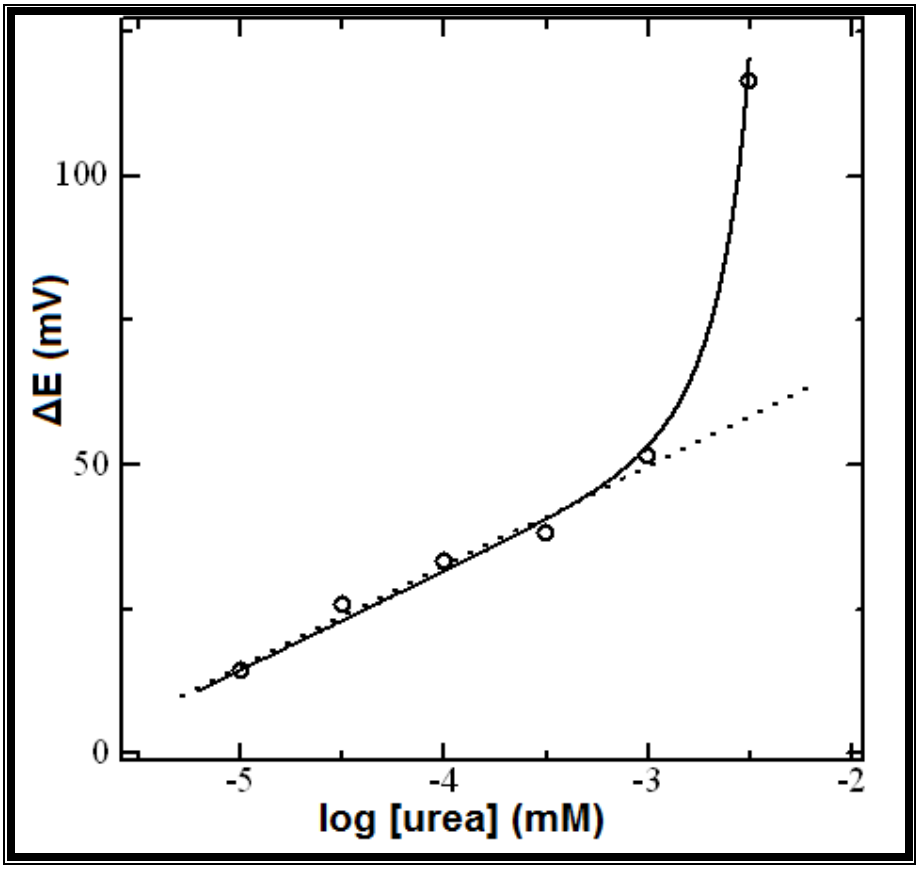

Fig. 2.9: Steady state potential dependence calibration curve of biosensor Urs/BSA-PPy/ITO to urea in 10 mM Tris-HCl buffer (pH 7.4)

A few common interfering reagents were studied for any possible interfering effects on the analysis of urea. Known concentrations of 1.0×10^{-4} M ascorbic acid .and 5.0×10^{-3} M glucose were added both individually and in combination to a sample of 1.0 mM urea solution. However, no significant interfering effects have been found using these reagents on the potential response of the electrode for the said sample.

2.3.4 Sensor stability and storage conditions

The Urs/BSA-PPy/ITO electrodes were studied for the enzyme stability, at a temperature of about 25°C and 4-5°C, respectively. The stability of the enzyme was monitored by conducting continuous measurement of the electrode potential response to a 1 mM urea sample, after an interval of 2 days for 4 months. The potential response of the electrode sharply decreases for 1 mM urea solution after 2 weeks when the said electrode is stored at about 25°C because of rapid enzyme inactivation. However, when the Urs/BSA-PPy/ITO electrodes are stored at 4-5°C, a very slow decrement in potential response was observed with time and it retained about 75% of its initial enzyme activity up to 2 months, thereafter it shows a rapid enzyme inactivation. This long-term stability of the enzyme over the surface modified polymer electrode is better than the recently reported urea biosensors (< 30 days) [46-48].

2.4 CONCLUSIONS

This study has demonstrated the advantages of developing a bovine serum albumin (BSA) embedded surface modified conducting polypyrrole film as an immobilizing matrix for the entrapment of enzyme, urease. The enzyme urease, efficiently binds with the free NH_2 groups provided by the BSA molecules at the surface of the polypyrrole film through carbodiimide coupling reaction. This has lead the surface modified polypyrrole film to have increased loading of enzyme, urease, which results in long term stability and a wide linear response range of detection, at much lower urea concentration in aqueous solution in comparison to the reported surface unmodified polypyrrole biosensor. The low cost and simple method of fabrication of surface modified immobilizing material also makes this biosensor more advantageous than recently reported biosensors. The experiments are presently in progress to further improve the shelf life of this Urs/BSA-PPy/ITO biosensor beyond 2 months at 4-5°C.

2.5 REFERENCES

1. Rajesh, Bisht V, Takashima W, Kaneto K. *Biomaterials* 26 (2005) 3683.
2. Mamiya G, Takishima K, Masakuni M, Kayumi T, Ogawa K. *J. Prot. Chem* 6 (1987) 55.
3. Vial S, Ghanbajab J, Forano C. *Chem. Commun,(* 2006) 290.
4. Dixon NE, Riddles PW, Gazzola C, Blakeley RL, Zerner B. *Can. J. Biochem.* 58 (1980) 1335.
5. Xie B, Danielsson B. *Anal. Lett.* 29 (1996) 1921.
6. Xie B, Mecklenburg M, Danielsson B, Ohman O, Nolin P, Winquist F. *Analyst* 120 (1995) 155.
7. Fulton SP, Cooney CL, Waever JC. *Anal. Chem.* 52 (1980) 505.
8. Adeloju SB, Shaw SJ, Wallace GG. *Anal. Chim. Acta* 323 (1996) 107.
9. Kuralay F, Ozyoruk H, Yildiz A. *Sens. & Actuators B* 114 (2006) 500.
10. Bertocchi P, Compagnone D, Palleshi G. *Biosens. Bioelectron.* 11 (1996) 1.
11. Rajesh, Bisht V, Takashima W, Kaneto K. *React. & Funct. Polym.* 62 (2005) 51.
12. Adeloju SB, Shaw SJ, Wallace GG. *Anal. Chim. Acta* 281 (1993) 621.
13. Komaba S, Seyama M, Momma T, Osaka T. *Electrochim. Acta* 42 (1997) 383.
14. Battilotti M, Colapicchioni C, Giannini I, Porcelli F, Campanella L, Cordatore M, Mazzei F, Tomassetti M. *Anal. Chim. Acta* 221 (1989) 157.

15. Sheppard Jr NF, Mears DJ, Guiseppi-Elie A. *Biosens. Bioeletron.* 11 (1996) 967.

16. Jdanova AS, Poyard S, Soldatkin AP, Jaffrezic-Renault N, Martelet C, *Anal. Chim. Acta* 321 (1996) 35.

17. Castillo-Ortega MM, Rodriguez DE, Encinas JC, Plascencia M, Mendez-Velarde FA, Olayo R. *Sens. and Actuators B* 85 (2005) 19.

18. Konck R, Lenarczuk T, Radomska A, Glab S. *Analyst* 126 (2001) 1080.

19. Stamm C, Seiler K, Simmon W. *Anal. Chim. Acta* 282 (1993) 229.

20. Correia DPA, Magalhaes JMCS, Machado AASC. *Talanta* 67 (2005) 773.

21. Lui B, Hu R, Deng J. *Anal. Chim. Acta* 341 (1997) 161.

22. Osaka T, Komaba S, Seyama M, Tanabe K. *Sens. & Actuators B* 36 (1996) 463.

23. Soldatkin AP, Montorial J, Sant W, Martelet C, Jaffrezic-Renault N. *Biosens. Bioelectron.* 19 (2003) 131.

24. Zamponi S, Ciero BL, Mascini M, Ciana LD, Sacco S. *Talanta* 43 (1996) 1373.

25. Cho W-J, Huang H-J. *Anal. Chem.* 70 (1998) 3946.

26. Gerard M, Chaubey A, Malhotra BD. *Biosens. Bioelectron.* 17 (2002) 345.

27. Rajesh, Takashima W, Kaneto K. *React. & Funct. Polym.* 59 (2005) 163.

28. Ahuja T, Mir IA, Kumar D, Rajesh. *Biomaterials* 28 (2007) 791.

29. Khan GF, Wernet W. *Thin Solid Films* 300 (1997) 265.

30. Minett AI, Barisci JN, Wallace GG. *React. & Funct. Polym.* 53 (2002) 217.

31. Cosnier S. *Appl. Biochem. Biotechnol.* 89 (2000) 127.

32. Killard AJ, Deasy B, O'Kennedy R, Smith MR. *Trends Anal. Chem.* 14 (1995) 257.

33. Barisci JN, Hughes D, Minett A, Wallace GG. *Anal. Chim. Acta* 371 (1998) 39.

34. Wise DL, Winek GE, Trantolo DJ, Cooper TM, Gresser JD. In *Electrical and Optical Polymer Systems*, Marcel Dekker, Inc., New York, 1998.

35. Rodriguez J, Grande HJ, Otero TF. In *Handbook of Organic Conductive Molecules and Polymers*, ed. H. S. Nalwa, John Wiley & Sons, New York, 1997.

36. Scrosati B, In *Applications of Electroactive Polymers*, Chapman & Hall, London, 1993.

37. Forsyth M, Truong VT. *Polymer* 36 (1995) 725.

38. Chen C-C, Gu Y. *Biosens. Bioelectron.* 23 (2008) 765.

39. Rajesh, Takashima W, Kaneto K. *Sens. and Actuators B* 102 (2004) 271.

40. Riklin A, Katz E, Willner I, Stocker A, Buckmann AF. *Nature* 376 (1995) 672.

41. Situmorang M, Gooding JJ, Hibbert DB, Barnet D. *Biosens. Bioelectron.* 13 (1998) 953.

42. Grdadolnik J. *Int. J. Vibr. Spec.* 6 (2002) 1.

43. Pizzariello A, Stredansky M, Stredanska S, Miertus S. *Talanta* 54 (2001) 763.

44. Stredansky M, Pizzariello A, Stredanska S, Miertus S. *Anal. Chim. Acta* 415 (2000) 151.

45. Chen J, Chou J, Sun T, Hsiung S. *Sens. and Actuators B* 91 (2003) 180.

46. Hamlaoui ML, Reybier K, Marrakchi M, Jaffrezic-Renault N, Martelet C, Kherrat R, Walcarius A. *Anal. Chim. Acta* 466 (2002) 39.

47. Lakard B, Herlem G, Lakard S, Antoniou A, Fahys B. *Biosens. Bioelectron.* 19 (2004) 1641.

48. Vostiar I, Tkac J, Sturdik E, Gemeiner P. *Bioelectrochemistry* 56 (2002) 113.

Chapter III

Carbon nanotubes/silica Composite based Potentiometric Urea Biosensor

3.1 INTRODUCTION

Carbon nanotubes (CNTs) have been used as an important component in electrochemical biosensor due to their unusual properties like their large length-to diameter aspect ratios which provides high surface-to-volume ratios, their ability to mediate fast electron-transfer kinetics for a wide range of electro-active species [1, 2]. In addition, CNTs chemical functionalization can be used to attach almost any desired chemical species to them, which allows us to enhance the solubility and biocompatibility of the tubes [3]. CNTs have been of great interest, both from a fundamental point of view and for potential applications. Their mechanical and unique electronic properties open a broad range of applications including nanoelectronic devices, composites, chemical sensors, biosensors and more. They also provide tremendous opportunities in the design of multifunctional materials systems. Particularly, they promise to provide solutions to many vexing problems encountered during the application of traditional composite materials. For example, they are electrically conductive and therefore are suitable for applications that require the capability to discharge electrostatic potentials.

Carbon nanotubes can be classified as single-walled carbon nanotubes (SWCNTs) and multi-walled carbon nanotubes (MWCNTs). SWCNTs consist of a cylindrical single sheet with a diameter between 1 and 3 nm and a length of several micrometers. They possess a cylindrical nanostructure formed by rolling up a single graphite sheet into a tube. MWCNTs consist of a coaxial arrangement of concentric single nanotubes like rings of a tree trunk

separated from one another by 0.34 nm. They usually have a diameter of about 2–20 nm. The production of SWCNTs or MWCNTs is highly dependent on the synthesis process and conditions [4]. CNTs are promising as an immobilization substance because of their significant mechanical strength, high surface area, excellent electrical conductivity and good stability [5]. Due to these properties, CNTs have the ability to promote electron transfer reactions when used as an electrode. Synthesis, processing and device fabrication techniques for nanotubes have greatly improved with recent intensive research [6]. Various electro analytical properties and applications of CNTs have appeared in the literature [7-9].

At present the dispersion of nanotubes in a matrix is a matter of experimenting. The problem of insolubility of carbon nanotubes due to strong van der Waals attractions and chemical inertness hinders their uniform dispersion and incorporation in any matrix. It was shown that the remarkable properties indigenous to the tubes could be transferred to the nanocomposite, in particular, to the polymer matrix. CNTs have the ability to promote electron transfer reactions when used as an electrode. As a result, the addition of CNTs can strongly modify the properties of polymers, especially theirs conductivity and mechanical properties. The combination of CNTs with polymers offers an attractive route to reinforce the polymer as well as to introduce electronic properties based on morphological modification or electronic interaction between the two components. A homogeneous dispersed filler in the polymer matrix reduces the possibility of nanotube entanglement, which can lead to significant changes in composite behavior

[10, 11]. The nanotube aggregation within a polymer system would certainly have a negative impact on its stiffening ability [12]. As yet, the nature of these entanglements and their influence on the composite properties is a little understood area. To overcome nanotube aggregation, functionalization of nanotubes with groups is done that facilitate their incorporation into a material through covalent bonding [1]. For example, SWCNT covalently functionalized with pyrrolidine by the 1,3-dipolar cycloaddition of azomethineylides show a solubility of 50 mg/mL in chloroform, even without sonication whereas the pristine SWNT is completely insoluble in this solvent [2]. Furthermore, covalent functionalization can provide a means for engineering the nanotube/polymer interface for optimal composite properties.

In polymer/CNTs composites, it has been suggested that either the polymer functionalizes the CNTs or the polymers are doped with CNTs, i.e., a charge transfer occurs between the two constituents [13]. It was shown that networks of carbon nanotubes in polymer matrix may be the first system that exhibits metallic, semiconducting and polymer-like properties within one material. According to Baibarac and Gymez-Romero, the main functionalization possibilities of CNTs reported until now are: (A) generation and functionalization of defect sites at the tube ends and side walls by oxidation and subsequent conversion into derivatives; (B) covalent side wall functionalization using addition reactions and subsequent nucleophilic substitution; and (C) non-covalent exohedral functionalization with surfactant-type molecules.

Nanotubes also have other advantages over conventional fillers, such as carbon black and carbon fibres, in that they are more amenable to processing and can be more easily dispersed throughout the matrix. Another interesting avenue of research involves manipulation of the tube chemistry, which also presents the opportunity to develop multifunctional composites with tailored physical properties. It was found that the CNTs addition may drastically change the electric properties of metal oxide matrix as well. Dispersing conductive materials into the nonconductive matrix can form conductive composites.

At that it was established that nanotube overlap is a very important parameter in nanocomposites. Well-dispersed systems possess very different rheological and electrophysical properties below and above the concentration of ‘‘mechanical percolation’’ or “electrical percolation”. At low volume fractions, the conductivity remains very close to the conductivity of the pure matrix. When a certain volume fraction is reached, the conductivity of the composite drastically increases by many orders of magnitude. The phenomenon is known as percolation and can be well explained by percolation theory. The electrical percolation threshold of conductive reinforcements embedded in an insulating matrix is sensitive to the geometrical shape of the conductive phase. The small size and large aspect ratio are helpful to lower the percolation threshold [14]. Because carbon nanotubes have tremendously large aspect ratios (100–10,000), many researchers have observed exceptionally low electrical percolation thresholds. Sandler et al. [15] and Moisala et al. [16] have reported ultra-low percolation

thresholds for multi-walled carbon nanotube composites. The percolation threshold for electrical conductivity of epoxy composites containing multi-wall carbon nanotubes was found to be 0.0025 wt% MWCNT considerably lower than nanoscale dispersed carbon black particles. Bryning et al. [26] reported very low percolation thresholds in single-walled nanotube composites. The threshold conductivity of single-walled carbon nanotubes in epoxy composites was noted to be a function of the SWCNT type with values as low as 0.00005 volume fraction.

CNTs-based composites have attracted a lot of attention of researchers for their applications in sensors [17]. The extended surface area provides greater substrate binding sites for sensing molecule attachment. Moreover, they are hollow tubes with high aspect ratio and propagate a signal fast. They serve as ideal substrates after being functionalized to form bonds with sensing molecules. Since their composition is uniform, they tend to give specificity to the overall sensing property. Orientation and structural uniformity of CNTs give additional advantages to nanocomposites on the basis of CNTs.

Recent reports have proposed the use of carbon nanotube/polymer-based composites as vapor sensors [18, 19]. In these reports the changes in electrical resistivity of the composite are measured and are attributed to swelling of the polymer matrix and/or conductive modification due to the solvent absorption. It was noted by Yoon et al. [20] that the different gas concentrations diffuse into the polymer affects the distance between carbon nanotubes through polymer swelling.

An et al. [21] have shown that SWCNT/PPY composite can be interesting for design of NO_2 sensors as well. The sensitivity of the gas sensor fabricated with the SWCNT/PPY nanocomposite towards NO_2, as measured by a direct voltage divider at room temperature, was very high of about ten times higher than that of PPY. It was supposed that by nano-dispersing of the SWCNT bundles, an increase of the specific surface area of the coated PPY took place and thereby a further increase of the sensitivity. It was also shown that the recovery time could be shortened, particularly in the nanocomposite, by taking advantage of the Joule-heating effect.

Recently, the sol-gel technology has been widely used for the development of biosensors due to their excellent processability, ability to form films and entrapping biomolecules like proteins, enzymes, antibodies etc. The immobilized biomolecules in sol-gel matrix exhibit structural integrity, very often full biological functions and also significant stability to resist chemical and thermal deactivation. This is due to simple sol–gel processing conditions and a possibility of tailoring the process for specific requirements and provides inherent versatility. Sol–gel-derived glasses can be a potential host matrix for chemical sensing and biosensing. It has been reported earlier that biomolecules immobilized in sol-gel are likely to have comparatively enhances shelf lives. Sol-gel offers a better way to immobilize biomolecules within its porous optically transparent matrix and demonstrated functional activity of encapsulated biomolecules [10]. Also by using different sol-gel precursors, doping polymers, additives and redox modifiers, the characteristics of silica matrix including pore size, pore distribution, flexibility, hydrophilicity and

conductivity can be modified for biosensing purposes [11, 12]. A few urea optodes based on sol-gel film have been reported. One example is urease immobilized in sol-gel matrix with fluorescein isothiocyanate-dextran as a florescence dye by Tsai et al. [22]. Another urea optode reported by Gulcev et al. [23] contained 500 nm thick film immobilized with urease enzyme or lipase and fluorescein/ carboxy-seminaphtharhodafluor-1 (SNARF-1) as the sensing materials.

Recently, MWCNTs with the property of sol-gel have been widely used for electrochemical biosensing for several analytes like lactate [24], choline [25] etc.

Urea is a bio-molecule that is known to play a variety of roles in the welfare of mankind. The well-known role of urea is as a fertilizer, which satisfies the nitrogen requirement of the plant. However, in human body, kidney excretes urea, an end product of protein metabolism. Blood urea nitrogen (BUN) is directly related to protein intake and nitrogen metabolism and inversely related to the rate of excretion of urea. The urea sensor becomes indispensable in diabetics monitoring to predict the nature and cause of diabetes and also as a direct indication for the onset of kidney failure or liver malfunction. The normal level of urea in serum is 8 to 20 mg dL^{-1} (1.3 to ~3.5 mM). An increase in urea concentration causes renal failure (acute or chronic), urinary tract obstruction, dehydration, shock, burns and gastrointestinal bleeding, whereas a decrease in urea concentration causes hepatic failure, nephrotic syndrome, cachexia (low-protein and high-carbohydrate diets).

Although a large number of studies dealing with the development of urea biosensors [26-30] are reported, the drawbacks related to their practical use are often not underlined. Stredansky et al. have reported the concept of an amperometric biosensor based on the use of pH-sensitive redox probe molecule [31], in which the enzyme urease was physically immobilized over the water insoluble pH-sensitive redox compound, 'lauryl gallate' for the construction of a bulk modified graphite composite electrode. However, the biosensor showed a slow response time of 3-5 min to a urea concentration. Recently, urease has been immobilized on polyethylenimine film [32], for the construction of urea potentiometric biosensor but the stability of the said biosensor is only 4 weeks.

In the present study, we have prepared a urea biosensor based on carboxyl functionalized multi wall carbon nano tubes- silica (F-MWCNTs/SiO_2) composite material. The biosensor was prepared by inserting the enzyme, urease, linked F-MWCNTs within the growing silica network over an indium tin oxide coated glass plate. The carboxyl groups of the functionalized carbon nano tubes (F-MWCNTs) were utilized for the covalent immobilization of enzyme, urease, for sensor application.

3.2 EXPERIMENTAL

3.2.1 Materials

Urease (EC 3.5.1.5, 95.9 Units/mg from jack beans) and N-(3-dimethylaminopropyl)-N'-ethyl carbodiimide hydrochloride (EDC) were obtained from Sigma Aldrich Corp. Tetraethyl orthosilicate (TEOS) was purchased from Merck chemicals (Germany). N-hydroxy succinimide (NHS) was obtained from Spectrochem. Purified carboxyl modified MWCNTs (F-MWCNTs) (20-30 nm OD, length 10-30 μm) were procured from "CheapTubes, USA." Urea was procured from CDH, India. Other chemicals were of analytical grade and used without further purification. Water used in all reactions was double de-ionized (DDI) water obtained from a Millipore purification system.

3.2.2 Equipments

Fourier transform infrared (FTIR) spectra of the films material were taken after making pallets in KBr and recorded on Nicolet FTIR-380 from Thermo Instruments. Scanning electron micrographs (SEM) were obtained with a ZEISS EVO series scanning electron micrograph model EVO50 at an acceleration voltage of 20.0 kV. UV-Vis measurements were carried out on a double beam UV-Vis spectrophotometer UV5704SS from Electronics Corporation India Ltd. Thermal Gravimetric Analysis was carried out on Q50

TA instruments. Potentiometric measurements were done on a PGSTAT302, AUTOLAB instrument from Eco Chemie, Netherlands, carried out in a conventional three-electrode cell configuration consisting of a working electrode (Urs/MWCNTs/SiO_2/ITO), Ag/AgCl reference electrode and platinum wire as a counter electrode. A stirring bar and magnetic stirrer provided convective transport. All measurements were performed at about 25°C in Tris-HCl buffer solution (pH 7.4).

3.2.3 Preparation of stock SiO_2 solution and F-MWCNT solution

A precursor SiO_2 solution was prepared by mixing 4 mL of TEOS, 1 mL of distilled water and 100 µL of 0.1 M HCl in a beaker. The mixture was stirred until a clear solution was obtained. This solution was diluted to four times with distilled water and used throughout the experiment. Two milligram of F-MWCNTs was suspended in a mixture of 200 µL (0.214 g) of triton X-100 and 800 µL of distilled water. It was further diluted with 1 mL of water, under continuous ultrasonic stirring. This black suspension was centrifuged for 30 min (4500 rpm) and the residue was discarded and the resultant suspension was used as F-MWCNT suspension.

3.2.4 Fabrication of enzyme electrode

The enzyme Urs (20mg) was dissolved in 1 mL of phosphate buffer (0.1 M, pH 7.4) containing 0.015 M EDC and 0.03 M NHS. 30 µL of this

enzyme solution was added to the 30 µL of F-MWCNTs suspension (different vials) for the attachment of enzyme to the carboxylic group of F-MWCNTs. This was kept in refrigerator for 1.5 h 10 µL of the above said solution mixture was added to 10 µL sol solution for simultaneous entrapment of the enzyme immobilized F-MWCNTs in the growing hydrolyzed gel-forming silica networks and 5 µL of this was used to cast the film on circular area of 0.28 cm^2 over an ITO glass plate. The film was dried at room temperature and then stored at 4°C.

3.4 RESULTS & DISCUSSION

3.4.1 Characterization of enzyme electrode (Urs/MWCNTs/SiO_2/ITO)

The scheme given in figure 3.1 shows the fabrication of enzyme electrode *(Urs/MWCNTs/SiO_2/ITO)*, wherein the free carboxyl groups present at the surface of the MWCNT/SiO_2 film have been utilized for the covalent attachment of enzyme, Urease, through peptide linkage with an amino group, using the linkage reagents EDC and NHS.

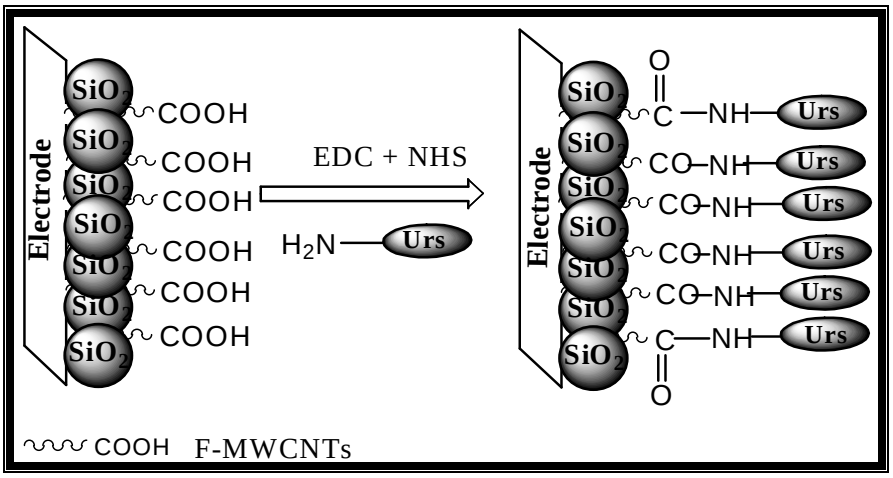

Fig. 3.1: Schematic representation of Urs/MWCNTs/SiO_2/ITO electrode

The Urs/MWCNTs/SiO_2/ITO film was characterized by FTIR spectroscopy. Figure 3.2a shows FTIR spectra of SiO_2. The peak seen at 1090 cm^{-1} was assigned to stretching vibration of Si–O–Si bond [33]. FTIR spectra of COOH modified MWCNTs (F-MWCNTs) shown in figure 3.2b shows a peak at 1634 cm^{-1}, which has been assigned to vibrational mode of carboxyl group [34]. The FTIR spectra of Urs/SiO_2/F-MWCNT (figure 3.2c) shows the characteristic peaks of both SiO_2 and F-MWCNTs at ~ 1086 and 1632 cm^{-1}, respectively, indicating the formation of Urs/MWCNTs/SiO_2 composite. The additional peak observed at ~1697 cm^{-1} which corresponds to C=O stretching (also called as amide I) [35, 36] indicates the presence of immobilized Urs enzyme.

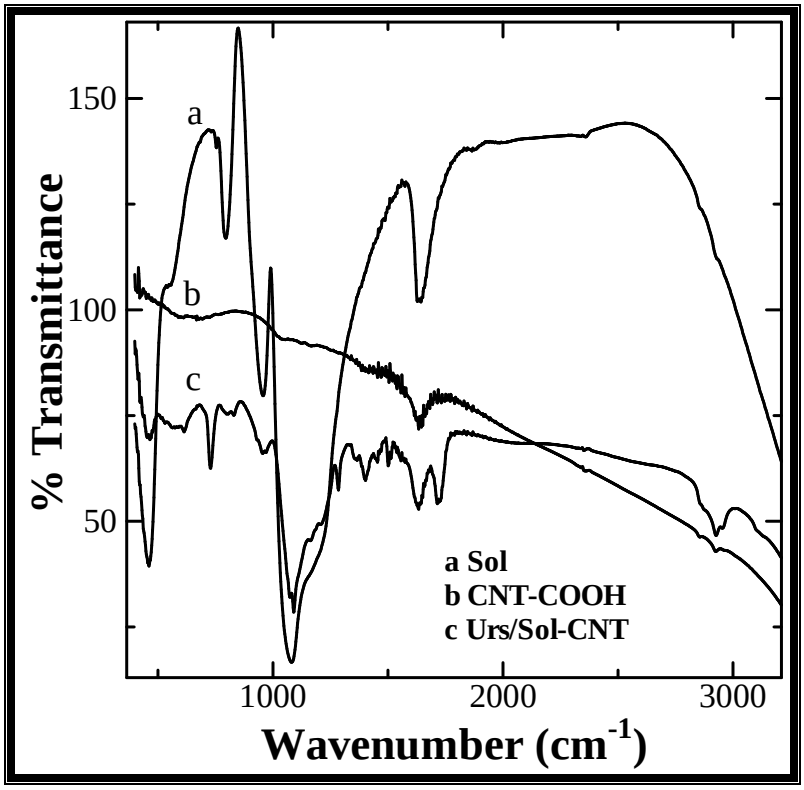

Fig. 3.2: FTIR spectra of (a) SiO_2; (b) F-MWCNT; (c) Urs/MWCNTs/SiO_2/ITO at 25°C

The physical morphology of the native SiO_2, SiO_2/F-MWCNT composite with and without enzyme (Urs) was characterized by scanning electron microscopy (SEM). A typical SEM micrograph of SiO_2 (figure 3.3a) at 20,000 magnifications displays a three- dimensional porous open structure. The SEM micrograph of SiO_2/F-MWCNT (figure 3.3b) shows fine nanotubular structures embedded within the circular particles of silica matrix, which indicate that carbon nanotubes have been well incorporated in the silica matrix. However, the SEM micrograph of enzyme immobilized

Urs/MWCNTs/SiO_2 composite depicted a different morphology having aggregation of globular shaped enzyme molecules surrounding the nanotubes in the silica matrix (figure 3.3c).

The thermal behavior of SiO_2, SiO_2/F-MWCNT and Urs/MWCNTs/SiO_2 were studied by thermal gravimetric analysis (TGA). All the samples were heated under nitrogen atmosphere from room temperature to 800°C, at a heating rate of 10°C/min. The TGA curves are displayed in figure 3.4. For the SiO_2 (sol-gel) and F-MWCNT, the TGA curves shows obvious mass losses at room temperature to about 150 and ~ 500°C, respectively. These mass losses correspond to vaporization of adsorbed water in silica matrix and degradation of MWCNT, respectively [37]. The thermal decomposition of Urs/MWCNTs/SiO_2 completed in three steps. The first step shows the vaporization and desorption of adsorbed water on the MWCNTs/SiO_2 composite surface, at room temperature to 200°C as was found in case of pure SiO_2 gel, whereas the second step shows the slow dehydration of SiO_2 in the said composite of Urs/MWCNTs/SiO_2 at 200-500°C [38]. The third step shows the degradation of carbon nanotubes at 500 to 800°C.

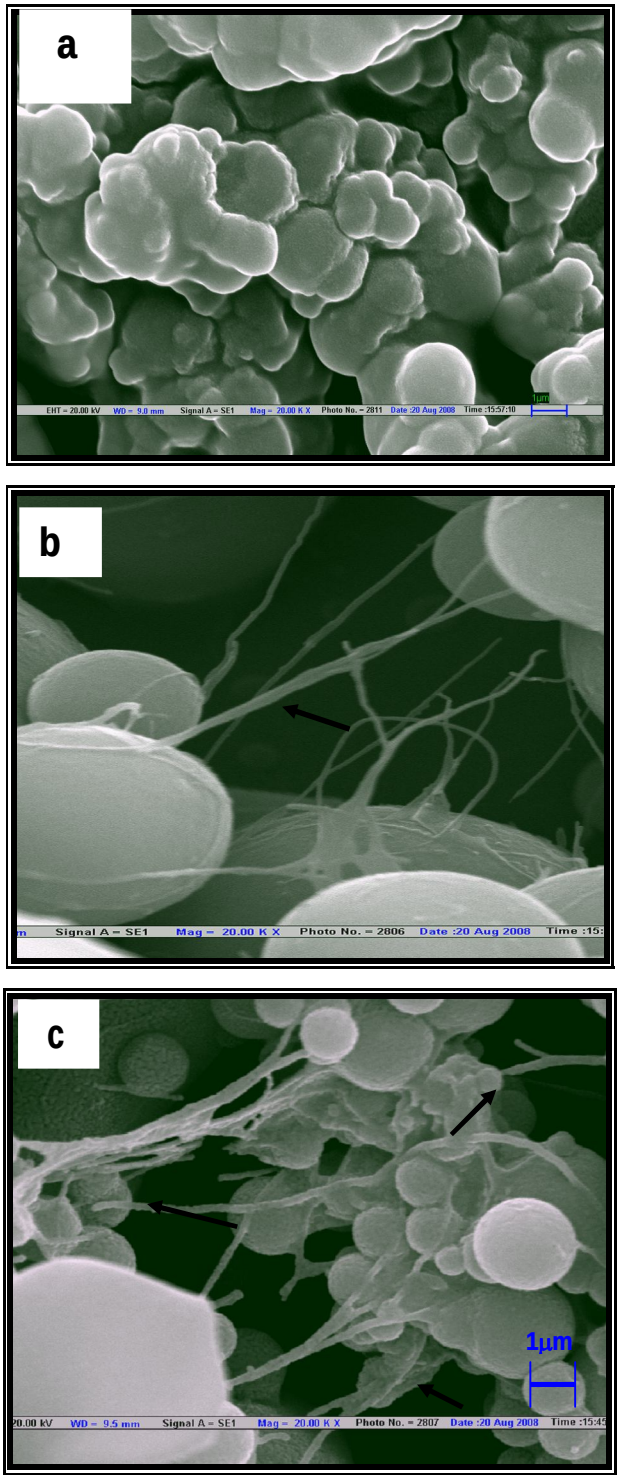

Fig. 3.3: SEM micrographs of (a) SiO_2; (b) MWCNTs/SiO_2; (c) Urs/MWCNTs/ SiO_2 at 20,000 magnification

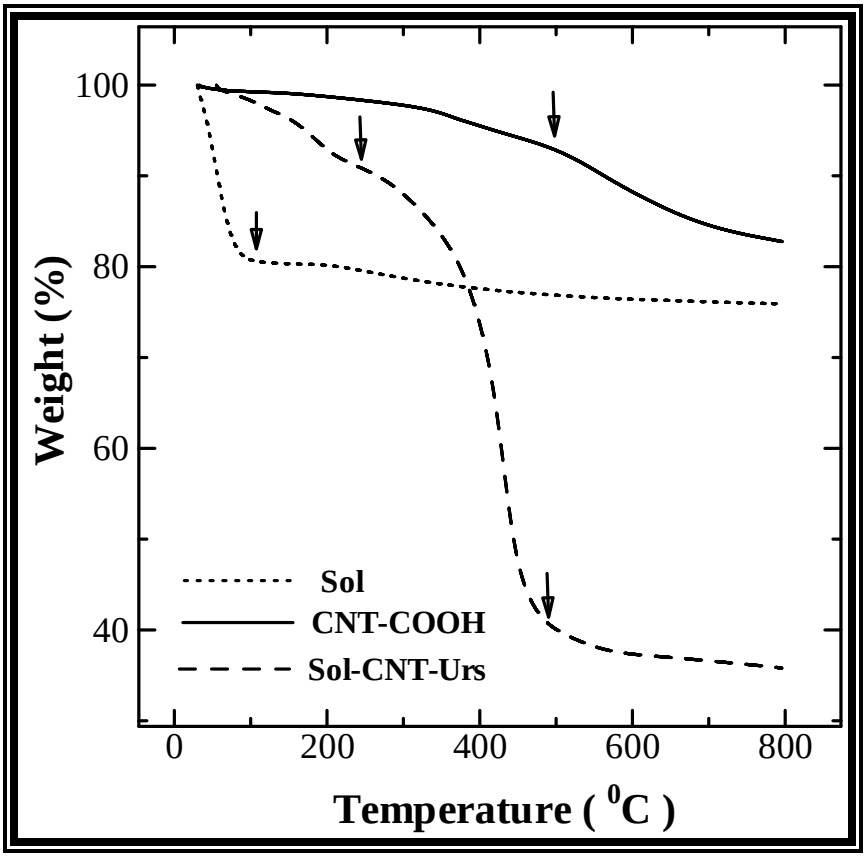

Fig. 3.4: TGA thermograms of SiO_2 (sol); F-MWCNT (CNT-COOH); Urs/MWCNT/SiO_2 (sol-CNT-Urs) measured from room temperature to 800°C, under nitrogen atmosphere

3.3.2 Spectrophotometric response studies

Urease catalyzes the hydrolysis of urea to produce ammonia, which in turn reacts with Nessler's reagent $K_2[HgI]_4$ to form a colored product $NH_2Hg_2I_3$ as shown in the reaction given below:

$$NH_2CONH_2 \text{ (urea)} + H_2O \xrightarrow{\text{Urease}} 2NH_3 + CO_2$$

$$2NH_3 + 2Hg^{II}I_4^{2-} \longrightarrow NH_2Hg_2I_3 (\lambda_{max} = 380 \text{ nm}) + NH_4^+ + 5I^-$$

The electrode (Urs/MWCNTs/SiO_2/ITO) was tested for the leaching of the enzyme, urease, from the surface of the film by placing it in 2 mL Tris-HCl buffer (pH 7.4) solution, for 20 min and assays the solution for urease. The film was taken out after 20 min from the buffer solution and 1 mL of 10 mM urea solution containing 200 µL Nessler's solution was added to check for any possible complex formation of Nessler's reagent with enzymatically produced ammonia in solution. However, no significant absorbance for urease was found in the solution, indicating an efficient covalent entrapment of enzyme, urease, through peptide linkage to the exposed carboxyl functional groups of functionalized MWCNTs.

By continuously monitoring the absorbance at 382 nm for the product $NH_2Hg_2I_3$, urea can be quantified and the analytical performance of the sensor was determined. The response time of the sensor (Urs/MWCNTs/SiO_2/ITO) to urea was tested by continuously monitoring the increasing absorbance at 382 nm with time period for 10 mM urea solution. The analytical response vs time profile of Urs/MWCNTs/SiO_2/ITO is shown in figure 3.5. The 95% response of

the Urs/MWCNTs/SiO_2/ITO to urea is achieved in approximately 15 min and there after the absorbance at 382 nm gets almost saturated. Figure 3.6 depicts the response of Urs/MWCNTs/SiO_2/ITO to varying concentrations of urea. The Urs/MWCNTs/SiO_2/ITO films were placed in different urea concentrations in Tris-HCl buffer (pH 7.4) solution (2 mL) containing identical amount of Nessler's reagent (200 µL) for 15 min before taking the absorbance at 382 nm for individual urea concentration. Figure 3.6 (inset) presents a typical calibration curve for urea.

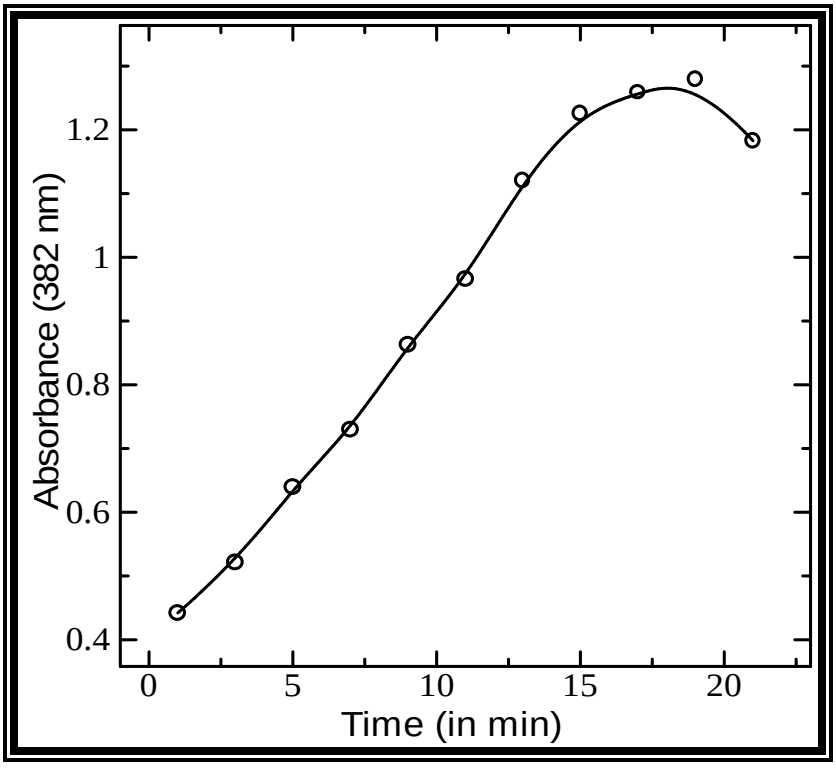

Fig. 3.5: Absorbance (382 nm) vs time profile for an Urs/MWCNTs/SiO_2/ ITO on exposure to Nessler's reagent with 10 mM urea

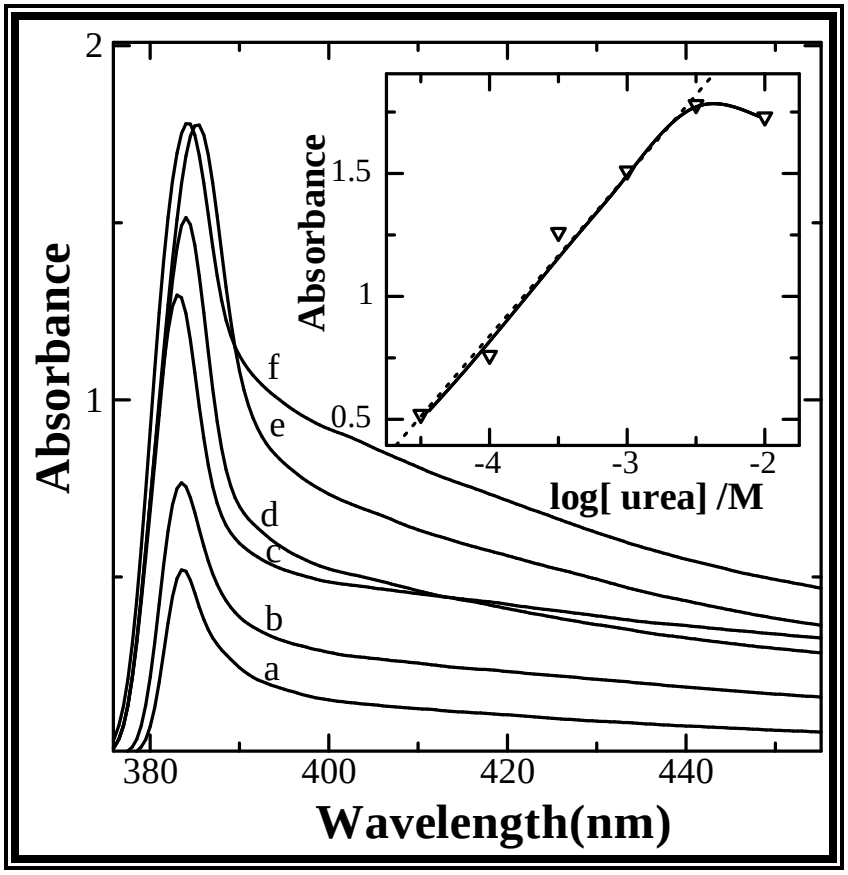

Fig. 3.6: Spectrophotometric response and calibration (λ_{382}) curve (inset) using an Urs/MWCNTs/SiO_2/ITO on exposure to varying concentrations of urea with identical amounts of Nessler's reagent

3.3.3 Potentiometric response characteristics

The potentiometric biosensor is based on the enzymatic reaction of urea hydrolysis catalyzed by urease (Urs) and is represented by the reaction as given below:

$$NH_2CONH_2 \text{ (urea)} + H^+ + 2H_2O \xrightarrow{\text{Urease}} 2NH_4^+ + HCO_3^-$$

By detecting ions consumed or produced in the above enzymatic reaction, urea concentrations are determined. The Urs/MWCNTs/SiO_2/ITO electrodes were tested for the potentiometric response measurements of urea concentration in working solution (10 mM Tris-HCl buffer, pH 7.4).

Potentiometric response were measured after the addition of successive aliquots of urea in Tris-HCl buffer solution (10 mM, pH 7.4, 10mL) under a slow constant stirring of 100 rpm, in accordance to the chronopotentiometric protocol. Figure 3.7 shows the sensitivity of enzyme electrode towards the addition of 100 µL aliquot of different urea concentration, at a time interval of 100 sec.

The enzyme electrode responded rapidly to the urea substrate and at 10-25 sec a 95% drop in the potential was achieved with respect to the potential obtained before the dispensation of urea sample. This quick response is attributed to the incorporation of F-MWCNTs within the silica network, which offers free terminal carboxyl group for the covalent immobilization of enzyme and an increased surface area for both the high enzyme loading and fast electro-catalytical activity.

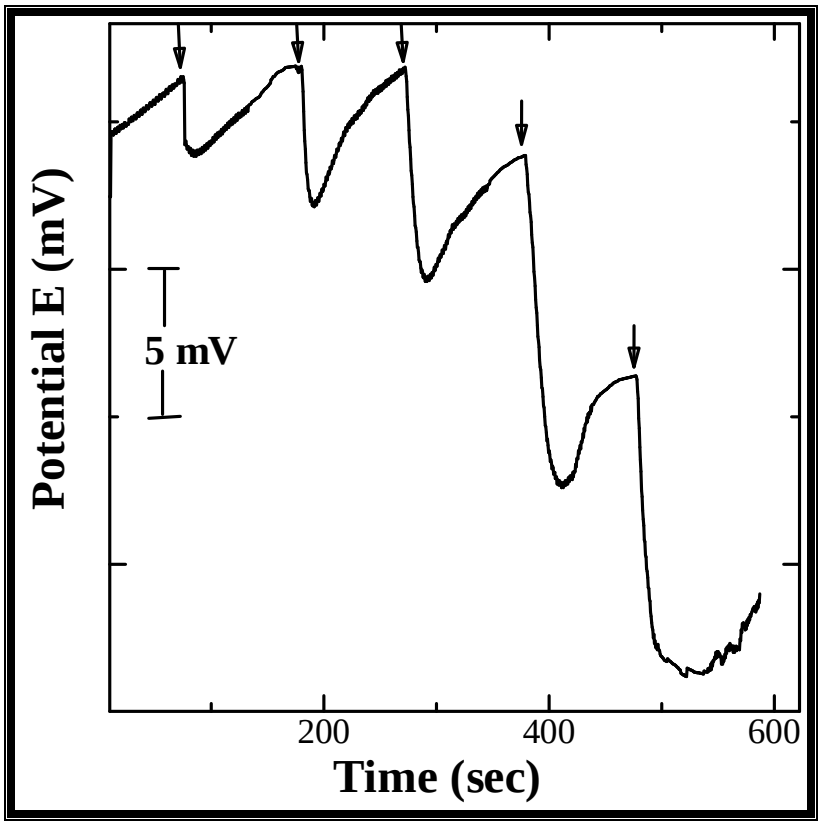

Fig. 3.7: Chronopotentiometric response of biosensor Urs/MWCNTs/SiO_2/ ITO to increasing urea concentration

Figure 3.8 shows the steady state potential dependence calibration curve for the each individual urea concentration. The response of enzyme electrode (Urs/MWCNTs/SiO_2/ITO) to urea was found to be linear in the range of 2.18 x 10^{-5} to 1.07 x 10^{-3} M (r=0.988). This linearity range is in well conformity with that obtained in the spectrophotometric response studies. The slope of the linearity, i.e., the sensitivity of the enzyme electrode towards urea concentrations was 23 mV per decade per cm^2. This low level detection of urea concentration below the physiological range of 1-100 mM urea of urine or blood serum sample would require a dilution of the sample before the analysis. Dilution of the sample is advantageous because the pH could be adjusted to the optimal value and the concentration of interfering species could be reduced in the same step [29, 39].

The reproducibility of the response of the enzyme electrode was investigated for a sample of 1 mM urea concentration. In a series of 10 Urs/MWCNTs/SiO_2/ITO electrodes of the same lot, prepared under identical conditions, give a reproducible response with a RSD of 12.6 % for a sample of 1 mM urea and the RSD value for each sample of different urea concentration is shown in the form of error bar in figure 3.8.

The reusability performance of the electrode was also studied and a continuous fall in the potential response was seen with each repetition, which may be attributed to the swelling of the sol-gel film in the aqueous solution resulting in leaching out of the enzyme immobilized F-MWCNTs from the sol-gel network.

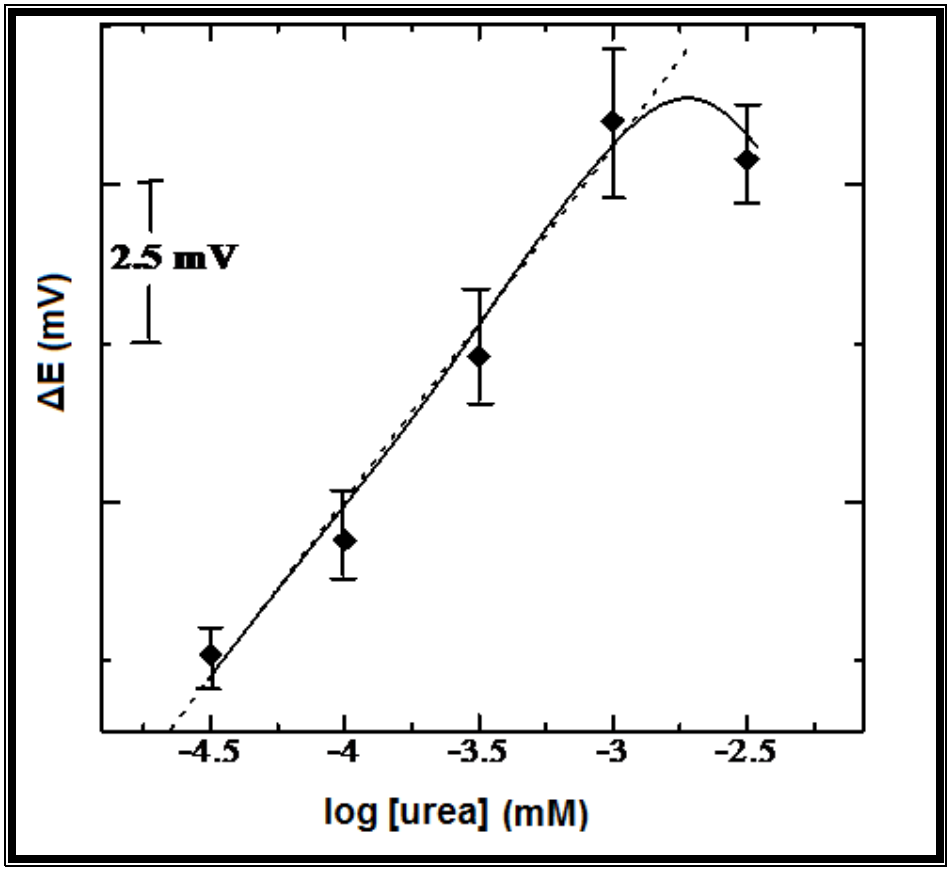

Fig. 3.8: Potential dependence calibration curve of biosensor Urs/MWCNTs/SiO_2/ITO to urea in 10 mM Tris-HCl buffer (pH 7.4)

A few common interfering reagents were studied for any possible interfering effects on the analysis of urea. Known concentrations of 1.0 x 10^{-4} M ascorbic acid .and 5.0 x 10^{-3} M glucose were added both individually and in combination to a sample of 1.0 mM urea solution. However, no significant

interfering effects have been found using these reagents on the potential response of the electrode for the said sample.

3.3.4 Sensor stability and storage conditions

The biosensor stability was studied by monitoring the potential response of at least 10 electrodes of the same lot, prepared under identical conditions, for a period of 10 weeks, at a temperature of about 25°C and 4-5°C, respectively. The potential response of the electrode sharply decreases for 1 mM urea sample after 2 weeks when stored at about 25°C because of rapid enzyme inactivation. However, the electrodes stored at 4-5°C, exhibit an average decrement of 8% in potential response (figure 3.9) up to a period of 7 weeks and thereafter show a sharp fall with an average decay of 22% in potential response. This long-term stability and response time (< 25 sec) of Urs/MWCNTs/SiO_2/ITO electrode is better than the recently reported urea biosensors [4, 6, 7, 29, 31, 40-43] as shown in table 3.1.

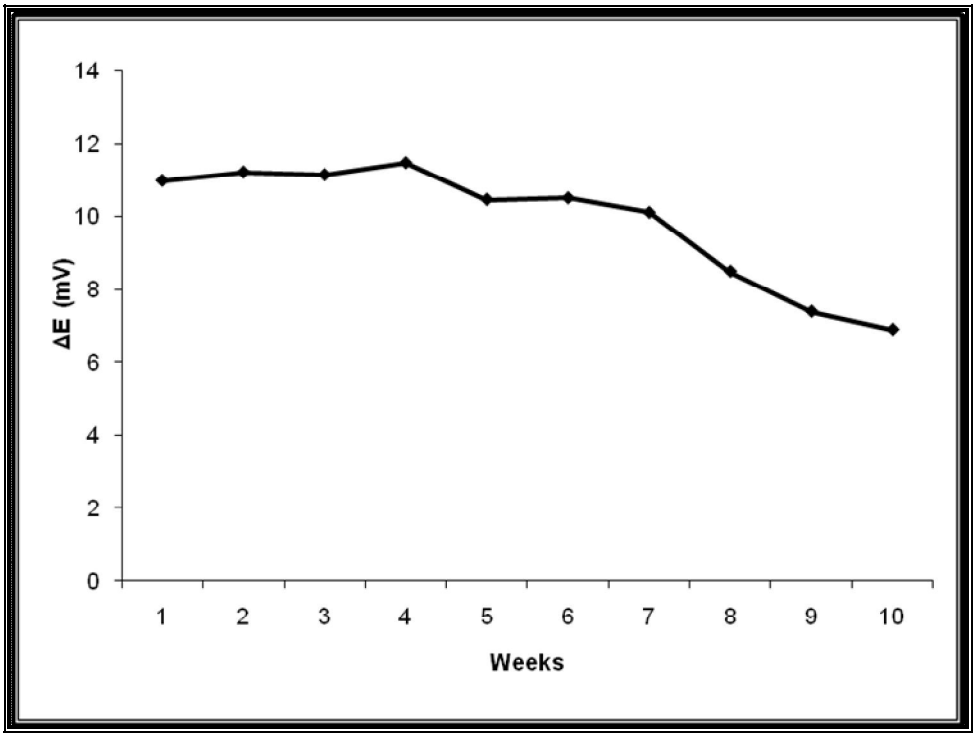

Fig. 3.9: Shelf life period of the Urs/MWCNTs/SiO_2/ITO electrode

Table 3.1: Characteristics of some urea biosensors

Matrix	Response time	Stability	Linear range	Sensitivity	Reference
SnO_2/ITO	2 min	--	0.31 to 120 mg/dl		4
PNVK/SA/urease LB film	2 min	5 weeks	0.5 to 68 mM	10 mV/mM	6
TMOS derived sol–gel silicate matrix	5 min	25 days		dpH/dp(C) = 2.4	7
Toluidine blue film/ graphite electrode	20-30 sec		up to 0.8 mM		29
poly(*o*-phenylenedi-amine) modified graphite electrode	3–5 min	--	0.002 to 0.75 mM	15.2 mA/M cm	31
Poly(N-3-aminopropyl pyrrole-co-pyrrole)	25–50 sec	2 months	6.3×10^{-6} to 4.07×10^{-4} M		40
PPy		--	0.5×10^{-3} to 100×10^{-3} M	17.5 mV/ decade	41
PPy/BSA	70-90 sec	2 months	6.6×10^{-6} to 7.5×10^{-4} M	17.3 mV/ decade	42
Polyvinyl alcohol	2–4 min	1 month			43
SiO_2/ MWCNT	10-25 sec	>2 months	2.18×10^{-5} to 1.07×10^{-3} M	23 mV /decade /cm^2	Present work

3.4 CONCLUSIONS

In this paper, carboxyl modified MWCNTs (F-MWCNTs) combined with sol-gel technique was used for the fabrication of potentiometric urea biosensors. The enzyme Urease (Urs) was covalently immobilized with the COOH group of F-MWCNTs through carbodimide coupling and was subsequently incorporated within the silica matrix. The sol-gel matrix provides a biocompatible environment for the entrapment of enzyme, Urs, linked F-MWCNTs. The F-MWCNTs offer an increased loading of enzyme, urease, with high electro-catalytical activity. This synergistic effect of biocompatible sol-gel matrix and electro catalytic active F-MWCNTs provide a stable and highly sensitive urea biosensor. The developed biosensor exhibited a wide linear range of urea detection in aqueous solution and fast response time in comparison to the recently reported urea biosensors.

3.5 REFERENCES

1. Rivas GA, Rubianes MD, Rodriguez MC, Ferreyra NF, Luque GL, Pedano ML, Miscoria SA, Parrado C. *Talanta* 74 (2007) 291.
2. Balasubramanian K, Burghard M. *Anal. Bioanal. Chem.* 385 (2006) 452.
3. Paradise M, Goswami T. *Mater. & Design* 28 (2007) 1477.
4. Chena J-C, Choub J-C, Sunc T-P, Hsiung S-K. *Sens.& Actuators B* 91 (2003) 180.
5. Xie B, Mecklenburg M, Danielsson B, Ohman O, Nolin P, Winquist F. *Analyst* 120 (1995) 155.
6. Singhal R, Gambhir A, Pandey MK, Annapoorni S, Malhotra BD, *Biosens. Bioelectron.*17 (2002) 697.
7. Tsai HC, Doong RA. *Biosens. Bioelectron.* 20 (2005) 1796.
8. Correia DPA, Magalhaes JMCS, Machado AASC, *Talanta* 67 (2005) 773.
9. Lui B, Hu R, Deng J. *Anal. Chim. Acta* 341 (1997) 161.
10. Gupta R, Chaudhury NK. *Biosens. Bioelectron.* 22 (2007) 2387.
11. Gill I. *Chem. Mater.* 13 (2001) 3404.
12. Tao Z, Tehan EC, Tang Y, Bright FV. *Anal. Chem.* 78 (2006) 1939.
13. Baibarac M, Gymez-Romero P. *J. Nanosci. Nanotechnology* 6 (2006) 1.
14. Wu HP, Wu XJ, Ge MY, Zhang GQ, Wang YW, Jiang JZ.. *Compos. Sci. Technol.* 67 (2007) 1116.
15. Sandler JKW, Kirk JE, Kinloch IA, Shaffer MSP, Windle AH. *Polymer* 44 (2003) 5893.

16. Moisala A, Li Q, Kinloch IA, Windle AH. *Compos. Sci. Technol.* 66 (2006) 1285.

17. Li C, Thostenson ET, Chou T-W. *Composites Sci. Technol*. 68 (2008) 1227.

18. Zhang B, Fu RW, Zhang MQ, Dong XM, Lan PL, Qiu JS. *Sens. Actuators B* 109 (2005) 323.

19. Wei C, Dai LM, Roy A, Tolle TB. *J. Am. Chem. Soc.* 128 (2006) 1412.

20. Yoon H, Xie JN, Abraham JK, Varadan VK, Ruffin PB. *Smart Mater. Struct*. 15 (2006) S14.

21. An KH, Jeong SY, Hwang HR, Lee YH. *Adv. Mater.* 16 (2004) 1005-1009.

22. Tsai HC, Doong RA, Chiang HC, Chen KT. *Anal. Chim. Acta* 481 (2003) 75.

23. Gulcev MD, Goring LG, Gillian RM, Brennan JD. *Anal. Chim. Acta*, 457 (2002) 47.

24. Huang J, Song Z, Li J, Yang Y, Shi H, Wu B, Anzai JI, Osa T, Chen Q. *Mater. Sci. & Eng. C* 27 (2007) 29.

25. Song Z, Zhao Z, Qin X, Huang J, Shi H, Wu B, Chen Q. *Front. Chem. China* 2 (2007) 146.

26. Alegret S, Bartroli J, Jimenez C, Martinezer-Fabregas E, Martorel D, Valdes-Perezgasga F. *Sens. Actuator B* 16 (1993) 453.

27. Soldatkin AP, Bubryak OA, Starodub NF, Elskaya AV, Shul'ga AK, Strikha AA. *Russ. J. Electrochem.* 29 (1993) 279.

28. Pijanovska D, Jaffrezic-Renault N, Martelet C, Torbicz W. *Recent Res. Devel. Electroanal. Chem.* 3 (2001) 7.

29. Vostiar I, Tkac J, Sturdik E, Gemeiner P. *Bioelectrochemistry* 56 (2002) 113.

30. Pizzariello A, Stredansky M, Stredanska S, Miertus S. *Talanta* 54 (2001) 763.

31. Stredansky M, Pizzariello A, Stredanska S, Miertus S. *Anal. Chim. Acta* 415 (2000) 151.

32. Lakard B, Herlem G, Lakard S, Antoniou A, Fahys B. *Biosens. Bioelectron.* 19 (2004) 641.

33. Riklin A, Katz E, Willner I, Stocker A, Buckmann AF. *Nature* 376 (1995) 672.

34. Situmorang M, Gooding JJ, Hibbert DB, Barnet D. *Biosens. Bioelectron.* 13 (1998) 953.

35. K. Babooram, R. Narain, *ACS Appl. Mater. Interfaces* 1 (2009) 181.

36. Kim W-J, Kang S-O, Ah CS, Lee Y-W, Ha DH, Choi IS, Yun WS. *Bull. Korean Chem. Soc.* 25 (2004) 1301.

37. Itoh K, Ohe C, Tsurumaru T, Yasukawa S, Yamaguchi T, Kasuya G. *Vibrational Spect.* 29 (2002) 197.

38. Hartgerink JD, Granja JR, Milligan RA, Ghadiri MR. *J. Am. Chem. Soc.* 118 (1996) 43.

39. Kovacs B, Nagy G, Dombi R, Toth K. *Biosens. Bioelectron.* 18 (2003) 111.

40. Rajesh, Bisht V, Takashima W, Kaneto K. *React. & Funct. Polym.* 62 (2005) 51.

41. Adeloju SB, Shaw SJ, Wallace GG. *Anal. Chim. Acta* 281 (1993) 621.

42. Ahuja T, Mir IA, Kumar D, Rajesh. *Sens. & Actuators B* 134 (2008) 140.

43. Ciurli S, Marzadori C, Benini S, Delana S, Gessa C. *Soil Biol. Biochem.* 28 (1996) 811.

Chapter IV

Self Assembled Monolayer of Silane based Uric Acid Biosensor

4.1 INTRODUCTION

Mostly, biological molecule links to an electrode surface by physical adsorption which produces a weak surface modification that can not resist to stirring, washing and the substrate is not biocompatible and thus inactivates the biomolecule. To prevent this, the substrate surface is modified with self assembled monolayer (SAM) of organic molecules having biocompatibility with biomolecules for efficiently coupling [1-4].

A SAM is an organized layer of amphiphilic molecules in which one end of the molecule, the “head group” shows a special affinity for a substrate. SAMs also consist of a tail with a functional group at the terminal end. SAMs are created by the chemisorption of hydrophilic “head groups” onto a substrate from either the vapor or liquid phase [5] followed by a slow two-dimensional organization of hydrophobic “tail groups” [6]. Initially, adsorbate molecules form either a disordered mass of molecules or form a “lying down phase”, and over a period of hours, begin to form crystalline or semicrystalline structures on the substrate surface [7, 8]. The hydrophilic “head groups” assemble together on the substrate, while the hydrophobic tail groups assemble far from the substrate. Areas of close-packed molecules nucleate and grow until the surface of the substrate is covered in a single monolayer. Self-assembled monolayers, SAMs, are formed when surfactant molecules spontaneously adsorb in a monomolecular layer on surfaces. Adsorbate molecules adsorb readily because they lower the surface energy of the substrate [7] and are stable due to the strong chemisorption of the “head

groups." These bonds create monolayers that are more stable than the physisorbed bonds of Langmuir–Blodgett films [9, 10].

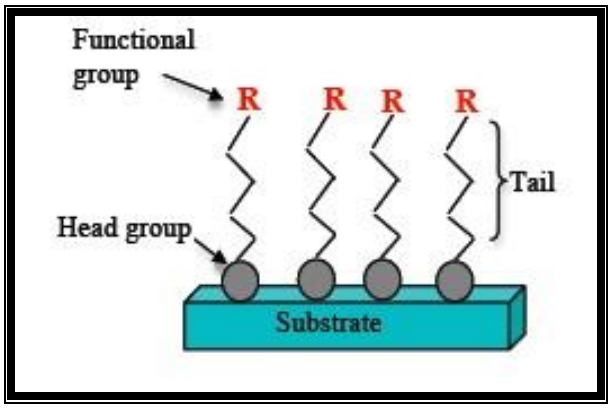

SAMs offer a unique combination of physical properties that allow fundamental studies of interfacial chemistry, solvent-molecule interactions and self-organization. Using SAMs to functionalize noble metal surfaces provides a simple route to functionalize electrode surfaces by organic molecules (both aliphatic and aromatic) containing free anchor groups such as thiols, disulphides, amines, acids or silanes for improved stability of biomolecules. This provides a simple route to organise suitable organic molecules on noble metal and selected nanocluster surfaces by using monolayers of long chain organic molecules with various functionalities like –SH, –COOH, $–NH_2$, silanes etc. These surfaces can be effectively used to build-up interesting nano level architectures. Due to high affinity of SH groups to metals, thiol-terminated SAMs have attracted tremendous attention for construction of biomolecular electronic devices. Thiols form SAMs on gold, silver, copper, platinum, palladium and copper, and on InP and GaAS. However, thiols on

gold make the strongest bond and are known to be very stable. Hence, oraganosulphur (thiols)-based SAMs, due to excellent stability and integration with biomolecular electronic devices, has been widely investigated for a variety of bioelectronic applications including biosensors

The stability, uniform surface structure and relative ease of varying thickness of a SAM make it suitable for development of biosensors. And the immobilization of biomolecules on a SAM requires very small amount and desired analytes can be easily detected via various transduction modes. The use of an appropriate SAM helps in oriented and controlled immobilization of biomolecules [11-13]. SAMs can be used to prevent protein denaturation at an electrode surface and for enhancing stability of biomolecules [14, 15]. SAMs can be utilized to functionalize gate material of a field-effect-transistor (FET) [16]. Aung et al. have investigated performance of streptavidin films immobilized using the biotin–thiol method and biotin–BSA method using quartz crystalmicro-balance (QCM) and surface Plasmon resonance (SPR). These studies suggest that streptavidin film assembled on the biotin–thiol-treated surface provides better platform and results in more efficient DNA capture ensuring better sensitivity for DNA hybridization detection [17].

One of the important advantages of SAM is that they can be prepared in the laboratory by simply dipping the desired substrate in the required millimolar solution for a specified time followed by thorough washing with the same solvent and drying. Gas-phase evaporation of the adsorbant can also form good monolayers, although structural control is difficult. Several factors affect the formation and packing density of monolayers, like nature and

roughness of substrate, solvent used, nature of the adsorbate, temperature, concentration of adsorbate etc. Cleanliness and crystallinity of the substrate also play a crucial role in determining the compactness, often quantitatively estimated by the pinhole distribution. 3-Aminopropyltriethoxysilane (APTES) provides aqueous solvent compatibility and is used to prevent dye leaching by covalently attaching the dye to a matrix through the amino group [18-21]. APTES is one of the most frequently used organosilane agents for the preparation of amino terminated films on silicon substrates [22-26]. A general consensus regarding the APTES film formation is that silanization begins with the hydrolysis of ethoxy groups in APTES, a process catalyzed by water, leading to the formation of silanols. APTES silanols then condense with surface silanols forming a monolayer of APTES via a lateral siloxane network in which amino groups are oriented away from the underlying silicon surface. Electrochemical techniques like cyclic voltammetry [27], and impedance measurements [28, 29] are easy techniques for monitoring monolayer characteristics. These electrochemical studies also provide useful information about the distribution of defects like pinholes, redox property of attached groups.

Uric acid (UA) or urate is the primary end-product of purine metabolism, which is present in biological fluids, such as blood and urine [30]. The normal level of UA in serum is between 0.13 and 0.46 mM (2.18–7.7 mg dL^{-1}) [31], and in urinary excretion is between 1.49 and 4.46 mM (25–74 mg dL^{-1}) [32, 33]. The presence of abnormal uric acid levels lead to gout, chronic renal disease, some organic acidemias, leukemia, pneumonia and Lesch–

Nyhan syndrome [34]. Hence, the detection of uric acid in body fluids is clinically important indicator. Different methods like colorimetric, flourometric, spectrophotometric, and electrochemical analysis have been used to determine the concentration of uric acid, but due to simplicity, selectivity, sensitivity and low cost instrumentation, electrochemical methods are favoured. Uricase also known as Urate oxidase (UOx) is a homotetrameric enzyme containing four identical active sites situated at the interfaces between its four subunits. UOx is made up of 301 residues and has a molecular weight of 33438 dalton. It is unique among the oxidase in that it does not require a metal atom or an organic co-factor for catalysis. UOx shows some very interesting properties: it does not need any co-factor nor any metal to catalyze its redox reaction, and no functional group seems to be directly involved in the catalytic mechanism. Today, the chemical reaction pathway of UOx is still largely unknown. A mechanism for the UOx reaction has been proposed earlier in which urate reacts directly with O_2 in a manner analogous to reduced flavin to form a urate hydroperoxide intermediate and produce allantoin and CO_2.

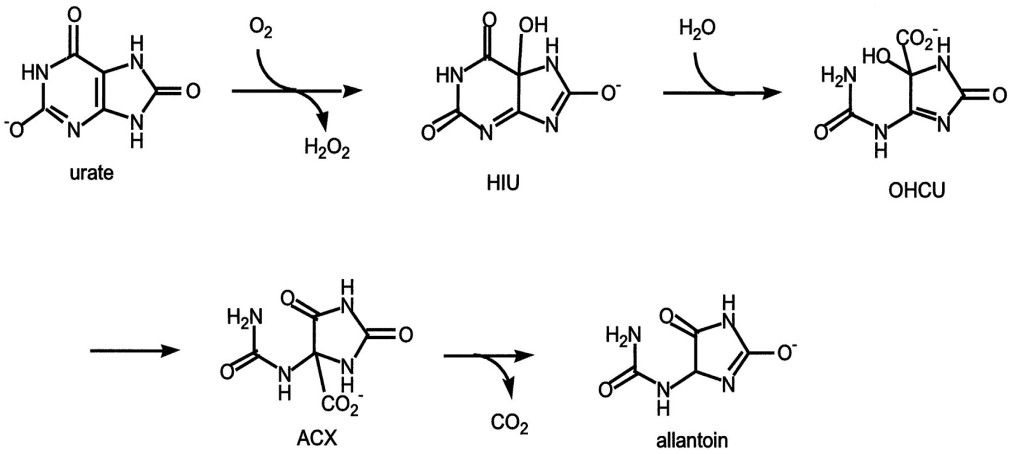

In the enzymatic reaction mechanism (figure 4.1), the enzyme, UOx, catalyzes the oxidation of urate to 5-hydroxyisourate; isotope labeling studies have shown that O_2 is reduced to H_2O_2 during the reaction, and the oxygen atom attached to C5 in the product is derived from solvent [35, 36]. Two intermediates have been reported wherein the first one was assigned to the urate dianion (**I**), which was presumed to be the species that reacts directly with O_2. The second intermediate was assigned to the urate hydroperoxide (**II**) formed from the urate dianion and O_2.

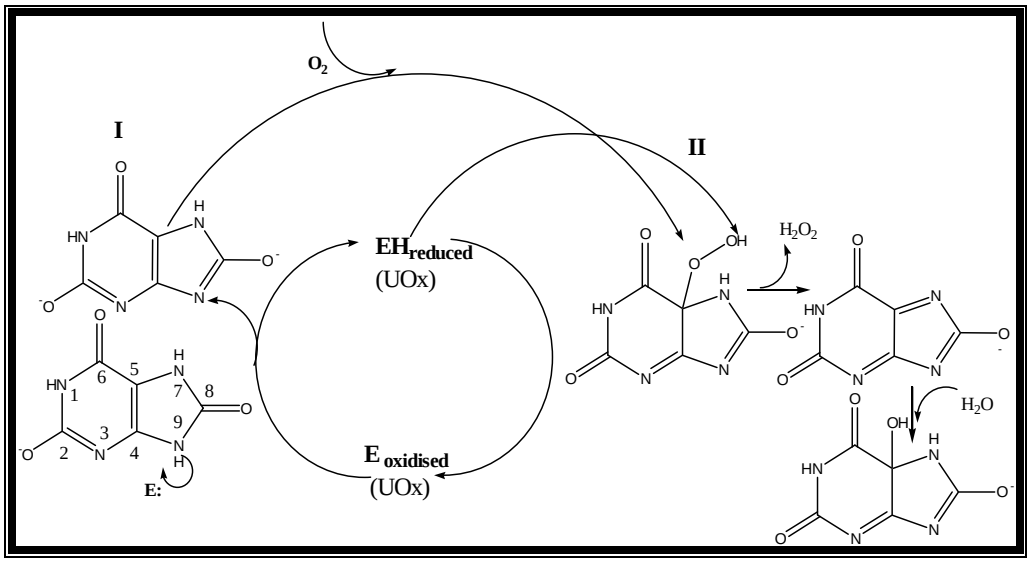

Fig. 4.1: Reaction mechanism of enzyme, UOx, with uric acid

The method based on the determination of H_2O_2 has received considerable interest because H_2O_2 can be detected either by its reduction or oxidation. Quantification of UA can be done conveniently by monitoring the

concentration of enzymatically generated H_2O_2. Since electrochemical oxidation of H_2O_2 requires high potential, other oxidizable species would interfere in the measurement of UA. Therefore, a low potential detection of H_2O_2 is required to avoid the interference from high potential oxidative species. This is done by using a low potential redox probe such as potassium ferricyanide as an electron mediator.

In this study, we describe an amperometric biosensor for the quantitative detection of uric acid in aqueous solution. The surface of the indium tin oxide (ITO) coated glass plate was modified by forming a SAM of 3-aminopropyltriethoxysilane, which was subsequently immobilized with uricase through strong amide bonding by utilizing Bis[sulfosuccinimidyl]suberate as a crosslinking reagent. Bis(sulfosuccinimidyl)suberate (BS^3) is a homobifunctional, water-soluble, non-cleavable and membrane impermeable crosslinker. It contains an amine-reactive *N*-hydroxysulfosuccinimide (NHS) ester at each end of an 8-carbon spacer arm. NHS esters react with primary amines at pH 7-9 to form stable amide bonds, along with release of the NHS leaving group. Proteins, including antibodies, generally have several primary amines in the side chain of lysine (K) residues and the N-terminus of each polypeptide that are available as targets for NHS-ester crosslinking reagents.

The biosensor (Uricase/BS^3/APTES/ITO glass electrode) was characterized by scanning electron microscopy, atomic force microscopy, cyclic voltammetry and electrochemical impedance spectroscopy.

4.2 EXPERIMENTAL

4.2.1 Materials

Enzyme Uricase (EC 1.7.3.3, 9 units/mg from *Bacillus fastidiosus*) was procured from Sigma Aldrich Corp. 3-aminopropyltriethoxysilane (APTES) was purchased from Merck chemicals (Germany). Bis[sulfosuccinimidyl]suberate (BS^3) was obtained from Pierce Biotechnology, USA. Uric acid with 99% purity was purchased from CDH, India. Other chemicals were of analytical grade and used without further purification. Water used in all reactions was double de-ionized (DDI) water obtained from a Millipore purification system.

4.2.2 Equipments

Contact angles were recorded on Drop Shape Analysis System, model DSA10MK2 from Kru''ss GmbH, Germany. Scanning electron micrographs (SEM) were obtained with a LEO 440 PC, UK based digital scanning electron micrograph at an acceleration voltage of 20.0 kV. Atomic force microscopy (AFM) images were obtained on a VEECO/ diCP2, USA scanning probe microscope. Cyclic voltammetry and electrochemical impedance measurements were done on a PGSTAT302N, AUTOLAB instrument from Eco Chemie, The Netherlands. The impedance measurements were performed in the presence of a redox probe $[Fe(CN)_6]^{3-}$ at the scanning frequencies from 0.1 to 100,000 Hz. All measurements were carried out in a

conventional three-electrode cell configuration consisting of a working electrode (Uricase/BS^3/APTES/ITO), Ag/AgCl reference electrode and platinum foil as a counter electrode.

4.2.3 Fabrication of Uricase/BS^3/APTES/ITO electrode

The ITO coated glass plates (1 x 1 cm^2) were cleaned by sequential ultrasonic cleaning in soapy water (extran), acetone, ethanol, isopropyl alcohol and distilled water for 10 min each, and drying in vacuum. Then, the cleaned ITO glass plates were put in plasma chamber and exposed to oxygen plasma for 5 min. Finally the ITO glass plates were once again washed with distilled water and dried in vacuum. Cleaned ITO glass plates were immersed in 2% APTES solution prepared in ethanol for 1.5 h, under ambient conditions, to form a SAM. The glass plates were then rinsed with ethanol in order to remove non-bonded APTES from the surface of the substrate and dried under N_2. 5mM Bis[sulfosuccinimidyl]suberate (BS^3) solution was prepared in sodium acetate buffer, pH 5.0. The APTES coated ITO glass plates were then treated with Bis[sulfosuccinimidyl]suberate (BS^3) solution for 1.0 h, followed by washing with doubled distilled water and dried under N_2. The BS^3 treated APTES/ITO glass plate (BS^3/APTES/ITO) was immersed in uricase solution (~3U) in phosphate buffer solution (PBS), pH 7.4, for a period of 1.5 h. The excess enzyme was removed by rinsing with PBS and finally dried under N_2, at room temperature and the biosensor (Uricase/BS^3/APTES/ITO) were stored at 4°C.

Figure 4.2 shows a scheme for the fabrication of Uricase/BS^3/APTES/ITO electrode, wherein the free NH_2 groups present at the surface of the APTES/ITO electrode have been utilized for the covalent attachment of uricase using the crosslinking reagent Bis[sulfosuccinimidyl]suberate (BS^3).

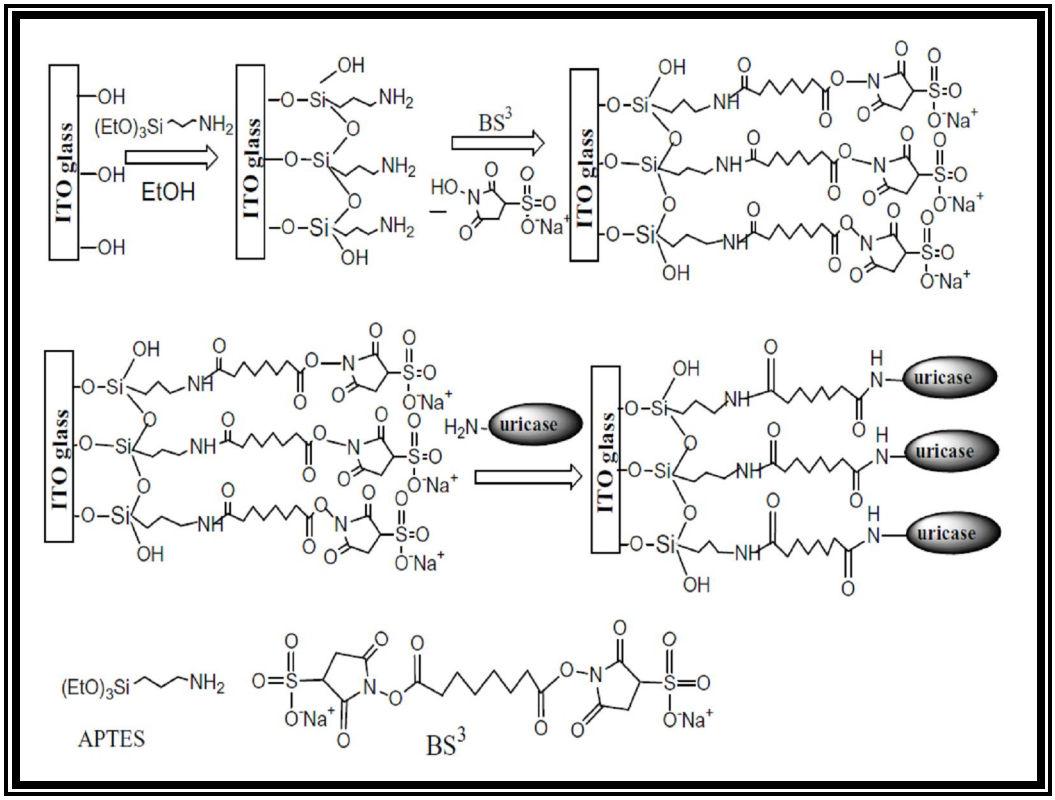

Fig. 4.2: Schematic illustration of each step of surface modification of ITO glass plate and immobilization of enzyme uricase

4.3 RESULTS & DISCUSSION

4.3.1 Characterization of enzyme electrode (Uricase/BS^3/APTES/ITO)

The various modification steps of the electrode surface was characterized by the static sessile drop method. The drop image was stored and an image analysis system calculated the contact angle (θ) from the shape of the drop. The contact angles for individual modification step of the electrode are listed in table 4.1. The hydrophilicity of the surface changes significantly with each step of surface modification. The initial low contact angle value of ~ 39° (figure 4.3a) obtained for bare ITO coated glass plate. This hydrophilic character of the surface is due to the presence of surface hydroxyl group. However, after treating the ITO glass plate surface with APTES, the contact angle was found to increase to ~ 73° (figure 4.3b), a value corresponding to that reported in the previous work [37]. This increase of water drop contact angle with respect to freshly cleaned ITO glass substrate is due to the presence of hydrophobic alkyl chains of APTES molecules. Surface free energy decreases upon silanization with respect to bare substrate (the polar component more than the dispersive component) due to the drastic decrease of hydroxyl groups at the surface because of reaction with silane molecules. The glass electrode surface showed even more hydrophobic character after the covalent immobilization of hydrophobic enzyme molecule crosslinked through Bis[sulfosuccinimidyl]suberate with an

increased contact angle of 90° (figure 4.3c). These results suggested the formation of Uricase/BS^3/APTES/ITO glass electrode.

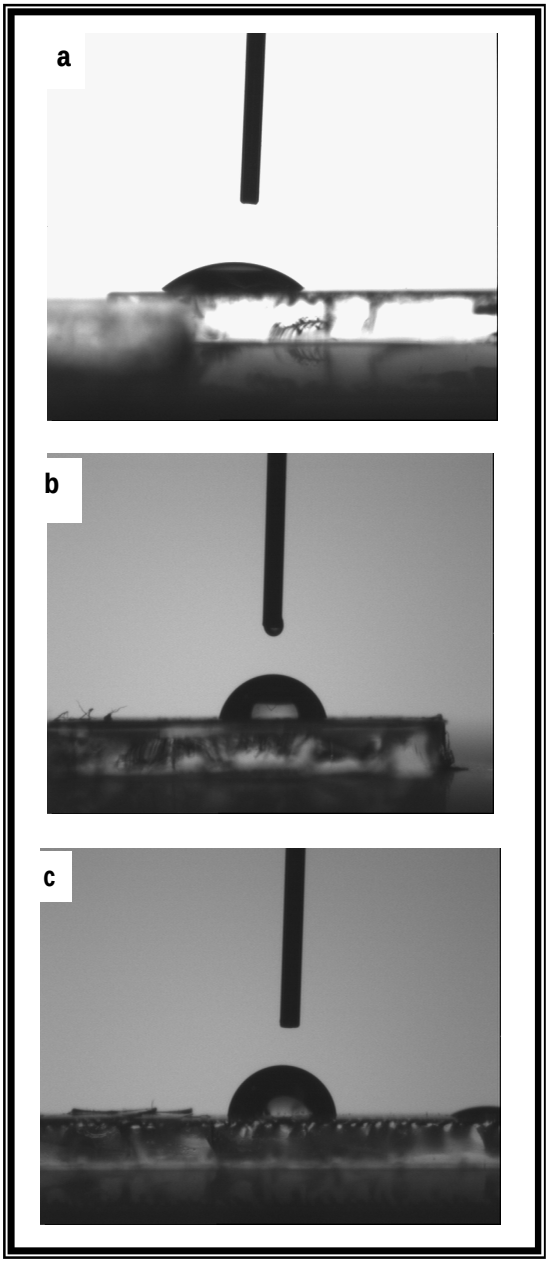

Fig. 4.3: Contact angle measurement images of (a) ITO coated glass plate; (b) APTES/ITO glass; (c) Uricase/BS^3/APTES/ITO glass

Table 4.1: Measurement of contact angle (in °) before and after surface modification of substrate and enzyme immobilization

Type of Electrode	Ist drop	IInd drop	IIIrd drop	IVth drop	Vth drop	Mean
Bare ITO	38.14	39.54	39.78	39.97	40.32	39.55
APTES/ITO	73.83	73.47	73.55	73.72	73.29	73.57
Uricase/BS^3/APTES/ITO	89.90	89.67	91.04	90.59	89.85	90.21

The surface morphology of modified electrode before and after enzyme immobilization was characterized by using scanning electron micrographs and atomic force microscopy (AFM) images. SEM micrograph of the APTES/ITO glass shows a smooth surface (figure 4.4a), whereas in the case of Uricase/BS^3/APTES/ITO glass it shows an aggregation of globular shaped cross-linked enzyme molecules (figure 4.4b) over APTES/ITO film. This has further been analyzed by AFM images taken in a contact mode. Figure 4.5 shows the AFM images of APTES/ITO films in the presence and absence of uricase. In contrast to the relatively globular shaped surface, the surface morphology of the uricase immobilized APTES/ITO glass exhibits the sharp regular island-like structure. The lateral size of the visible features is strongly affected by the convolution effect between the sample and the AFM tip. An average vertical height of about 8 nm in the AFM image of uricase modified APTES/ITO glass surface seems to be in accordance with the size of the uricase enzyme molecule [38].

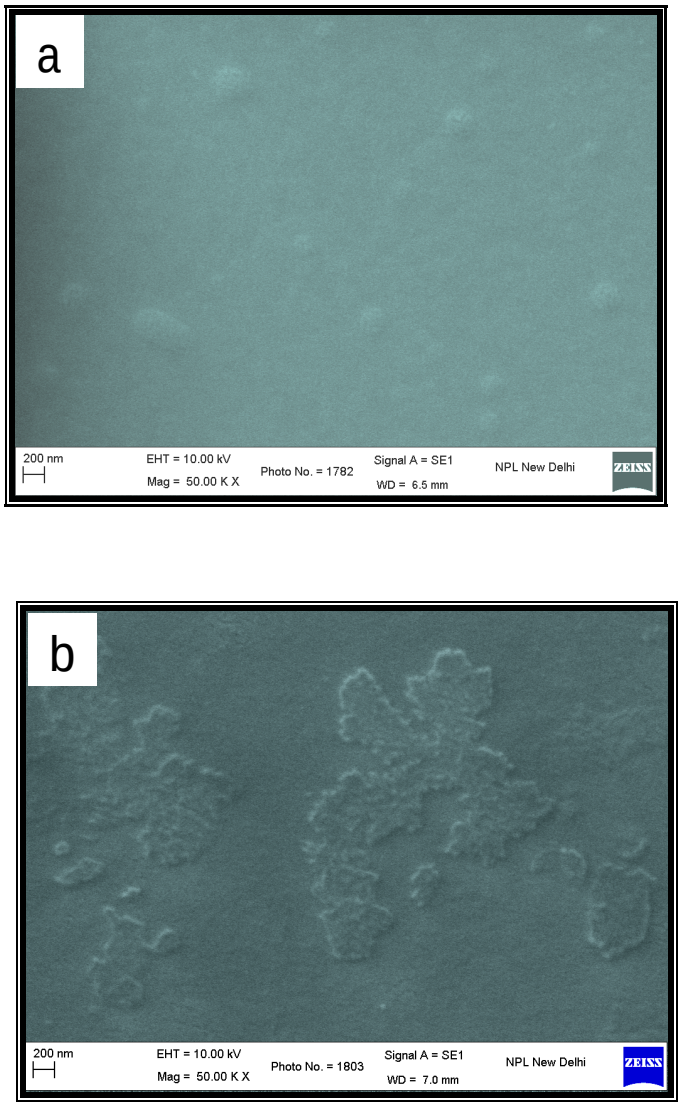

Fig. 4.4: SEM micrographs of (a) APTES/ITO glass; (b) Uricase/BS^3/APTES/ ITO glass at 50,000 magnification

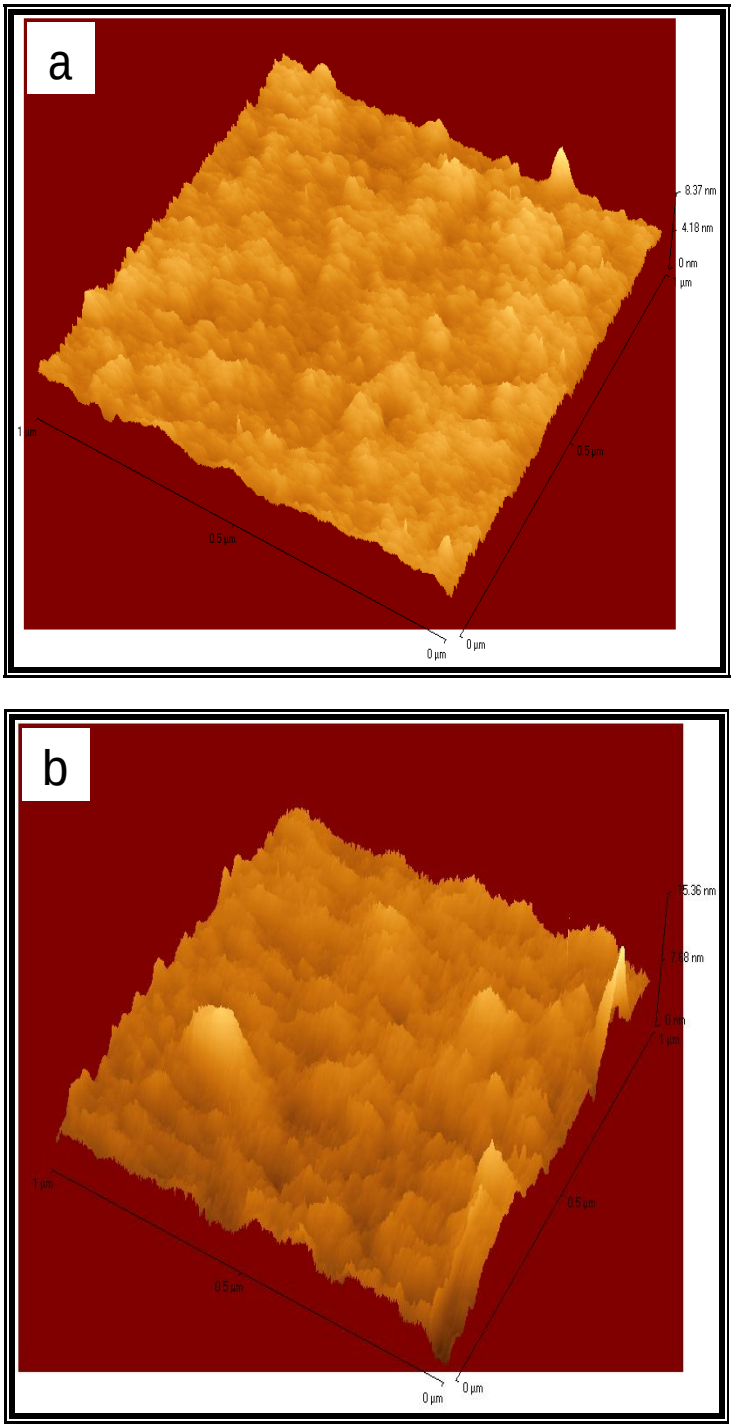

Fig. 4.5: AFM images (1 x 1 μm^2) of: (a) APTES/ITO glass;

(b) Uricase/BS^3/APTES/ITO glass

The Uricase/BS^3/APTES/ITO glass electrode was characterized by cyclic voltammetry and electrochemical impedance spectroscopy. All electrochemical measurements were performed in PBS solution, pH 7.4, containing 0.1 M KCl and 2 mM $[Fe(CN)_6]^{3-}$. The $[Fe(CN)_6]^{3-}$ probe was used as a marker to investigate the changes in electrode behavior after each surface modification step. Each step of surface modification of ITO-glass plate and enzyme immobilization were monitored by cyclic voltammetry. The cyclic voltammogram of the modified electrode before and after the enzyme immobilization is shown in figure 4.6. In all the CV experiments, 3rd cycle was considered as stable one since no significant changes were observed in the subsequent cycles. The bare ITO glass shows a quasi reversible cyclic voltammogram with a peak separation of oxidation and reduction potential (ΔE_p) of 170 mV. On modification with SAM of APTES, it shows a more reversible signal with an increased oxidation and reduction peak current (ΔI_p) of 0.23 mA and a decreased peak separation (ΔE_p) of 128 mV between the cathodic and anodic waves of the redox probe. This reduction in peak potential separation after the formation of APTES layer is attributed to an increased interfacial concentration of the anionic probes ($[Fe(CN)_6]^{3-}$) due to its strong affinity towards the polycatonic (NH_2) layer [39]. However, in contrary to above a decrease in redox peak current (ΔI_p) of 0.19 mA and a significant increase in the peak potential separation (ΔE_p) of 169 mV was observed when APTES modified ITO-glass electrode was treated with a crosslinker, Bis[sulfosuccinimidyl]suberate.

This increased separation of peak potentials indicates a repulsive interaction of polyanions (SO_3^-) with anionic probe $[Fe(CN)_6]^{3-}$, at the surface interface, conforming the formation of a crosslinker BS^3 layer over the surface of APTES/ITO glass. The CV curve shows a further decrease in redox peak current (ΔI_p) of 0.18 mA and an increased peak separation (ΔE_p) of 214 mV between redox waves after the immobilization of enzyme molecules at the surface of the modified electrode (BS^3/APTES/ITO glass). This may be attributed to the formation of insulating layer of uricase enzyme molecule, at the electrode surface, which perturbs the interfacial electron transfer considerably indicating an efficient covalent bonding of enzyme through a crosslinker BS^3.

Each assembled step involved in the fabrication of Uricase/BS^3/APTES/ITO glass electrode was further characterized by electrochemical impedance spectroscopy. The impedance spectroscopy was represented as an equivalent circuit [40] as shown in the inset of figure 4.7. The impedance spectrum, which includes a semicircle portion at higher frequencies, corresponds to the electron transfer limiting process and a linear part at the low frequencies resulting from diffusion limiting step of the electrochemical process. The ohmic resistance of the electrolyte solution (R_s) and the Warburg impedance (Z_w) represents the bulk properties of the electrolyte solution and diffusion features of the redox probe in solution, respectively. The diameter of the semicircle in the Nyquist plots represents the electron-transfer resistance of the layer, and this can be used to describe the interface properties of the modified electrode.

Figure 4.7 shows the electrochemical impedance spectra of the bare and the modified ITO glass electrode before and after the immobilization of the enzyme uricase and the corresponding electron-transfer resistance values are listed in table 4.2. The bare ITO glass shows an electron transfer resistance (R_{et}) value of 3.40 kΩ. The R_{et} value for APTES/ITO glass was strongly reduced to 1.41 kΩ, which indicates an easy electronic transport at the electrode surface interface after the APTES modification of ITO. However, the treatment of the above electrode surface with a crosslinker, BS^3 and its subsequent immobilization with enzyme uricase results in an increased R_{et} values of 3.20 and 5.01 kΩ, respectively. These results are in conformity with the pattern obtained in cyclic voltammetry measurements, further confirming the formation of the Uricase/BS^3/APTES/ITO glass electrode.

Table 4.2: CV peak potential difference (ΔE_p) and the charge-transfer resistance of biosensor before and after each step of ITO glass surface modifications and enzyme immobilization

Type of Electrode	E_{oxi} (mV)	E_{red} (mV)	ΔE_p (mV)	ΔI_p (mA)	Charge transfer resistance R_{et}(kΩcm^{-2})
Bare ITO	243	71	170	0.218	3.40
APTES/ITO	207	79	128	0.231	1.41
BS^3/APTES/ITO	232	63	169	0.196	3.20
Uricase/BS^3/APTES/ITO	260	46	214	0.180	5.01

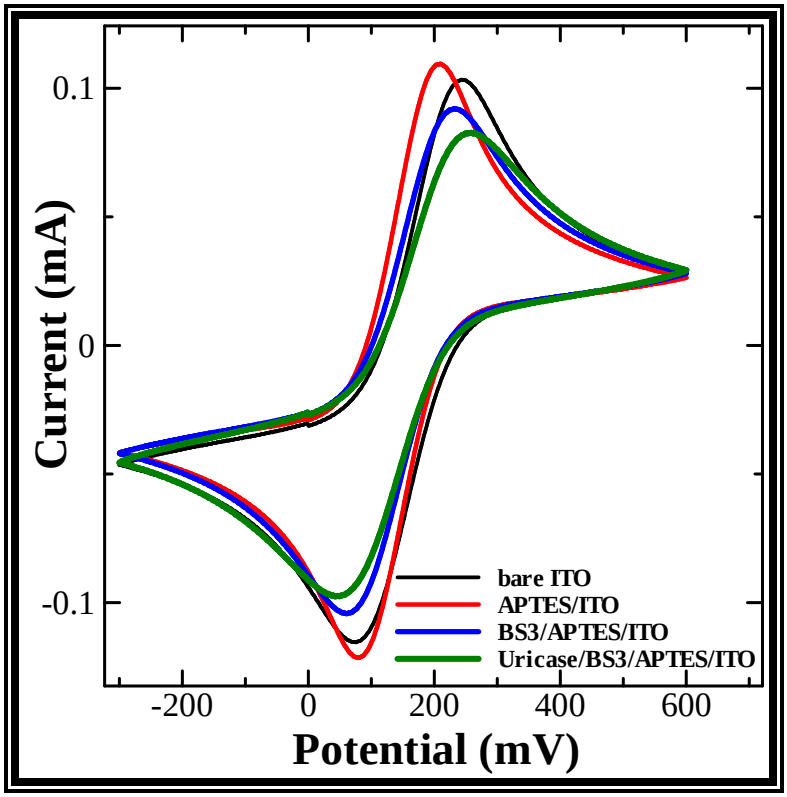

Fig. 4.6: Cyclic voltammograms of: bare ITO glass; APTES/ITO glass; BS^3/APTES/ITO glass and Uricase/BS^3/APTES/ITO glass in 0.1 M KCl solution containing 2 mM $[Fe(CN)_6]^{3-}$; scan rate 25 mV/s; 3rd cycle voltammogram is shown

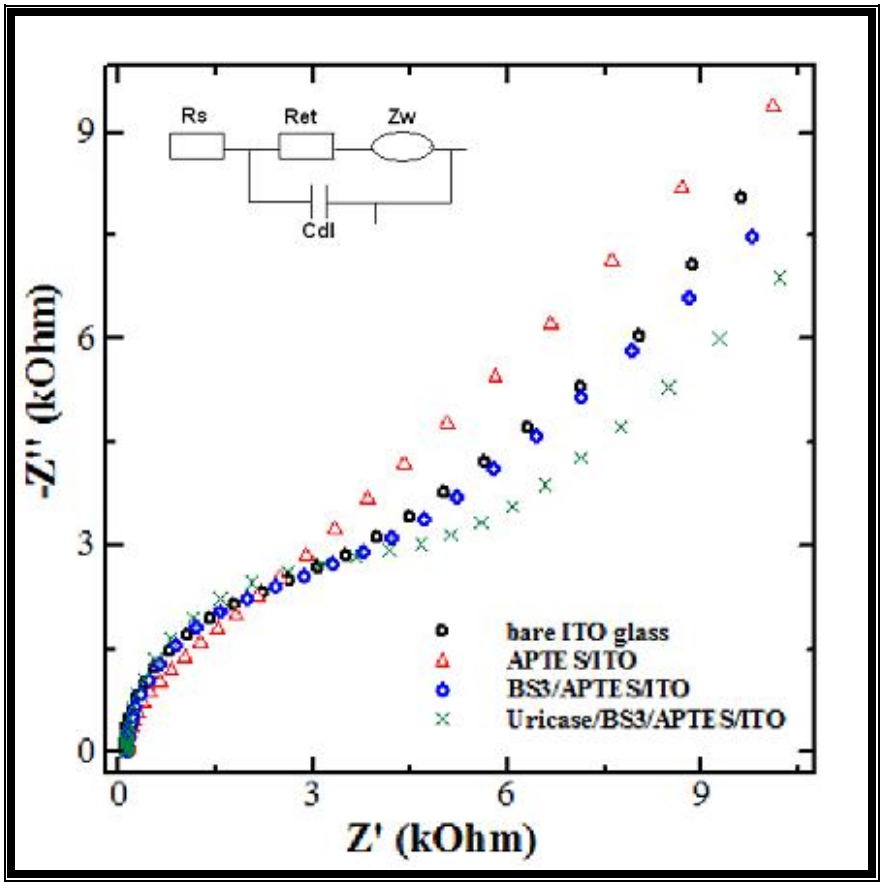

Fig. 4.7: Nyquist plots obtained for bare ITO glass, APTES/ITO glass, BS^3/APTES/ITO glass and Uricase/BS^3/APTES/ITO glass electrodes in 0.1 M KCl solution containing 2 mM $[Fe(CN)_6]^{3-}$. Inset shows a schematic diagram of equivalent circuit for impedance spectroscopy in the presence of redox couple: R_s, resistance of the electrolyte solution; Ret, electron-transfer resistance; Z_w, Warburg impedance; C_{dl}, double-layer capacitance

4.3.2 Amperometric response of Uricase/BS^3/APTES/ITO glass electrode

Chronoamperometric response studies were conducted with Uricase/BS^3/APTES/ITO glass electrode, at a bias voltage of 0.26 V vs Ag/AgCl in PBS; pH 7.4 containing 2 mM $[Fe(CN)_6]^{3-}$. The amperometric response was measured with the successive addition of each 100 µL aliquot of uric acid in 2 mL PBS solution, at an interval of 100 sec. The scheme of amperometric response obtained in an enzymatic reaction mechanism is shown in figure 4.8.

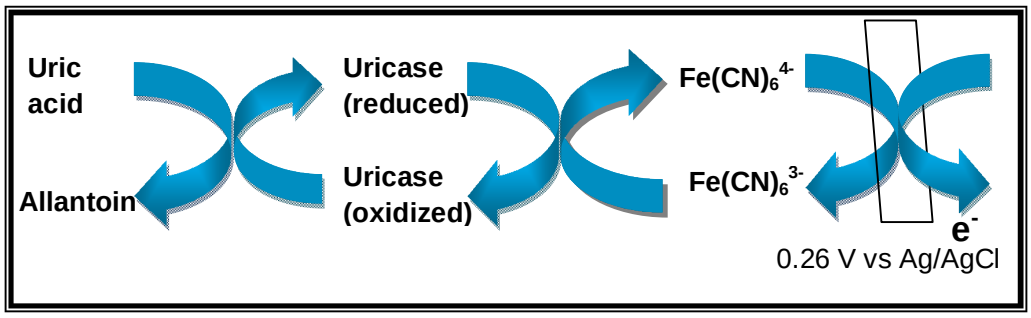

Fig. 4.8: Enzymatic reaction mechanism of working of Uricase/BS^3/ APTES/ITO electrode

Figure 4.9 depicts the chronoamperometric response of Uricase/BS^3/ APTES/ITO glass electrode along with the reusable response performance as a function of uric acid concentration in aqueous solution. An increasing order of amperometric response was observed after each successive addition of the aliquot of increasing uric acid concentration. The 95% steady state current response to uric acid was obtained in about 50 sec.

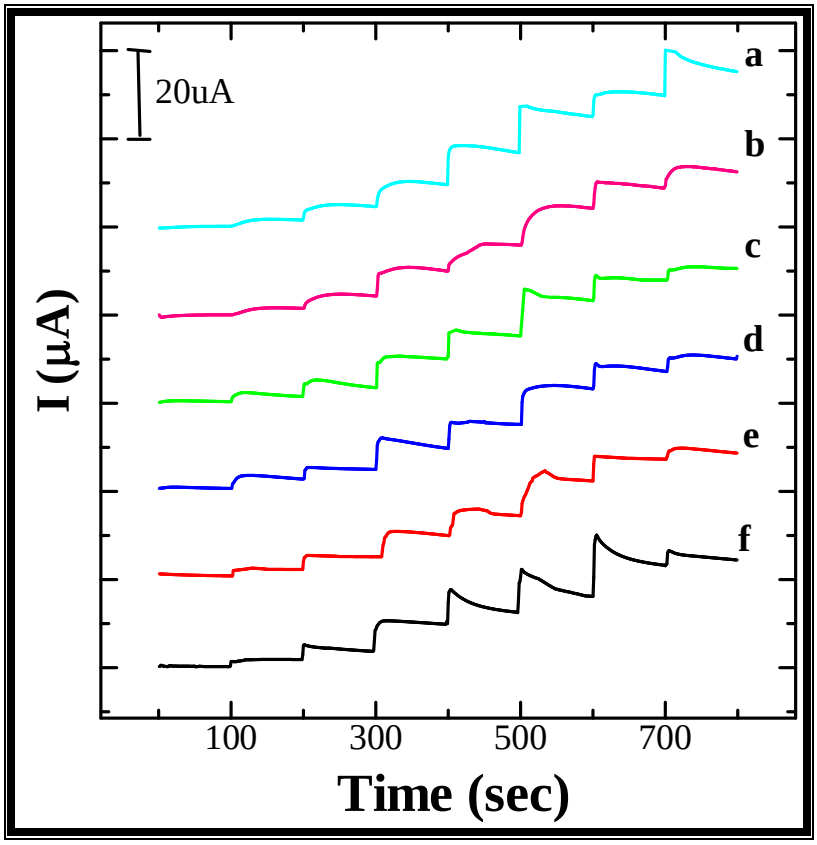

Fig. 4.9: (a) Chronoamperometric response curve of uricase/BS^3/APTES/ITO with addition of different concentration of uric acid; repeatability performance of the same electrode from n = 2-6 time (b-f)

Figure 4.10 shows the steady state current dependence calibration curve to uric acid concentration. The response of the Uricase/BS^3/APTES/ITO glass electrode to uric acid was found to be linear in the range of 0.05 to 0.58 mM with a correlation coefficient of 0.993 (n=5). The lowest detection limit of the electrode was 0.037 mM at a signal-to-noise ratio of 3. The slope of the linearity, i.e., the sensitivity of the enzyme electrode towards uric acid was 39.35 $\mu AmM^{-1}cm^{-2}$, which is relatively better than the recently reported biosensors.

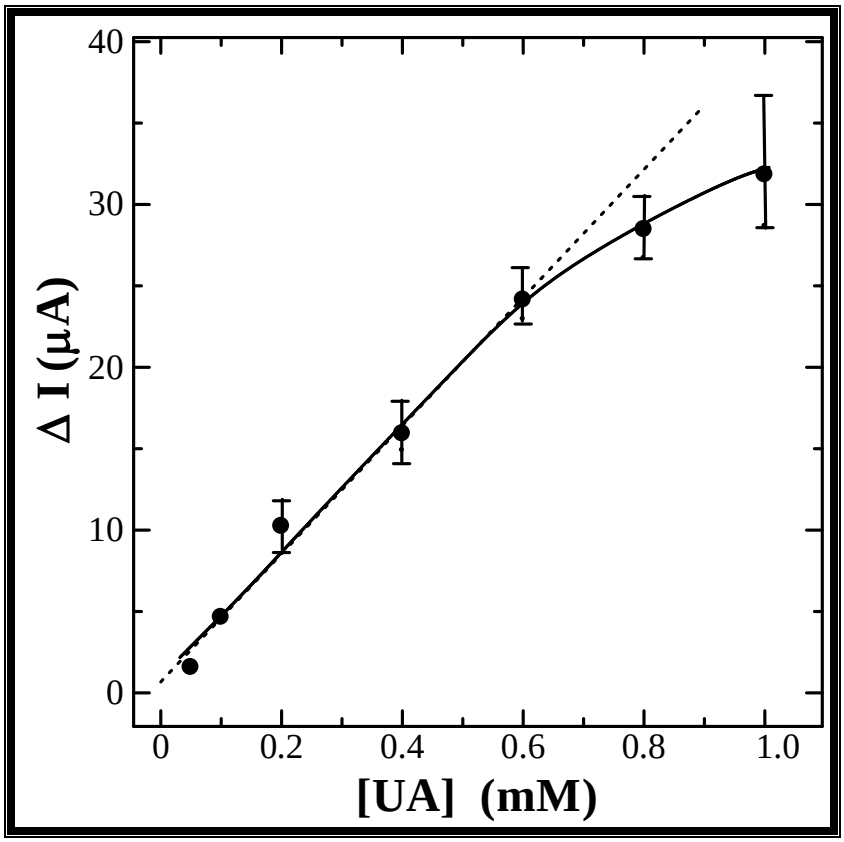

Fig. 4.10: Steady state current dependence calibration curve of Uricase/BS^3/ APTES/ITO biosensor to uric acid

The reusability of the modified electrode was also tested by conducting the same experiment for several times, under identical conditions. The results were found to be reproducible within a range of the RSD value of 2.5 to 5.1% for 0.05 to 0.6 mM uric acid concentration (n = 3-5), as shown in figure 4.11. The reproducibility of the Uricase/BS^3/APTES/ITO glass electrode was investigated in a series of 10 electrodes for 0.2 mM uric acid sample and a relative standard deviation of 7.9% was obtained.

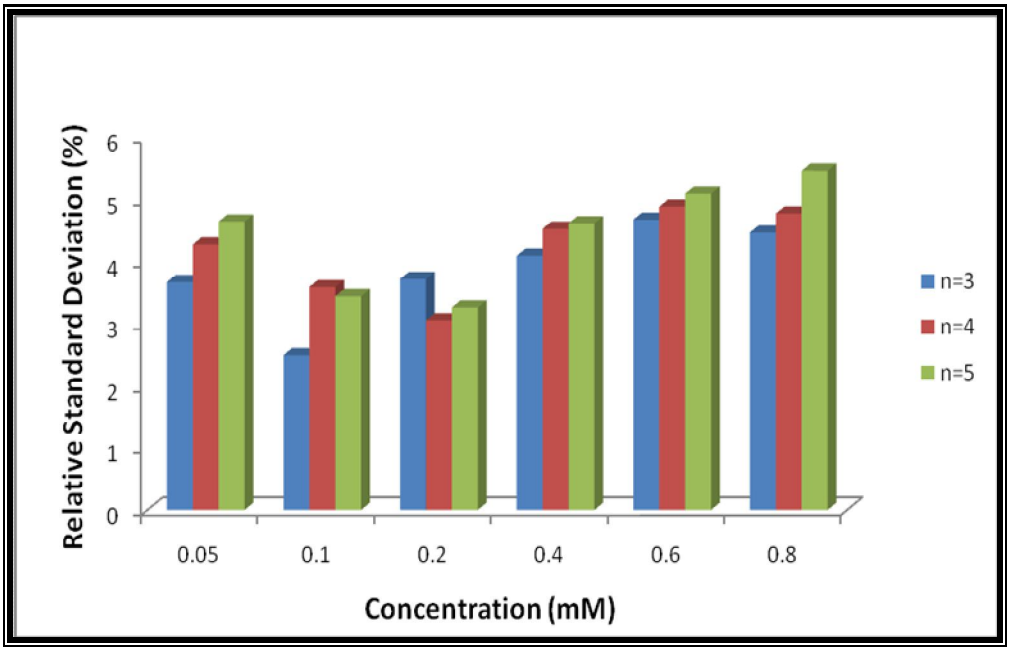

Fig. 4.11: Reusability performance (n = 3-5) of the Uricase/BS^3/APTES/ ITO electrode in terms of relative standard deviation at different concentrations of uric acid in PBS

4.3.3 Stability and storage

The stability of Uricase/BS^3/APTES/ITO electrode was studied at an interval of 7 days, when stored at 4-5ºC by continuously monitoring the current response to uric acid, under identical experimental conditions, as shown in figure 4.12. A slow decrement of 5.8% in current response was observed for 50 days of storing after which a sharp decrease of about 15.18 % was observed.

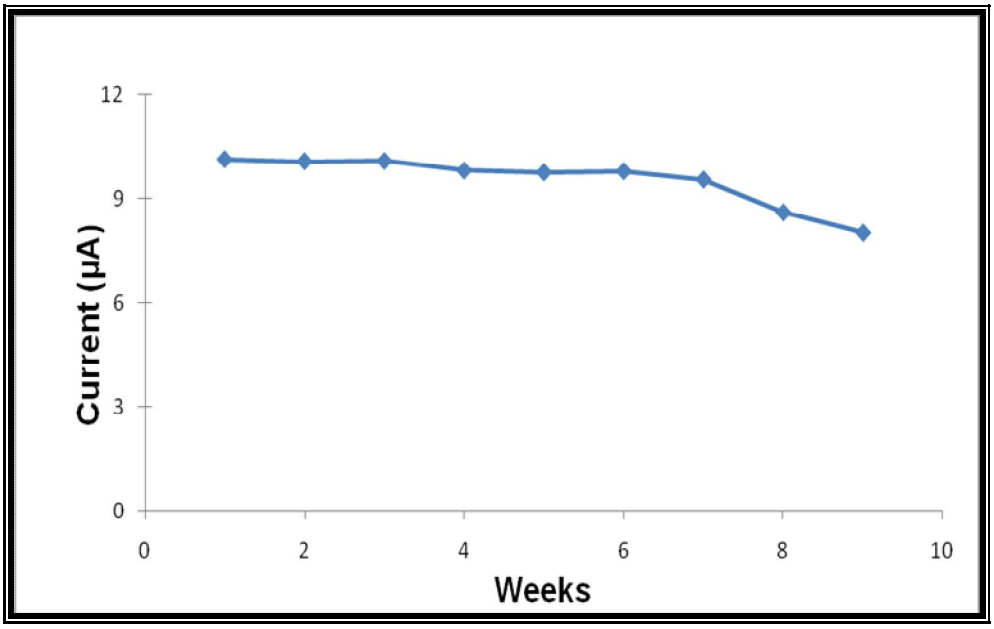

Fig. 4.12: Effect of storage time on the amperometric response of Uricase/BS^3/APTES/ITO electrode

4.4 CONCLUSION

Uric acid biosensor was fabricated by immobilizing enzyme uricase on SAM of APTES via a crosslinker BS^3 on an ITO-glass plate. Uricase/BS^3/APTES/ITO electrode was characterized by electrochemical techniques and amperometric response was studied as a function of uric acid concentration. The biosensor Uricase/BS^3/APTES/ITO showed a linear range of 0.05 to 0.58 mM with a lower detection limit of 0.037 mM. The response time was found to be 50 sec reaching to a 95% steady state current value. The efficient bonding of enzyme on the electrode surface exhibits an improved sensitivity of 39.35 $\mu AmM^{-1}cm^{-2}$. The low cost, easy method of fabrication and high sensitivity makes it advantageous to the recently reported uric acid biosensors.

4.5 REFERENCES

1. Dannenberger O, Weiss K, Woll C, Buck M. *Phys. Chem. Chem. Phys.* 2 (2000) 1509.
2. Yun DH, Song MJ, Hong SI, Kang MS, Min NK. *J. Kor. Phys. Soc*. 47 (2005) S445.
3. Mendes RK, Carvalhal RF, Kubota LT. *J. Electroanal. Chem.* 612 (2008) 164.
4. Satjapat M, Sanedrin R, Zhou F. *Langmuir* 17 (2001) 7637.
5. Schwartz DK. *Annu. Rev. Phys. Chem.* 52 (2001) 107.
6. Gary W, Bowlin GL. *Encyclopedia of Biomaterials and Biomedical Engineering*. Informa Healthcare, 2004.
7. Love JC, Estroff LA, Kriebel JK, Nuzzo RG, Whitesides GM. *Chem. Rev.* 105 (2005) 1103.
8. Vos, JG, Forster RJ, Keyes TE. *Interfacial Supramolecular Assemblies*. Wiley, 2003.
9. Madou M. *Fundamentals of Microfabrication: The Science of Miniaturization* CRC, 2002.
10. Kaifer A. *Supramolecular Electrochemistry. Coral Gables*. Wiley VCH. 2001.
11. Jung SH, Son HY, Yuk JS, Jung JW, Kim KH, Lee CH, Hwang H, Ha KS. *Colloids Surf. B* 47 (2006) 107.
12. Kim SJ, Gobi KV, Tanaka H, Shoyama Y, Miura N. *Sens. Actuators B* 130 (2008) 281.

13. Cheng F, Gamble LJ, Castner DG. *Anal. Chem.* 80 (2008) 2564.
14. Kafi AKM, Lee DY, Park SH, Kwon YS. *Microchem. J.* 85 (2007) 308.
15. Babu VRS, Kumar MA, Karanth NG, Thakur MS. *Biosens. Bioelectron.* 19 (2004) 1337.
16. Kharitonov AB, Zayats M, Lichtenstein A, Katz E, Willner I. *Sens. Actuators B* 70 (2000) 213.
17. Aung KMM, Ho XN, Su XD. *Sens. Actuators B* 131 (2008) 371.
18. Degrandpre MD. *Anal. Chem.* 65 (1993) 331.
19. Moreno-Bondi MC, Orellana G, Camara C, Wolfbeis OS. *Proc. SPIE* 1368 (1990) 157.
20. Parker JW, Laskin O, Yu C, Lau M, Klima S, Fisher R, Scott I, Atwater BW. *Anal. Chem.* 65 (1993) 2329.
21. Wolfbeis OS. In Fiber OpticChemical Sensors and Biosensors, vol. II, CRC, Press, Boca Raton, 1991.
22. Saprigin AV, Thomas CW, Dulcey CS, Patterson CH, Spector Jr MS. *Surf. Interface Anal*. 36 (2004) 24.
23. Hooper AE, Werho D, Hopson T, Palmer O. *Surf. Interface Anal.* 31 (2001) 809.
24. Charles PT, Vora GJ, Andreadis JD, Fortney AJ, Meador CE, Dulcey CS, Stenger DA. *Langmuir* 19 (2003) 1586.
25. Flink S, Schonherr H, Vancso GJ, Geurts FAJ, Leerdam van KGC, Veggel van F, Reinhoudt DN. *J. Chem. Soc. Perkin Trans.* 2 (2000) 2141.
26. Howarter JA, Youngblood JP. *Langmuir* 22 (2006) 11142.

27. Bandyopadhyay K, Sastry M, Paul V, Vijayamohanan K. *Langmuir* 13 (1997) 866.
28. Bandyopadhyay K, Vijayamohanan K. *Langmuir* 14 (1998) 625.
29. Finklea HO, Snider DA, Fedyk J, Sabatani E, Gafni Y, Rubenstein I. *Langmuir* 9 (1993) 3660.
30. Eswara US, Dutt H, Mottola A. *Anal. Chem.* 46 (1974) 1777.
31. Raj CR, Ohsaka T. *J. Electroanal. Chem.* 540 (2003) 69.
32. Matos RC, Angnes L, Araujo MCU, Saldanha TCB. *Analyst* 125 (2000) 2011.
33. Matos RC, Augelli MA, Lago CL, Angnes L. *Anal. Chim. Acta* 404 (2000) 151.
34. Burtic CA, Ashwood ER. Teitz Textbook of Clinical Chemistry, second ed. WB Saunders, Philadelphia, 1994.
35. Kahn K, Tipton PA. *Biochemistry* 36 (1997) 4731.
36. Kahn K, Serfozo P, Tipton PA. *J. Am. Chem.Soc.* 119 (1997) 5435.
37. Jain SC, Tanwar VK, Dixit V, Verma SP, Samanta SB. *Appl. Surf. Sci.* 182 (2001) 350-356.
38. Akgo S, Ozturka N, Karagozler AA, Uyguna DA, Uygun M, Denizli A. *J. Mol. Cat. B: Enzy.* 51 (2008) 36.
39. Zhao J, Bradbury CR, Huclova S, Potapova I, Carrara M, Fermin DJ. *J. Phys. Chem. B* 109 (2009) 22985.
40. Randles JBB. *Disc Faraday Soc.* 1 (1947) 11.

Chapter V

Self Assembled Gold Nanoparticles based Uric Acid Biosensor

5.1 INTRODUCTION

With recent advances in nanotechnology, electrochemical biosensors, in combination with nanomaterials, have become simple, efficient tools to measure the concentration of analytes and the response- time functions of target biomolecules to the drugs or the toxic reagents. Nanomaterials have been applied to modify metal, glass or carbon surfaces in connection with electrochemical and optical sensing.

The modification of the electrode material with metal nanoparticles enabled a larger active surface area for the immobilization of the biomolecules as well as facilitated the flow of electrons between the solid surface and the biomolecules. Thus, better detection limits were obtained than with the biosensors without nanoparticle modification. The use of metal nanoparticles as catalysts in biosensors is due to their superior stability and complete recovery in biochemical redox processes.

Incorporation of metal nanoparticles (MNPs) into electrochemical applications has attracted extensive interest owing to their extraordinary catalytic properties and their interfacedominated properties over bulk-metal electrodes. These MNPs-modified electrodes have been focused on studying the direct electrochemistry of protein, especially heme protein (such as cytochrome *c* [1, 2], hemoglobin (Hb) [3–5], myoglobin [6, 7], horseradish peroxidase [8, 9] and so on), and further applications in mediator-free biosensors and catalysis [10, 11]. Many kinds of metal and their oxide nanoparticles, such as Au, Ag, Pt, TiO_2, Fe_3O_4, ZrO_2 and MnO_2 nanoparticles,

were imposed to catalyze electrochemical reaction and enhance the electron transfer between enzyme and electrodes.

Gold nanoparticles (GNPs) have emerged as a promising new material and their widespread application in the fields of electronics, catalysis and biosensors has received worldwide attention in recent years [12-17]. The affinity of certain thiol-containing substrates to GNPs has especially caused dramatic changes in the electrochemistry of substrate enzyme interactions. GNPs in biosensors also provide a biocompatible microenvironment for biomolecules and greatly increase the amount of immobilized biomolecules on the electrode surface, thus improving the sensitivity of the biosensor [18-20]. Electrochemical studies have revealed that GNPs can enhance electrode conductivity, facilitating the electron transfer and improving the detection limit for biomolecules [21, 22]. Recently, a great deal of methods has been developed to prepare stable gold nanoparticles with controllable size. The synthesized gold nanoparticles are always capped with a certain stabilizer, which involves alkanethiols [23-25], amines [26], nucleotides [27] and polymers [28-32] to avoid the aggregation of gold nanoparticles resulting from Van der Waals attractions [33]. Modification of metal-nanoparticle surfaces with targeted ligands provides endless opportunities to prepare metal nanoparticles with desired properties and functions. As shown in figure 5.1, metal nanoparticles have been successfully applied to modify electrode surfaces.

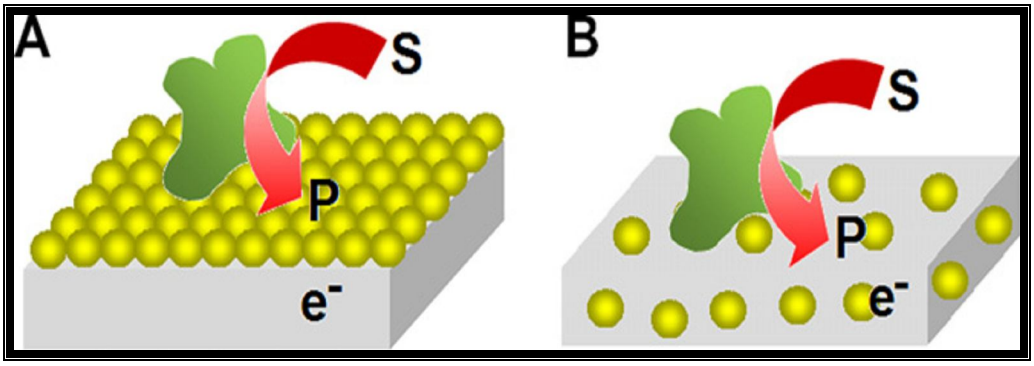

Fig. 5.1: (A) Self-assembled monolayer formation of Au nanoparticles on solid surfaces enhances the redox process that provides the electrochemical detection of the enzymatic product (P) from the substrate (S); (B) Metal nanoparticles embedded inside the matrices allow the direct connection between the enzyme and the electrode surface

Caruso and co-workers [34] fabricated dense GNPs films by the hybrid of GNPs in polyelectrolyte multifilms, and revealed that GNPs could improve the electron-transfer characteristics of the films and they further utilized the films as high-sensitive electrochemical sensors for nitrous oxide. Recently, Hempelmann and co-workers [35] fabricated highly ordered macroporous gold films for increasing electroenzymatic oxidation of glucose with glucose dehydrogenase.

To utilize GNPs for the fabrication of novel electrochemical sensors, they must be attached to electrode substrates [36, 37]. Attachment of GNPs with self-assembled monolayers (SAMs) of alkane or aromaticthiols terminated with -SH or -NH_2 functional groups is useful for the preparation of

GNPs-modified electrodes because controllable surface coverage of GNPs with good stability can be achieved by this method [38, 39]. Although GNPs modified electrodes have shown electrocatalytic activity towards several biomolecules, the sensitivity of these electrodes towards some bio- molecules is not encouraging [40-42]. It has been reported that only 25–30% coverage of GNPs can be achieved at sol-gel and alkanethiols terminated with -SH and -NH_2 functional groups [43], and this is one of the possible reasons for the lower sensitivity for biomolecules.

Various strategies have been reported to obtain GNPs linked on suitable functionalized surfaces and among these the self assembly approach represents a simple, fast and versatile method to obtain nanoparticles arrays in which coverage and distributions can be easily controlled [44-46]. The design and preparation of an optimum interface between the bio-components and the detector material is the key part of sensor development [47-49].

The detection of uric acid (UA) in body fluids is clinically important indicator. Uricase catalyzes the *in vivo* oxidation of uric acid in the presence of oxygen to produce allantoin and CO_2 as oxidation products of uric acid and hydrogen peroxide as a reduction product of O_2.

$$\text{Uric acid} + O_2 + H_2O \xrightarrow{\text{uricase}} \text{allantoin} + CO_2 + H_2O_2$$

The electrochemical oxidation of H_2O_2 requires high potential, at which the other oxidizable species may also interfere in the measurement of UA. Therefore a low potential detection of H_2O_2 is required to avoid the interference from high potential oxidative species. This is done by using a low potential redox probe such as potassium ferricyanide as an electron mediator.

The uricase oxidizes UA to allantoin and itself is reduced to its reduced form which is oxidized back to its initial oxidated form by ferricyanide as redox mediator.

$$UA + 2[Fe(CN)_6]^{3-} + H_2O \xrightarrow{\text{uricase}} \text{allantoin} + 2[Fe(CN)_6]^{4-} + CO_2 + 2H^+$$

$$2[Fe(CN)_6]^{4-} \xrightarrow{\text{anodic electrode}} 2[Fe(CN)_6]^{3-} + 2e^-$$

Keeping the above facts in view, we describe a highly sensitive and selective UA amperometric biosensor using self assembled GNPs for the quantitative detection of uric acid in aqueous solution. The GNPs were self assembled over a SAM of APTES modified surface of the indium tin oxide (ITO) coated glass plate, which was further modified by forming a mixed SAM of 11-Mercapto Undecanoic acid (MUA) and 3-Mercapto Propionic acid (MPA) for the immobilization of uricase through carbodiimide coupling reaction. The biosensor (Uricase/MUA-MPA/GNPs/APTES/ITO glass electrode) was characterized by cyclic voltammetry and electrochemical impedance spectroscopy in the presence of $[Fe(CN)_6]^{3-}$ as a redox probe.

5.2 EXPERIMENTAL

5.2.1 Materials

Enzyme Uricase (EC 1.7.3.3, 9 units/mg from *Bacillus fastidiosus*) was procured from Sigma Aldrich Corp. 3-aminopropyltriethoxysilane (APTES) was purchased from Merck chemicals (Germany). Tetrachloroauric (III) acid ($HAuCl_4$) was obtained from Himedia Pvt. Ltd., India for preparation of GNPs.

11-Mercapto Undecanoic acid 95% (MUA), 3-Mercapto Propionic acid 99% (MPA), *N*-(3-Dimethylaminopropyl)-*N'*-ethyl carbodiimide hydrochloride (EDC) and *N*-Hydroxy Succinimide 98% (NHS) were obtained from Sigma-Aldrich chemicals. Uric acid with 99% purity was purchased from CDH, India. Other chemicals were of analytical grade and used without further purification. Water used in all reactions was double de-ionized (DDI) water obtained from a Millipore purification system.

5.2.2 Equipments

Contact angles were recorded on Drop Shape Analysis System, model DSA10MK2 from Kru''ss GmbH, Germany. Atomic force microscopy (AFM) images were obtained on a Nanoscope 5, VEECO Instrument Ltd., USA. Transmission electron microscopy (TEM) images were taken on high resolution TM model Technai G2 F30 S Twin, The Netherlands. Cyclic voltammetry and electrochemical impedance measurements were done on a PGSTAT302N, AUTOLAB instrument from Eco Chemie, The Netherlands. The impedance measurements were performed in the presence of a redox probe $[Fe(CN)_6]^{3-}$ at the scanning frequencies from 0.1 to 100,000 Hz. All measurements were carried out in a conventional three-electrode cell configuration consisting of a working electrode (Uricase/MUA-MPA/GNPs/APTES/ITO), Ag/AgCl reference electrode and platinum foil as a counter electrode.

5.2.3 Fabrication of Uricase/MUA-MPA/GNPs/APTES/ITO glass electrode

The ITO coated glass plates (1 x 1 cm^2) were cleaned by sequential ultrasonic cleaning in soapy water (extran), acetone, ethanol, isopropyl alcohol and distilled water for 10 min each, and drying in vacuum. Then, the cleaned ITO glass plates were exposed to oxygen plasma for 5 min in a plasma chamber. Finally the ITO glass plates were once again washed with doubled distilled water and dried in vacuum. Cleaned ITO glass plates were immersed in 2% APTES solution prepared in ethanol for 1.5 h, under the ambient conditions, to form a SAM. The glass plates were then rinsed with ethanol in order to remove non-bonded APTES from the surface of the substrate and dried under N_2. Colloidal GNPs were prepared by citrate reduction of $HAuCl_4$ in aqueous solution with an average particle diameter of 10-12 nm [50]. The APTES modified ITO glass plates were then immersed in the above colloidal solution of GNPs for a period of 1 h, followed by washing with distilled water and dried under N_2 to form the GNPs/APTES/ITO glass plates. These were then immersed in mixture of MUA and MPA (20 mM; 1:9; v/v) in ethanol for 16 h to form a mixed SAM of MUA and MPA over the GNPs modified surface. These plates were then washed in ethanol to remove the unbound MUA/MPA molecules and dried under N_2. The combination of MPA and MUA was used to obtain the SAMs not as compact as those formed with long-chain alkanethiols, thus allowing access of chemical species in solution, such as redox mediator, to the electrode surface. The mixture of MPA and MUA thus provide the characteristics of both, long and short-chain alkanethiol

monolayers, which offers a better loading of proteins molecules, as reported earlier [51].

The above MUA-MPA/GNPs/APTES/ITO glass plates were then further immersed in an aqueous solution containing 30 mM NHS and 150 mM EDC for 1 h, followed by washing with distilled water and dried under N_2 to obtain the NHS/MUA-MPA/GNPs/APTES/ITO glass plates. These glass plates were utilized for the immobilization of enzyme by immersing them in an uricase solution (~ 3U) prepared in phosphate buffer solution (PBS) of pH 7.4, for a period of 1.5 h. The excess enzyme was removed from the glass plates by rinsing them with PBS and finally dried under N_2 and stored at 4°C. These Uricase/MUA-MPA/GNPs/APTES/ITO glass plates were used as working electrode.

5.3 RESULTS AND DISCUSSION

5.3.1 Characterization of enzyme electrode

The figure 5.2 shows a schematic representation of the stepwise fabrication of Uricase/MUA-MPA/GNPs/APTES/ITO electrode. Colloidal GNPs obtained from $[AuCl_4]^-$ has an intrinsic fixed negative charge resulting from strongly adsorbed Cl^- / or a coating of $[AuCl_2]^-$ (produced by incomplete reduction of $[AuCl_4]^-$) [52]. The 10-12 nm GNPs colloidal solution was characterized by TEM (Fig. 5.3). The free NH_2 groups of APTES/ITO electrode get ionized in the pH 4-10 regime to form NH_3^+ and these positively

charged amino groups are responsible for the electrostatic interaction with the negatively charged GNPs for the formation of the self assembly of GNPs. Adsorption of GNPs by this method results in a monolayer coverage, further adsorption on the surface being limited by repulsion between the charged particles. The GNPs were further modified with a mixed SAM of MUA-MPA (1:9) and the freely available carboxylic groups were utilized for the immobilization of uricase enzyme.

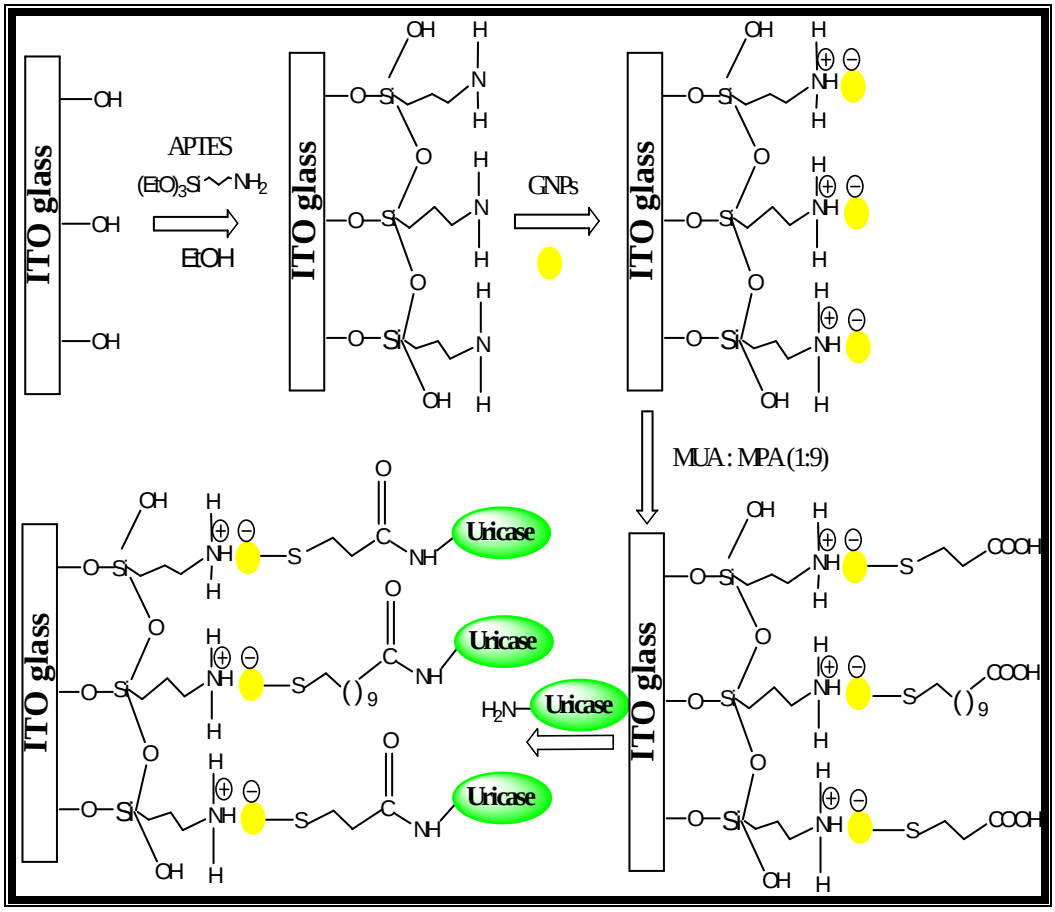

Fig. 5.2: Schematic illustration of the step wise surface modification of ITO glass plate and immobilization of enzyme uricase

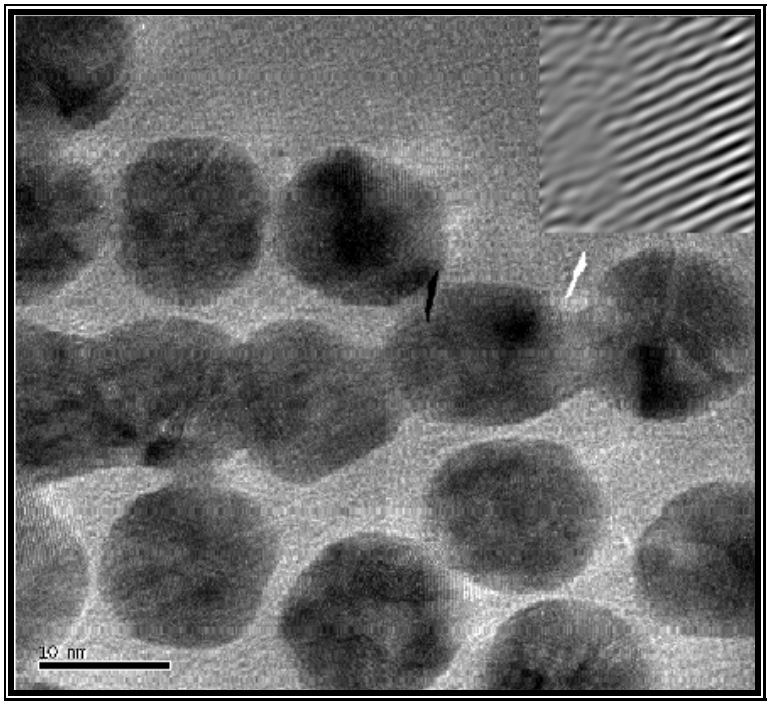

Fig. 5.3: TEM micrograph of GNPs with an average size of 10-12 nm

The various modification steps of the electrode surface were characterized by the static sessile drop method. The drop image was stored and an image analysis system calculated the contact angle (θ) from the shape of the drop. Measurements were repeated on four drops at different regions. The hydrophilicity of the surface changes significantly with each step of surface modification. The initial low contact angle value of 40±1° (Fig. 5.4a) obtained for bare ITO coated glass plate. This hydrophilic character of the surface is due to the presence of surface hydroxyl group. However, after treating the ITO glass plate with APTES, the contact angle was found to increase to 73±1° (Fig. 5.4b), a value corresponding to that reported in the

previous work [53]. This increase in water drop contact angle with respect to freshly cleaned ITO glass substrate is due to the presence of hydrophobic positively charged amino group of APTES molecules. Surface free energy decreases upon silanization with respect to bare substrate (the polar component more than the dispersive component) due to the drastic decrease of hydroxyl groups at the surface because of reaction with silane molecules. The self assembly of GNPs over APTES modified ITO glass surface exhibits a further increase in water contact angle to 93±2° (Fig. 5.4c) due to the hydrophobic character of gold surface [54]. The modification of GNPs/APTES/ITO surface with a mixed SAM of MUA and MPA results in the reduction of water contact angle to 86±2° (Fig. 5.4d). This may be due to the presence of terminal hydrophilic carboxyl ions at the surface of the electrode. Further, on EDC/NHS treatment a slight increase in hydrophilicity was observed, as evident from a small decline in the water contact angle to 80±2° (Fig. 5.4e). This may result from the replacement of terminal carboxyl groups with little more hydrophilic succinimide groups. This on further subsequent treatment with uricase enzyme results in a significant increment in water contact angle to 105±2° (Fig. 5.4f) due to the substitution of succinimide group with hydrophobic amino acid chain of enzyme molecules during carbodimide coupling reaction, thereby indicating the attachment of enzyme molecules over the GNPs modified electrode.

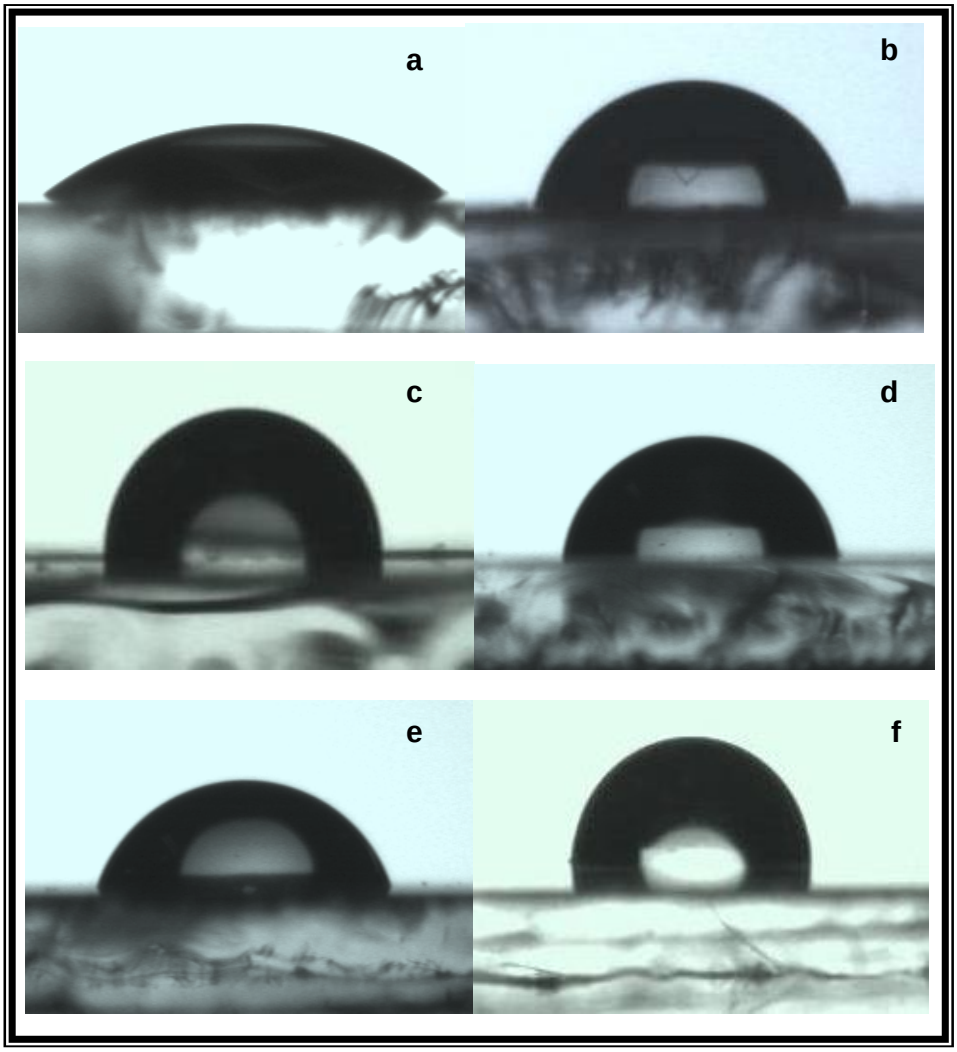

Fig. 5.4: Contact angle measurement images of (a) ITO coated glass plate; (b) APTES/ITO glass; (c) GNPs/APTES/ITO glass; (d) MUA-MPA /GNPs/APTES/ITO glass; (e) NHS/MUA-MPA/GNPs/APTES/ITO glass; (f) Uricase/NHS/MUA-MPA/GNPs/APTES/ITO glass

The surface morphology of the each modified step involved in the fabrication of GNPs modified electrode was characterized by using atomic force microscopy (AFM) images taken in a non contact mode. The AFM images of GNPs modified APTES/ITO surface (Fig. 5.5a) indicate the well coverage of the APTES surface by the GNPs having a regular island-like structure with an average roughness parameter value of 0.431 nm and maximum average height of 11.9 nm. However, the AFM images of MUA/MPA modified GNPs/APTES/ITO glass exhibits an asymmetrical globular shaped surface (Fig. 5.5b) with an increased roughness parameter value of 0.984nm and increased average maximum height of 16.3 nm. This may be due to the attachment of long thio-alkyl chain of MUA/MPA surrounding well over the GNPs surface. In contrast to the relatively globular shaped surface, the surface morphology of the uricase immobilized MUA-MPA/GNPs/APTES/ITO glass exhibits a highly asymmetrical sharp regular island-like structure (Fig. 5.5c) with an average roughness parameter value of 2.81 nm and average maximum height of 32.9 nm. This significant increase in both the average roughness parameter and average maximum height values is a clear indication of the immobilization of the uricase enzyme molecules well over the surface of MUA-MPA/GNPs/APTES/ITO.

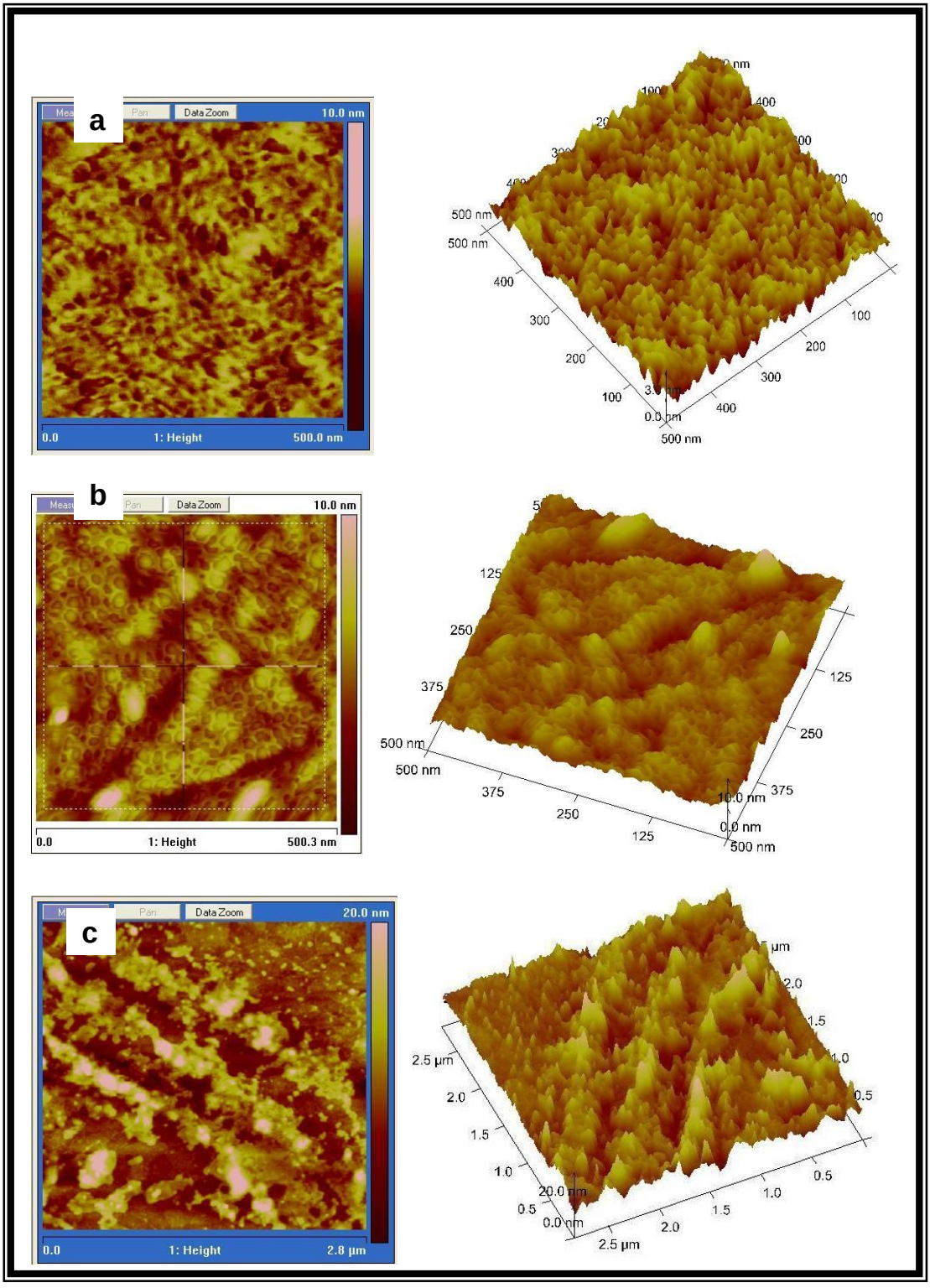

Fig. 5.5: 2D and 3D AFM images of (a) GNPs/APTES/ITO glass; (b) MUA-MPA/ GNPs/APTES/ITO glass; (c) Uricase//MUA-MPA/GNPs/APTES/ITO glass

The Uricase/MUA-MPA/GNPs/APTES/ITO glass electrode was characterized by cyclic voltammetry and electrochemical impedance spectroscopy. All the electrochemical measurements were performed in PBS solution, pH 7.4, containing 0.1 M KCl and 2 mM $[Fe(CN)_6]^{3-}$. The $[Fe(CN)_6]^{3-}$ probe was used as a marker to investigate the changes in electrode behavior after each surface modification step. Each step of surface modification of ITO-glass plate and enzyme immobilization were monitored by cyclic voltammetry. The cyclic voltammograms of the modified electrode before and after the enzyme immobilization is shown in figure 5.6. In all the CV experiments, 3rd cycle was considered as stable one since no significant changes were observed in the subsequent cycles. The bare ITO glass shows a quasi reversible CV with a peak-to-peak separation between the oxidation and reduction potentials (ΔE_p) of 231 mV. This upon modification with a SAM of APTES exhibits a more reversible CV cycle with an increased peak-to-peak oxidation and reduction current (ΔI_p) of 0.24 mA and a decreased potential difference (ΔE_p) of 149 mV between the cathodic and anodic waves of the redox probe. This reduction in the potential difference is attributed to an increased interfacial concentration of the anionic probes ($[Fe(CN)_6]^{3-}$) due to its strong affinity towards the polycatonic layer as the amino groups of the APTES get protonated (NH_3^+) in aqueous solution [55]. A further increase in the redox current (ΔI_p 0.30 mA) and a reduction in the potential difference (ΔE_p 133 mV) was observed with the GNPs modified APTES. This may be due to the fact that the large surface area of the conducting GNPs provides a fast exchange of electrons and thus indicating the formation of the self assembly

of GNPs over the APTES surface. However, in contrary to the above a large decrement in the redox peak current (ΔI_p 0.20 mA) and an increment in the potential difference (ΔE_p 156 mV) was observed when the GNPs modified surface was treated with a mixed SAM of MUA and MPA. These results indicate a repulsive interaction of terminal carboxyl ions (COO^-) with ionic probe $[Fe(CN)_6]^{3-}$, at the surface interface, conforming the formation of a mixed SAM of MUA and MPA layer over the surface of GNPs/APTES/ITO glass. The CV curve shows a further decline in the redox peak current (ΔI_p 0.19 mA) and a large potential difference (ΔE_p 276 mV) between the redox waves after the immobilization of enzyme molecules at the surface of the modified electrode. This may be attributed to the formation of insulating layer of uricase enzyme molecule, at the electrode surface, which perturbs the interfacial electron transfer considerably indicating an efficient covalent bonding of enzyme through a mixed SAM of MUA and MPA.

Each assembled step towards the fabrication of Uricase/MUA-MPA/ GNPs/APTES/ITO glass electrode was further characterized by electrochemical impedance spectroscopy. The impedance spectroscopy was represented as an equivalent circuit [56] as shown in the inset of figure 5.7. The impedance spectrum, which includes a semicircle portion at higher frequencies, corresponds to the electron transfer limiting process and a linear part at the low frequencies resulting from diffusion limiting step of the electrochemical process. The ohmic resistance of the electrolyte solution (R_s) and the Warburg impedance (Z_w) represents the bulk properties of the

electrolyte solution and diffusion features of the redox probe in solution, respectively.

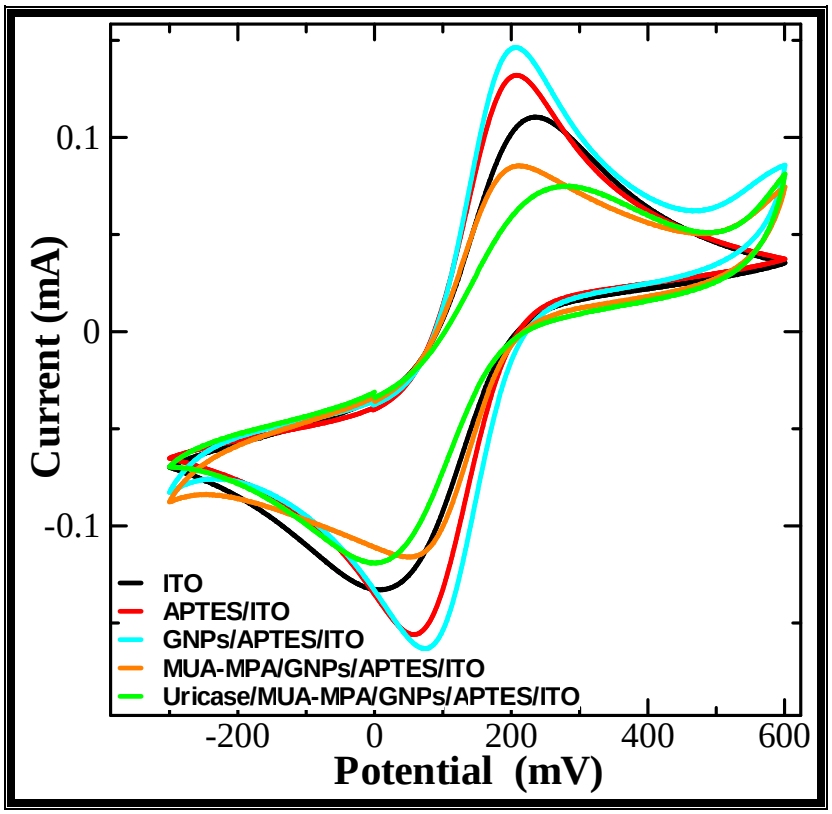

Fig. 5.6: Cyclic voltammograms of: bare ITO glass; APTES/ITO glass; GNPs /APTES/ITO glass; MUA-MPA/GNPs/APTES/ITO glass and Uricase/MUA-MPA/GNPs/APTES/ITO glass in 0.1 M KCl solution containing 2 mM $[Fe(CN)_6]^{3-}$; scan rate 25 mV/s; 3rd cycle voltammogram is shown

Figure 5.7 shows the electrochemical impedance spectra of the bare and the GNPs modified ITO glass electrode before and after the immobilization of the enzyme uricase and the corresponding electron-transfer resistance values are listed in table 5.1. The bare ITO glass shows an electron transfer resistance (R_{et}) value of 1039.80 Ω. The R_{et} value for APTES/ITO glass was strongly reduced to 807.33 Ω, which indicates an easy electronic transport at the electrode surface interface after the APTES modification of ITO. A further decrease in the R_{et} value of 461.44 Ω was observed for the GNPs modified APTES/ITO glass, which indicates a fast exchange of electrons at the electrode surface interface. However, the treatment of the above GNPs modified electrode surface with a mixed SAM of MUA and MPA and their subsequent attachment with the enzyme uricase results in an increased R_{et} values of 1445.31 and 1603.66 Ω, respectively. These results are in conformity with the pattern obtained in cyclic voltammetry measurements, further confirming the formation of the Uricase/MUA-MPA/GNPs/APTES/ITO glass electrode.

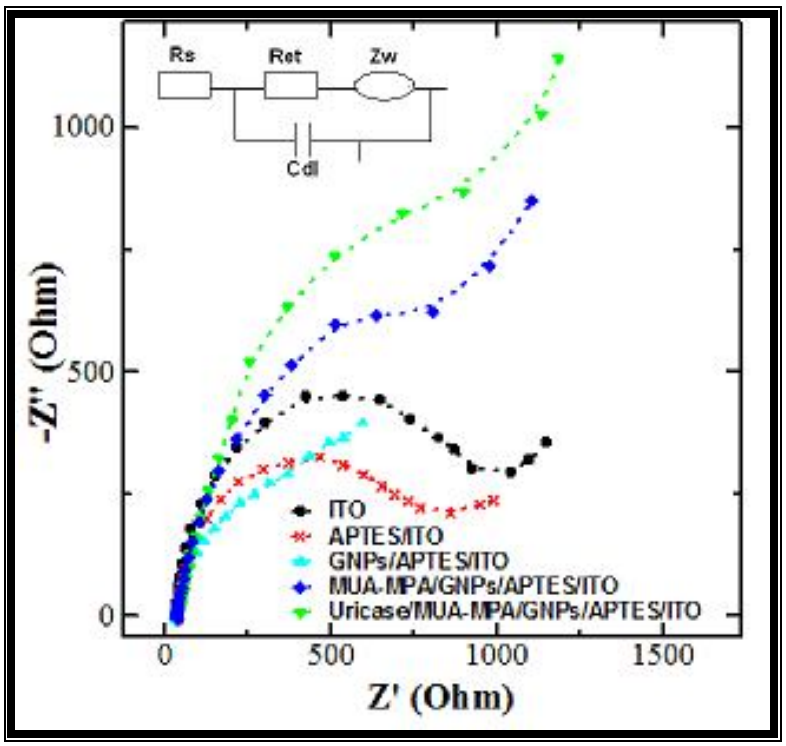

Fig. 5.7: Nyquist plots obtained for bare ITO glass, APTES/ITO glass; GNPs /APTES/ITO glass; MUA-MPA/GNPs/APTES/ITO glass and Uricase/MUA-MPA/GNPs/APTES/ITO glass electrodes in 0.1 M KCl solution containing 2 mM $[Fe(CN)_6]^{3-}$. Inset shows a schematic diagram of equivalent circuit for impedance spectroscopy: R_s, resistance of the electrolyte solution; Ret, electron-transfer resistance; Z_w, Warburg impedance; C_{dl}, double-layer capacitance

Table 5.1: CV peak potential difference (ΔE_p) and the charge-transfer resistance of biosensor before and after each step of ITO glass surface modifications and enzyme immobilization

Type of Electrode	E_{oxi} (mV)	E_{red} (mV)	ΔE_p (mV)	ΔI_p (mA)	Charge transfer resistance R_{et}(Ωcm^{-2})
ITO	235	4	231	0.242	1039.80
APTES/ITO	206	57	149	0.287	807.33
GNPs/APTES/ITO	205	72	133	0.309	461.64
MUA-MPA/GNPs/ APTES/ITO	209	53	156	0.200	1445.31
Uricase/MUA-MPA/ GNPs/APTES ITO	279	3	276	0.193	1603.66

5.3.2 Amperometric response of Uricase/MUA-MPA/GNPs/APTES/ITO glass electrode

Chronoamperometric response studies were conducted with Uricase/MUA-MPA/GNPs/APTES/ITO glass electrode, at a bias voltage of 0.27 V vs Ag/AgCl in PBS; pH 7.4 containing 2 mM $[Fe(CN)_6]^{3-}$. The amperometric response was measured with the successive addition of 100 µL aliquot of different uric acid concentration in PBS solution, at an interval of 100s.

Figure 5.8 depicts the chronoamperometric response of Uricase/MUA-MPA/GNPs/APTES/ITO glass electrode along with the reusable response performance as a function of uric acid concentration in aqueous solution. An increasing order of amperometric response was observed after each successive addition of an aliquot of increasing uric acid concentration. The 95% steady state current response to uric acid was obtained in about 25 sec. Figure 5.9 shows the steady state current dependence calibration curve to uric acid concentration. The response of the Uricase/MUA-MPA/GNPs/APTES/ITO glass electrode to uric acid was found to be linear in the range of 0.07 to 0.63 mM with a correlation coefficient of 0.991 (n = 10). The lowest detection limit of the electrode was found to be 0.054 mM, at a signal-to-noise ratio of 3. The slope of the linearity i.e. the sensitivity of the enzyme electrode towards uric acid was 19.27 µA mM^{-1}, which is relatively better than the recently reported biosensors and a comparative performance is given in table 5.2. [57-71]

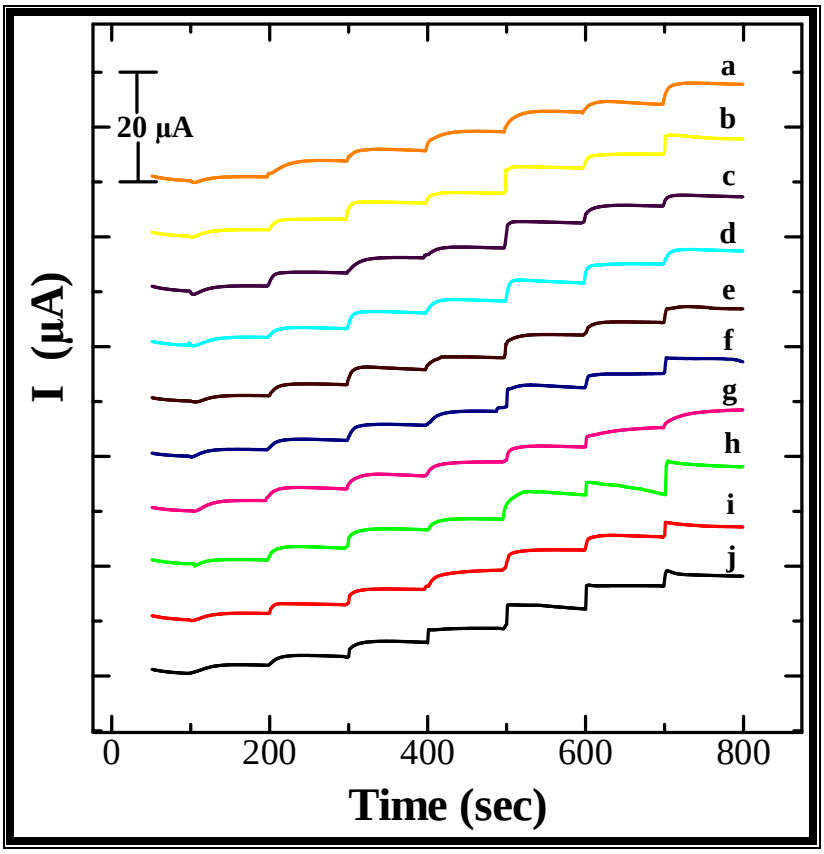

Fig. 5.8: Chronoamperometric response curve of Uricase/MUA-MPA/GNPs/ APTES/ITO with subsequent addition of increasing uric acid concentration (a); reusability response of the same electrode for n = 2-10 (b-j)

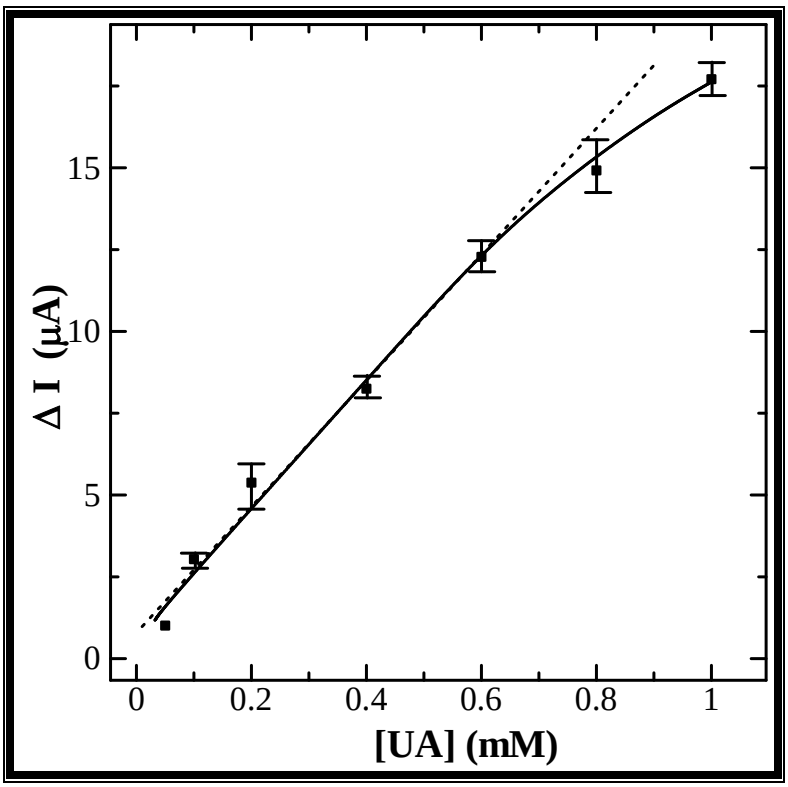

Fig. 5.9: Steady state current dependence calibration curve of Uricase/MUA-MPA/GNPs/APTES/ITO biosensor to uric acid

Table 5.2: Characteristics of some amperometric uric acid biosensors

Matrix	Response time	Stability	Linear range	Sensitivity	Working potential	Reference
Ir-C	41 s	-	0.1 to 0.8 mM	16.60 μA mM^{-1}	0.25 V	[57]
o-aminophenol-aniline copolymer	-	~50 days	0.0001 to 0.5 mmol dm^{-3}	~2.65 μA mM^{-1}	0.4 V	[58]
Polyaniline	-	~60 days	0.0036 to 1.0 mmol dm^{-3}	~ 1 μA mM^{-1}	0.4 V	[59]
Polyaniline-polypyrrole	70 s	4 weeks	$2.5x10^{-6}$ to $8.5x10^{-5}$ M	1.12 μAmM^{-1}	0.4 V	[60]
CNT/Screen printed carbon electrode	-	2 months	20 to 200 mg/L	0.0568 to 0.0721 μA/mgL^{-1}	0.3 V	[61]
Polyaniline			1.0×10−3 to 1.0 mmol dm^{-3}.	<7μA mM^{-1}	0.4 V	[62]
poly(allylamine) (PAA) / poly(vinyl sulfate) (PVS)			10^{-6} to10^{-3} M	<5 μA mM^{-1}	0.6 V	[63]
Zinc sulfide (ZnS) quantum dots		20 days	$5.0×10^{-6}$ to $2.0×10^{-3}$ mol L^{-1}	2.2 μA mM^{-1}	0.45 V	[64]

Polypropylene			4.82-10.94 mg/dL	0.0029 μA mM^{-1}		[65]
Carbon paste	70 s	> 100 days	upto100 μmol dm^{-3}		0.34 V	[66]
self-assembled monolayer of *n*-octanethiolate on Au	20 s		0.15-0.4 mmol dm^{-3}	< 1.0 μAmM^{-1}	0 V	[67]
self-assembled monolayer of 2-(2-mercaptoethylpyrazine) (PET) and 4,4_-dithiodibutyric acid (DTB) on gold (Au) electrode	80–100 s		5–150μM	3.4±0.08 nA cm^{-2} μM^{-1}.	-0.1 V	[68]
Poly(*o*-aminophenol)	37 s	20 days	up to 1×10^{-4} M		0.05 V	[69]
ZnO nanorods			5.0×10^{-6} to 1.0×10^{-3} mol L^{-1}			[70]
SAM of heteroaromatic thiol/Au	-	1 day	1 to 300 μM	0.0149± 0.0005 μA mM^{-1}	~0.4 V	[71]
MUA-MPA/ GNPs/APTES/ITO	25 s	63 days	0.07 to 0.63 mM	19.27 μAmM^{-1}	0.27V	Present work

A few common interfering reagents were studied for any possible interfering effects on the analysis of uric acid. Known concentrations of 1.0×10^{-4} M ascorbic acid, 5.0×10^{-3} M glucose and 1.0×10^{-4} urea were added both individually and in combination to a sample of 0.2 mM uric acid solution. However, no significant interfering effects have been found using these reagents on the current response of the electrode for the said sample.

The reusability of the modified electrode was also tested by conducting the same experiment for several times, under identical conditions. The relative standard deviation determined by 10 successive analyses of using a single Uricase/MUA-MPA/GNPs/APTES/ITO glass electrode was found to less than 4% for 0.1 to 1.0 mM uric acid concentration, as shown in figure 5.10. In a series of 5 Uricase/MUA-MPA/GNPs/APTES/ITO glass electrodes, a relative standard deviation of about 7% was obtained for the individual current response for the same sample (0.2 mM uric acid).

5.3.3 Stability and storage

The stability of Uricase/MUA-MPA/GNPs/APTES/ITO electrode was studied at an interval of 7 days, when stored at 4-5ºC by continuously monitoring the current response to uric acid, under identical experimental conditions, as shown in figure 5.11. A slow decrement of about 10% in current response was observed up to 63 days of storage beyond which a sharp declinment of about 18.3 % was observed.

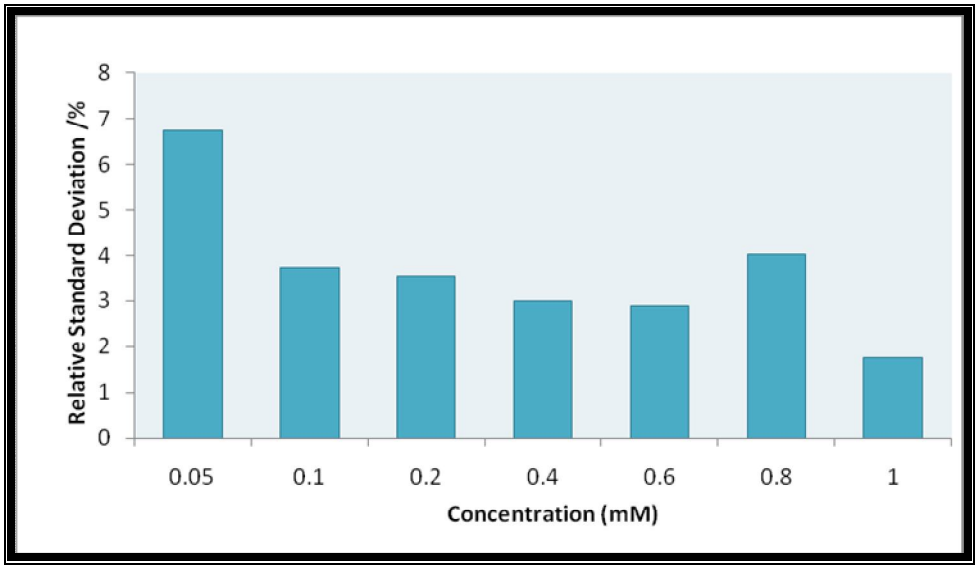

Fig. 5.10: Reusability performance (n = 10) of the Uricase/MUA-MPA/GNPs/ APTES/ITO electrode in terms of relative standard deviation at different concentrations of uric acid in PBS

5.4 CONCLUSION

Uric acid biosensor was fabricated by immobilizing enzyme uricase on a GNPs modified APTES through a mixed SAM of MUA and MPA on an ITO-glass plate. Uricase/MUA-MPA/GNPs/APTES/ITO glass electrode was characterized by AFM and electrochemical techniques. Chronoamperometric response of the modified electrode was studied as a function of uric acid concentration, at a bias voltage of 0.27 V vs Ag/AgCl. The biosensor Uricase/MUA-MPA/GNPs/APTES/ITO exhibits an amperometric response to uric acid concentration in the linear range of 0.07 to 0.63 mM with a sensitivity of 19.27 μA mM^{-1}. The response time was found to be about 25 sec reaching to a 95% steady state current value. The high enzyme loading and fast electron exchange on the large surface of GNPs at the electrode surface results in an improved sensitivity of 19.27 μA mM^{-1}. The low cost and easy method of fabrication are the added advantages which makes it superior over the recently reported uric acid biosensors.

5.5 REFERENCES

1. Haymond S, Babcock GT, Swain GM. *J. Am. Chem. Soc.* 124 (2002) 10634.
2. Liu T, Zhong J, Gan X, Fan C, Li G, Matsuda N. *Chem. Phys. Chem.* 4 (2003) 1364.
3. Liu HY, Hu NF. *J. Phys. Chem. B* 109 (2005) 10464.
4. Topoglidis E, Astuti Y, Duriaux F, Gratzel M, Durrant JR. *Langmuir* 19 (2003) 6894.
5. Wang C, Yang C, Song Y, Gao W, Xia X. *Adv. Funct. Mater.* 15 (2005) 1267.
6. Liu A, Wei M, Honma I, Zhou H. *Anal. Chem.* 77 (2005) 8068.
7. Immoos CE, Chou J, Bayachou M, Blair E, Greaves J, Farmer PJ. *J. Am. Chem. Soc.* 126 (2004) 4934.
8. Liu S, Chen A. *Langmuir* 21 (2005) 8409.
9. Wang L, Wang EK. *Electrochem. Commun.* 6 (2004) 225.
10. Hirsch R, Katz E, Willner I. *J. Am. Chem. Soc.* 122 (2000) 12053.
11. Zhou H, Gan X, Wang J, Zhu X, Li G. *Anal. Chem.* 77 (2005) 6102.
12. Alivisatos AP. *Science* 271 (1996) 933.
13. Rao CNR, Muller A, Cheetham AK. The Chemistry of Nanomaterials: Synthesis, Properties and Applications, Wiley-VCH Verlag GmbH & Co, Weinheim, 2004.
14. Daniel MC, Astruc D. *Chem. Rev.* 104 (2004) 293.
15. Jena BK, Raj CR. *Langmuir* 23 (2007) 4064.
16. Brown KR, Fox AP, Natan MJ. *J. Am. Chem. Soc.* 118 (1996) 1154.
17. Rosi NL, Mirkin CA. *Chem. Rev.* 105 (2005) 1547.

18. Liang KZ, Qi JS, Mu WJ, Chen ZG. *J. Biochem. Biophys. Meth.* 70 (2008) 1156.

19. He X, Yuan R, Chai Y, Shi Y. *J. Biochem. Biophys. Meth.* 70 (2008) 823.

20. Li NB, Park JH, Park K, Kwon SJ, Shin H, Kwak, J. *Biosens. Bioelectron.* 23 (2008) 1519.

21. Song W, Okamura M, Kondo T, Uosaki K. *J. Electroanal. Chem.* 554 (2003) 385.

22. Stoeva SI, Lee J-S, Thaxton CS, Mirkin CA. *Angew. Chem. Int. Ed.* 45 (2006) 3303.

23. Yang Y, Chen S, *Nano Lett.* 3 (2003) 75.

24. Wang G, Huang T, Murray RW, Menard L, Nuzzo RG. *J. Am. Chem. Soc.* 127 (2005) 812.

25. Wang G, Guo R, Kalyuzhny G, Choi JP, Murray RW. *J. Phys. Chem. B* 110 (2006) 20282.

26. Isaacs SR, Cutler EC, Park J, Lee TR, Shon Y. *Langmuir* 21 (2005) 5689.

27. Zhao W, Gonzaga F, Li Y, Brook MA. *Adv. Mater.* 19 (2007) 1766.

28. Murphy CJ, Orendorff CJ. *Adv. Mater.* 17 (2005) 2173.

29. Wu H, Hong R, Wang X, Arvizo R, You C, Samarrta B, Patra D, Tuominen MT, Rotello VM. *Adv. Mater.* 19 (2007) 1383.

30. Abraham S, Kim I, Batt CA. *Angew. Chem. Int. Ed.* 46 (2007) 5720.

31. Miyamura H, Matsubara R, Miyazaki Y, Kobayashi S. *Angew. Chem, Int. Ed.* 46 (2007) 4151.

32. Shi F, Zhang Q, Ma Y, He Y, Deng Y. *J. Am. Chem. Soc.* 2005, 127, 4182.

33. Bhargava SK, Booth JM, Agrawal S, Coloe P, Kar G. *Langmuir* 21 (2005) 5949.

34. Yu A, Liang Z, Cho J, Caruso F. *Nano Lett.* 3 (2003) 1203.

35. Szamocki R, Reculusa S, Ravaine S, Bartlett PN, Kuhn A, Hempelmann R. *Angew. Chem. Int. Ed.* 45 (2006) 1317.

36. Bharathi S, Nogami M, Ikeda S. *Langmuir* 17 (2001) 1.

37. El-Deab MS, Ohsaka T. *J. Electroanal. Chem.* 553 (2003) 107.

38. Abdelrahman AI, Mohammad AM, Okajima T, Ohsaka T. *J. Phys. Chem. B* 110 (2006) 2798.

39. Raj CR, Okajima T, Ohsaka T. *J. Electroanal. Chem.* 543 (2003) 127.

40. Zhang L, Jiang X. *J. Electroanal. Chem.* 583 (2005) 292

41. Sun Y, Bai Y, Yang W, Sun C. *Electrochim. Acta* 52 (2007) 7352.

42. Wu B-Y, Hou S-H, Yin F, Zhao Z-X, Wang Y-Y, Wang X-S, Chen Q. *Biosens. Bioelectron.* 22 (2007) 2854.

43. Sagara T, Kato N, Nakashima N. *J. Phys. Chem. B* 106 (2002) 1205.

44. Musick MD, Pena DJ, Botsko SL, McEvoy TM, Richardson JN, Natan MJ. *Langmuir* 15 (1999) 844.

45. Nakanishi T, Ohtani B, Uosaki K. *J. Phys. Chem. B* 102 (1998) 1571.

46. Ballarin B, Cassani MC, Scavetta E, Tonelli D. *Electrochimica Acta*, 53 (2008) 8034.

47. Ahuja T, Mir IA, Kumar D, Rajesh. *Biomaterials* 28 (2008) 791.

48. Rajesh, Ahuja T, Kumar D. *Sens. Actuators B* 136 (2009) 275.

49. Rajesh, Sharma V, Tanwar VK, Biradar AM. *Sensor Lett*. 8 (2010) 362.

50. Frens G. *Nature Phys. Sci.* 241 (1973) 20.

51. Campuzano S, Pedrero M, Montemayor C, Fatas E, Pingarron JM. *J. Electroanal. Chem.* 586 (2006) 112.

52. Grabar KC, Freeman RG, Hommer MB, Natan MJ. *Anal. Chem.* 67 (1995) 735.

53. Jain SC, Tanwar VK, Dixit V, Verma SP, Samanta SB. *Appl. Surf. Sci.* 182 (2001) 350.

54. Notsu H, Kubo W, Shitanda I, Tatsuma T. *J. Mater. Chem.* 15 (2005) 1523.

55. Grabar KC, Smith PC, Musick MD, Davis JA, Walter DG, Jackson MA, Guthrie AP, Natan MJ. *J. Am. Chem. Soc.* 118 (1996) 1148.

56. Randles JBB. *Disc Faraday Soc.* 1 (1947) 11.

57. Luo Y-C, Do J-S, Liu C-C. *Biosens Bioelectron.* 22 (2006) 482.

58. Pan X, Zhou S, Chen C, Kan J. *Sens Actuators B* 113 (2006) 329.

59. Kan J, Pan X, Chen C. *Biosens Bioelectron*. 19 (2004) 1635.

60. Arslan F. *Sensors* 8 (2008) 5492.

61. Xu H, Li G, Fu M, Wang Y, Liu J. *Proc. of the 2005 IEEE* 1-4 (2005) 255.

62. Jiang Y, Wang A, Kan J. *Sens. Actuators B* 124 (2007) 529.

63. Hoshi T, Saiki H, Anzai J. *Talanta* 61 *(*2003) 363.

64. Zhang F, Li C, Li X, Wang X, Wan Q, Xian Y, Jin L, Yamamoto K. *Talanta* 68 (2006) 1353.

65. Chen J-C, Chung H-H, Hsu C-T, Tsai D-M, Kumar AS, Zen J-M. *Sens. Actuators B* 110 (2005) 364.

66. Dutra RF, Moreira KA, Oliveira MIP, Araujo AN, Montenegro MCBS, Filho JLL, Silva VL. *Electroanalysis* 17 (2005) 701.

67. Nakaminami T, Ito S, Kuwabata S, Yoneyama H. *Anal. Chem.* 71 (1999) 4278.

68. Behera S, Raj CR. *Biosens. Bioelectron.* 23 (2007) 556.

69. Miland Em Miranda Ordieres AJ, Tunon Blanco P, Smyth MR, Fagain CO. *Talanta* 43 (1996) 785.

70. Zhang F, Wang X, Ai S, Sun Z, Wan Q, Zhu Z, Xian Y, Jin L, Yamamoto K. *Anal. Chim. Acta* 519 (2004) 155.

71. Raj CR, Ohsaka T. *J. Electroanal. Chem.* 540 (2003) 69.

Presentation in conferences and workshop attended

1. Presented a poster titled “An amperometric uric acid biosensor based on Bis[sulfosuccinimidyl]suberate crosslinker/3-Aminopropyltriethoxysilane surface modified ITO glass electrode” in Indo-Japan Workshop on Biomolecular Electronics & Organic Nanotechnology for Environment Preservation, 17-20 Dec 2009, NPL, Delhi, India.
2. Participated in National Seminar on Chemistry Industry Interface-2005, December 2005, ARSD College, University of Delhi, Delhi.
3. Participated in National seminar on Bio-nanotechnology and engineering materials (NSBNEM-07), 26th October, 2007, Delhi College of Engineeering, Delhi.
4. Presented a poster in NPL, on the occasion of National Science Day, 26th Feb 2010. **This poster won the best presentation.**
5. Presented a poster titled “An amperometric uric acid biosensor based on gold nanoparticles modified 3-aminopropyltriethoxysilane/indium tin-oxide electrode” in a National seminar on “Frontiers in polymeric nanomaterials and composites”, 18-19 March, 2010, B.S. Abdur Rehman University, Vandulur, Chennai . **This poster won best poster award.**
6. Presented a poster titled “Electrochemical uric acid biosensor using interdigitated microelectrode” in Recent advances in Analytical Sciences, 12-14 April 2010, Himachal Pradesh University, Shimla, India. **This poster won Best poster award.**
7. Presented a poster entitled “A Modified Interdigitated Micro-Electrode Embedded Micro-Fluidic Device for the Detection of Uric Acid” in International Conference on Science & Technology of Synthetic Metals, 4-10 July 2010 in Kyoto, Japan.

List of Publications

1. **Tarushee Ahuja**, I.A. Mir, D. Kumar, Rajesh, "Biomolecular immobilization on conducting polymers for biosensing applications", *Biomaterials (Elsevier Press)*, 28 **(2007)** 791-805.
2. **Tarushee Ahuja**, I.A.Mir, D. Kumar, Rajesh, "Potentiometric urea biosensor based on BSA embedded surface modified polypyrrole film", *Sensors and Actuators B: Chemical (Elsevier Press)*, 134 **(2008)** 140-145.
3. **Tarushee Ahuja**, D. Kumar, and Rajesh, "Polymer Based Urea Biosensors: A Brief Overview", *Sensor Letters (American Academic Press)*, 6 **(2008)** 663–674.
4. Rajesh, **Tarushee Ahuja**, D.Kumar, "Recent progress in the development of nano-structured conducting polymers/nanocomposites for sensor applications", *Sensors and Actuators B: Chemical (Elsevier Press)*, 136 **(2009)**275–286.
5. **Tarushee Ahuja**, D. Kumar, Rajesh, V. K. Tanwar, V. Sharma, N. Singh, A. M. Biradar, "An amperometric uric acid biosensor based on Bis[sulfosuccinimidyl]suberate crosslinker/3-Aminopropyltriethoxysilane surface modified ITO glass electrode", *Thin Solid Films*, *(Elsevier Press),* 519(**2010)**1128-1134.
6. **Tarushee Ahuja**, D. Kumar, N. Singh, Rajesh, "Potentiometric urea biosensor based on multi-walled carbon nanotubes (MWCNTs)/silica composite material", Material Science & Engineering C, *(Elsevier Press),* **2010**, I*n Press*.
7. **Tarushee Ahuja**, V. K. Tanwar, S. B. Samanta, D. Kumar, A.M. Biradar, Rajesh, "An amperometric uric acid biosensor based on self assembled gold nanoparticles modified indium tin-oxide electrode" communicated.

Book chapter

"Nanocomposites: from fabrication to chemical sensor applications" by Rajesh, Tarushee Ahuja, D. Kumar in "Chemical Sensors" Momemtum Press, LLC, New York, 2010.

SYNTHESIS & CHARACTERIZATION OF IMMOBILIZING MATERIALS FOR BIOSENSING APPLICATION

Thesis submitted to the

FACULTY OF TECHNOLOGY
UNIVERSITY OF DELHI

for the award of the degree of the

DOCTOR OF PHILOSOPHY

in

APPLIED CHEMISTRY

by

TARUSHEE AHUJA

Department of Applied Chemistry,
DELHI COLLEGE OF ENGINEERING,
BAWANA ROAD, DELHI-110042
2010

Summary

Urea and uric acid are the most important end product of protein degradation and purine metabolism, thus their proper balance in blood is essential for overall well being and for renal health specifically. The optimal concentration of urea in blood is an indication of proper renal functioning, its high level in blood causes urinary tract obstruction, dehyradation, shock, burns and gastrointestinal bleeding, whereas a substantial low level of urea concentration causes hepatic failure, nephrotic syndrome, cachexia. Similarly abnormal uric acid levels lead to gout, chronic renal disease, some organic acidemias, leukemia, pneumonia and Lesch–Nyhan syndrome. Hence, the detection of these analytes in body fluids is clinically important indicator. Although direct spectroscopic methods can be used for their determination, but these methods are dependent on the pre-treatment of sample and cannot be used for onsite monitoring. The primary focus of this work is to develop urea and uric acid biosensors with improved properties such as sensitivity and response time by using different substrates on indium tin-oxide (ITO) glass plates and different methods of immobilization.

The first part of the dissertation focuses on the development of urea biosensor with improved properties based on conducting polymer polypyrrole (PPy). PPy is synthesized electrochemically on ITO glass plates using p-toluene sulphonic acid as dopant. However, the absence of active binding sites in PPy, which can bind the biomolecule, limits its application to some extent. Also simultaneous electrochemical deposition of enzyme, during polymerization showed decrease in background current. This degradation of the polymer was attributed to the denaturing of the enzyme. This problem can

be overcome by incorporating an actively binding group containing substances into the polymer film that provides free NH_2 group to enhance the immobilization as well as electrochemical properties. In this investigation, electrodes are fabricated by embedding bovine serum albumin (BSA) in PPy during electrochemical synthesis on an ITO glass electrode. The free NH_2 groups of embedded BSA at the surface of the PPy film were exploited for the covalent binding of enzyme via carbodiimide coupling reaction. The advantage of using BSA embedded surface modified PPy films for efficient enzyme loading is described. PPy film was characterized with scanning electron microscopy, infrared spectroscopy and UV visible spectroscopy before and after each step of surface modification and enzyme immobilization. Potentiometric and spectrophotometric response of the enzyme electrode (Urs/BSA-PPy/ITO) were measured as a function of urea concentration.

In the following section, the use of carbon nanotubes in a silica matrix is studied to develop urea biosensor. Tetraethyl orthosilicate (TEOS) is used to prepare SiO_2 solution which provides a network for incorporation of carbon nanotubes. Functionalized multiwalled carbon nanotubes are used to supply free COOH groups, on which the enzyme can covalently immobilize. The synergistic effect of silica matrix, F-MWCNTs and biocompatibility of Urs/MWCNTs/SiO_2 made the biosensor to have the excellent electro catalytic activity and high stability. Electrodes were characterized at each step of formation and potentiometric response was measured as a function of urea concentration.

The next part of the dissertation focuses on the development of uric acid biosensor by immobilizing enzyme uricase through a self assembled

monolayer (SAM) of 3-aminopropyltriethoxysilane (APTES) using a crosslinker, Bis[sulfosuccinimidyl]suberate (BS^3) on an indium-tin-oxide (ITO) coated glass plate. Electrodes fabricated were characterized by scanning electron microscopy (SEM), atomic force microscopy (AFM) and electrochemical techniques. Chronoamperometric response was measured as a function of uric acid concentration in aqueous solution (pH 7.4).

Last part of the theisi focuses on the modification of above SAM layer on ITO with gold nanoparticles. Chronoamperometric response was measured as a function of uric acid concentration in aqueous solution. The results indicates better reproducibility and response time of the electrode.

This research work provides a comprehensive study of fabricating different biosensors by using different matrixes and different techniques of transducing.

The development of biosensors has come from the rapid advances in health care technology as a frequent measurement of biochemical parameters such as blood cations, gases and metabolites required for effective patient care. The need for cheap and reliable sensors for monitoring such parameters has lead to exponential increase in the research and development of biosensors.

Electrochemical biosensors have emerged as the most commonly used biosensors as they have been found to overcome most of the disadvantages, which inhibit the use of other types of biosensors. They are rapid, easy to handle, simple and low cost. The basic fact behind this bio-interaction process is that the electrochemical species such as electrons are consumed or

generated producing an electrochemical signal, which can be measured by the detector. These biosensors are usually based on potentiometry and amperometry.

This study identifies the already established materials for developing different biosensor which may be used for the detection of urea and uric acid in aqueous solution. The main objective of this dissertation is to use modified electrode such as BSA/PPy, MWCNT/SiO_2, APTES/BS_3 and GNPs/APTES as matrix for the development of urea and uric acid biosensors.